THE INTERACTION SPECIFICITIES OF SELECTED SMALL MOLECULES WITH NUCLEIC ACIDS

By

Ronald Phillip DeStefano

A DISSERTATION PRESENTED TO THE GRADUATE COUNCIL OF THE UNIVERSITY OF FLORIDA IN PARTIAL FULFILLMENT OF THE REQUIREMENTS FOR THE DEGREE OF DOCTOR OF PHILOSOPHY

UNIVERSITY OF FLORIDA
1973

To my girls. . . . . Karen and Kimberly.

ACKNOWLEDGMENTS

The author extends his appreciation to Dr. E. J. Gabbay for his guidance during the course of these studies. Thanks are also due Dr. C. S. Baxter for his technical assistance in obtaining the XL-100 pmr spectra. The encouragement and support of his wife and daughter are also deeply appreciated.

TABLE OF CONTENTS

LIST OF TABLES

Table | Page

LIST OF FIGURES

Abstract of Dissertation Presented to the
Graduate Council of the University of Florida in Partial
Fulfillment of the Requirements for the Degree of Doctor of Philosophy

THE INTERACTION SPECIFICITIES OF SELECTED SMALL MOLECULES WITH NUCLEIC ACIDS

By

Ronald Phillip DeStefano

December, 1973

Chairman: Dr. E. J. Gabbay
Major Department: Chemistry

This research deals with the use of small molecules to probe the structure of nucleic acids in solution. The first part of the work deals with the assertion that nucleic acids exist in equilibrium with a certain percentage of "open" structures even at temperatures far below the melting temperature of the double helix. A new class of reporter molecules was utilized to probe this open structure to determine possible specificity which might arise due to the somewhat lower stability of sections of the DNA rich in adenine and thymine as opposed to sections rich in guanine and cytidine. These reporter molecules were so designed that intercalation in the usual sense of insertion between base pairs of the intact double helix was impossible due to steric bulk. The interactions were investigated in detail by subtle variations in the structure of the probes and also by utilizing a number of different nucleic acid systems.

The investigations consisted of a series of stopped-flow kinetic measurements wherein rapid mixing of the reactants and observation of the developing hypochromic effect on the spectral transitions of the reporters were used to monitor the complex formation. The use of

sodium dodecyl sulfate (SDS) to dissociate the premade complexes also allowed the investigation of the reverse reaction. Variations in the reaction temperature allowed an investigation of the thermodynamic parameters associated with the reaction.

The data point to the following mechanism: (1) The nucleic acid double helix, due to natural thermal motions such as twisting of the phosphodiester chains relative to each other and consequent underwinding, "cracks" to reveal an open but still stacked segment several base pairs long which may then unstack in a manner dependent upon its base content and sequence. (2) The bulky reporters then insert themselves between adjacent bases. (3) The strands of the double helix reclose to form the original native structure, thus trapping the intercalated reporter molecule. (4) Kinetic evidence suggests that the reclosure step is rate-controlling for the association reaction. (5) Further, the experiments using SDS to dissociate the premade complexes provide additional information on the interaction. It appears that the nucleic acids richer in A-T base pairs dissociate more easily than do those richer in G-C base pairs. This fits in with the experimental observation that the association is three times faster with poly dAT-poly dAT than with poly dG-poly dC.

Another line of investigation involved comparing the interactions of a number of differently substituted p-nitroanilines with nucleic acids. The techniques of proton magnetic resonance (pmr), circular dichroism, ultraviolet-visible spectroscopy, viscometry, direct binding studies, and melting temperature profiles were utilized. The goals of this research were to investigate the possibility of specificity arising from the intercalation process and to gain a better understanding

of the interactions of "reporter" molecules in general with nucleic acids. A model utilizing opposing steric and hydrophobic forces serves to correlate a great deal of the data. The presence of hydrophobic substituents tends to cause a more intimate complex to form, while the increase in steric bulk obtained upon substitution with very large groups makes the insertion between base pairs more difficult. In addition, a number of results suggest that there is a certain degree of specificity in the intercalation reaction. (1) A different circular dichroism spectrum is seen depending upon the ratio of reporter molecules to nucleic acid base pairs in solution. (2) The binding constants decrease as the base pair-reporter concentration ratio drops. (3) The binding constants depend upon the base content of the nucleic acid as well as upon its sequence. In general, this class of molecules is found to be specific for A-T base pairs in the intercalation reaction.

INTRODUCTION

The determination of the fiber structure of deoxyribonucleic acid in 1953 by Watson and Crick[1,2] was undoubtedly one of the most significant breakthroughs of the century. To quote Watson himself,[3] "the gene was no longer a mysterious entity whose behavior could be investigated only by breeding experiments. Instead, it became a real molecular object about which chemists could think objectively in the same manner as smaller molecules." Their discovery generated a fantastic amount of research into not only the role of the nucleic acids in the mechanism of heredity but also the finer points of the structure itself. While the x-ray structure is indeed very significant, it must also be realized that DNA in aqueous solution is the real determinant of heredity in the living organism. It is the determination of the solution structure of nucleic acids that continues to busy countless researchers around the world. It is becoming increasingly clear that DNA is a very complex beast in solution, with eight different structures having been reported.[4] While the use of x-ray diffraction has been applied to DNA structure determination,[4,5,6] serious questions have been raised about the reliability of such techniques, as the fibers do not provide enough data points to unambiguously define a structure. Instead, a combination of model-building studies and x-ray data is used to fit a structure to the data. These techniques are undoubtedly open to question in many instances due to their indirectness.[7,8,9]

In short, less direct methods of probing the structure of nucleic acids in solution must, at least for the present, be depended upon. The x-ray structure should, however, be carefully considered as a sort of "jumping-off" point for the analysis of solution studies. Even a cursory examination of the original structure, subsequently refined by Wilkins,[10] reveals the delicately balanced forces at work which might be expected to cause complex changes in structure upon transfer to an aqueous environment.

Briefly, the model of Watson, Crick, and Wilkins consists of two helical arrays wound about a common axis with a right-handed sense. Two types of forces maintain this geometry and consist of hydrogen bonding between the complementary bases and hydrophobic stacking forces generated by the release of solvent molecules due to the clustering of bases in the nonpolar atmosphere of the helix interior. The gross structure, shown in Figure 1, thus has both vertical and horizontal stabilizing forces.

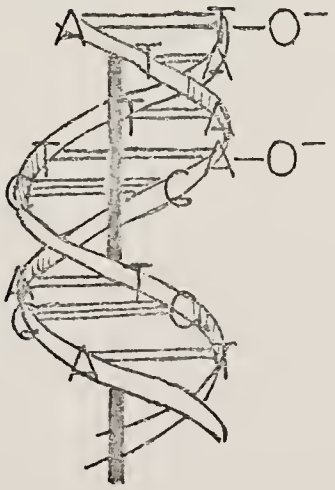

Figure 1. The DNA Double Helix. The vertical line is the helical axis, and the horizonital lines represent hydrogen bonds between bases.

The bases are somewhat complex in themselves, allowing for a keto-enol tautomerization equilibrium. The keto tautomers are used in the model, with the G-C and the A-T base pairs having, respectively, three and two hydrogen bonds. The model studies of Watson and Crick and also the chemically determined relations due to Chargaff[11] ruled out any but A-T and G-C base pairs. The connecting chains between bases consist of sugar phosphodiester links. The sugar moiety is D-deoxyribose and exists in the furanoside form with two hydroxyl groups at the 3' and 5' positions of the pentose ring. It was proven somewhat later that the two sugar phosphate chains are oriented antiparallel to each other.[12]

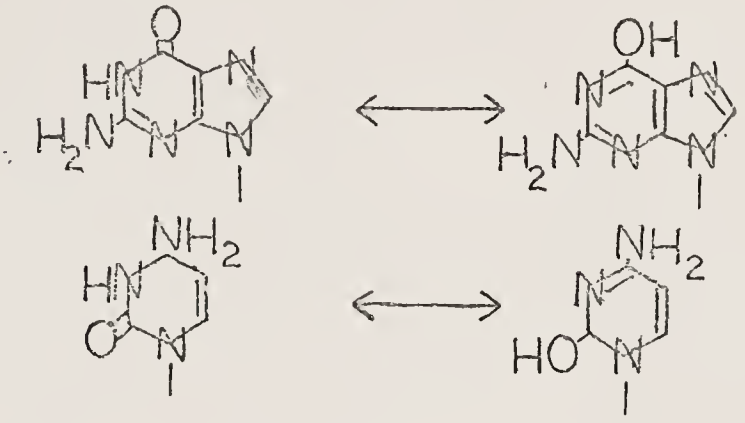

Figure 2. Keto-Enol Tautomers for the Bases Guanine and Cytosine.

Since the phosphodiesters are monoanions at physiological pH's and the interior of the helix is quite nonpolar, the charged oxygens are directed outward into the solution. They are not identical, however--the one being at right angles and the other being parallel to the helix axis. The charged nature of the phosphates is actually a destabilizing force, since the charge repulsion between phosphates is expected to be considerable. Due to the position of substitution of

the sugars on the bases, the distance from one phosphate chain to the other is not the same on both sides of the helix. In other words, a major (larger) groove and a minor (smaller) groove are created. The bases are oriented perpendicular to the axis of the helix, and the distance between bases is 3.4 angstroms since the pitch is 34 angstroms with ten bases per turn.[13]

It can be seen that a number of considerations enter into the possible consequences of transfer of this complex assemblage to an aqueous medium. Temperature, pH, counterions, relative humidity, and even the A-T/G-C ratio have been found to cause structural alteration to the DNA structure.[5,6] For example, it has been found that a number of A-T rich DNA's (e.g., Cl. perfringens, B. cereus) are quite different in the solution state from their structure in the fiber state. The pitch of the helix is at least 10 percent longer in the solution state.

Hydrogen Bonding Forces

While the geometrical constraints of colinear hydrogen bonds and hydrogen bonding lengths of 2.8-3.0 angstroms would allow for the formation of twenty-nine possible base pairs connected by two or three hydrogen bonds,[14,15] it has been found that even rather simple base derivatives exhibit surprising specificity in the hydrogen bonding schemes employed in practice. In fact, only three different schemes have been found in the crystal state. Calculations based on dipole-dipole interactions have shown that the Watson-Crick scheme is favored markedly for guanine-cytosine base pairing,[16] but adenosine-uracil pairs can exist in three forms, two of them of approximately equal energy. Indeed, two crystal structures have been found for substituted A-T base pairs. Cocrystals of 9-methyl adenine and 1-methyl thymine

have been found to assume the Hoogstein base-pairing scheme (Figure 3b).[17] It was postulated by these authors that this structure was not seen in

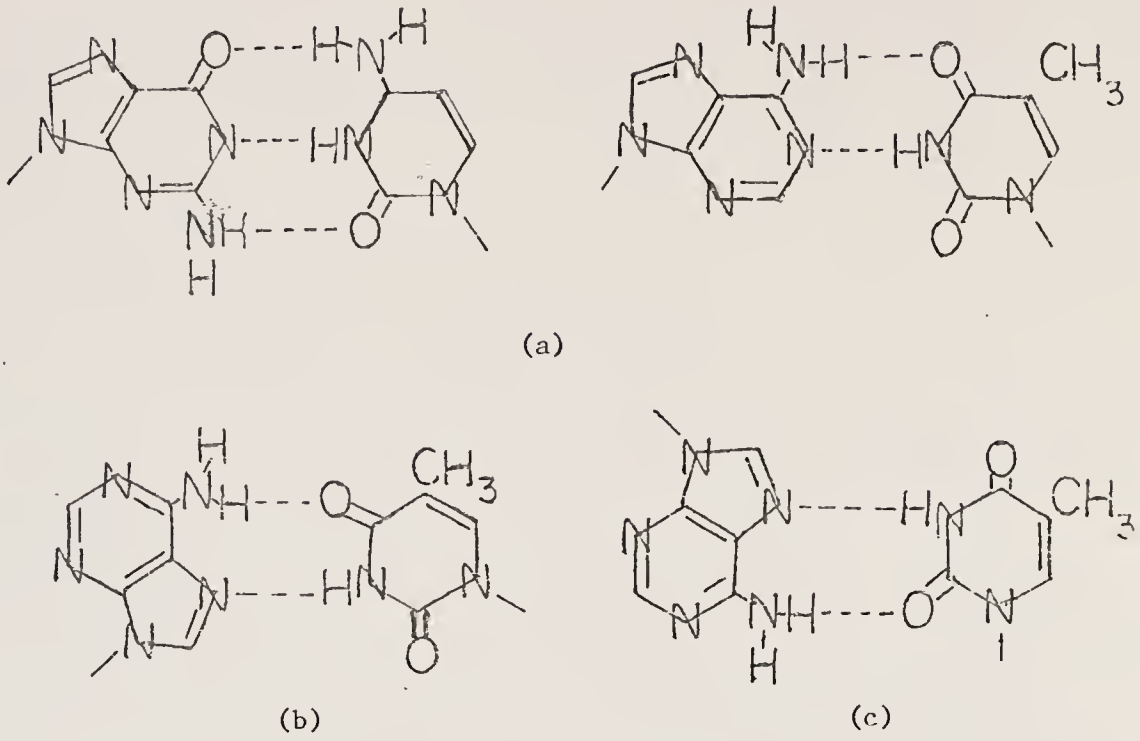

Figure 3. Base Pairing Schemes.

a) Adenine-thymine and guanine-cytosine Watson-Crick pairs.

b) Hoogstein adenine-thymine pair.

c) Anti-Hoogstein adenine-thymine pair.

nucleic acids due to the fact that the electrostatic repulsion between strands was lower in the Watson-Crick base-pairing scheme. This assertion was based on the fact that the two phosphodiester chains are farther apart in the Watson-Crick scheme than they are in the Hoogstein scheme. Further, adenosine and 5-bromouridine have been found to

assume the anti-Hoogstein base-pairing scheme (Figure 3c).[18,19] On the other hand, single crystals of guanine and cytosine have yielded only the expected Watson-Crick base-pairing scheme.[20,21] This may well be due to the fact that the Watson-Crick scheme has three hydrogen bonds while the others have only two. Hydrogen bonding also appears to be quite specific in the presence of aqueous solvent. It was found that when a given nucleoside was covalently attached to an insoluble support and a mixture of the other three nucleosides was passed through this modified support, only the complement to the covalently bound nucleoside was retarded.[22] In addition, elution of the column with aqueous urea instead of water abolished the association, thus strongly implicating hydrogen bonding as the force responsible for the very specific binding of the complementary nucleoside. Another study[23] utilized proton magnetic resonance in a variety of solvents to show that base pairing, as monitored by the downfield shift due to the decrease in electron density about the proton nucleus, decreases as the hydrogen bonding ability of the solvent increases. Still another study using proton magnetic resonance showed that the base pairing was quite specific.[24] The N-1 proton of guanosine was shifted drastically only when the complement cytosine was added, with little effect being seen upon addition of the other nucleosides. Likewise, the N-3 proton of uridine was shifted only in the presence of adenine. While these studies show that hydrogen bonding may be quite specific in organic solvents of various types, it is hard to imagine that hydrogen bonding plays the major part in stabilizing the double helical structure. In aqueous solution, the competition for the hydrogen bonding sites on the bases by water would minimize the importance of these forces. Further, though hydrogen bonding is quite specific in nonpolar solvents, it is known that these

same solvents cause the disruption of the double helix. The answer to the question of the importance of hydrogen bonding in the aqueous environment lies in the realization that the double helix has a nonpolar interior region where the bases are located. The aqueous solvent is excluded from this region due to the hydrophobic nature of the bases, thus making this region ideal for the formation of extensive hydrogen bonding.

Stacking Forces

A number of observations suggest that stacking interactions are the main force for stabilizing the double helix. First, it is known that the double helix can exist even in the presence of high concentrations of protons which might be expected to cause disruption of hydrogen bonding due to protonation of the amino groups on the bases. A lowered temperature to reduce the thermal motion is all that is necessary to maintain this structure. Vapor pressure studies by Ts'o and coworkers[25,26] showed that the bases do aggregate in water solution and that the association is not due to hydrogen bonding.[27] This type of interaction is quite complex, as shown by futher observations on these phenomena. Methylation of the bases increases the aggregation, while methylation of the sugar ring has no effect. However, if the purine nucleoside is modified by adding an amino group to the 6-position, stacking increases. Further, 5-bromouridine stacked better than the more hydrophobic thymidine. A correlation of base stacking ability with polarizability was noted by Hanlon.[28] Pmr has also been quite useful for further defining the stacking phenomenon. It was found that the ring protons of the bases experienced increased shielding as the concentration of the base was increased.[29] By measuring the differential shielding of the various positions of the aromatic systems of the bases, a geometry

was assigned to the stacked adenosine molecule.[30] The two possible arrangements are shown in Figure 4.

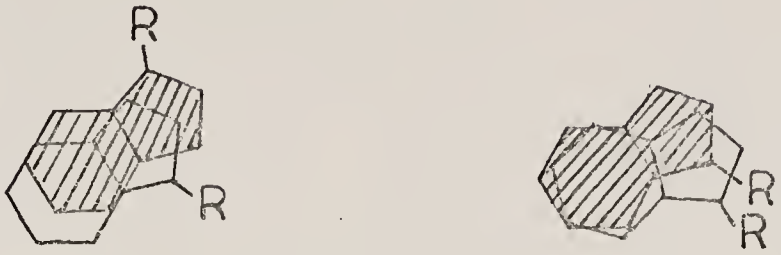

(a) (b)

Figure 4. Nucleoside Stacking Schemes.

a) Alternate Stack

b) Straight Stack.

Extension of these investigations to dinucleoside phosphates has provided further information on the details of the stacking interactions. Chan and Nelson[31] used pmr techniques to show that ApA exists in the 3'-anti-5'-anti right-handed stack. Further, striking differences have been observed from one dinucleoside phosphate to another regarding their stacking ability.[32] It was found that UpU lost its ordered structure readily upon elevation of the temperature, while ApA's structure persisted. This was explained as being due to differing solvation capabilities for the two dinucleoside phosphates.

The stacking phenomenon is also of marked importance in more complex systems. For example, single-stranded polynucleotides are highly structured at ambient temperatures, as seen by the observation that they possess a high degree of temperature-dependent hypochromism and optical activity.[33,34] Although originally thought to be due to hydrogen bonding, the structuring is now known to be due to base

stacking.[35,36] It was found that blockage of the hydrogen bonding sites in polyriboadenylic acid and polyribocytidylic acid did not abolish the temperature-dependent hypochromism and optical activity.[33,34] The evidence for stacking in the double-stranded nucleic acids will be discussed in a separate section, as the methods for observing these effects are not so straightforward.

Electrostatic Effects

The main destabilizing influence in the double helix is the presence of the phosphate-phosphate ionic repulsions. In fact, it is known that DNA spontaneously denatures if a minimum concentration of positive ions is not present to at least partially shield the negative charges from each other.[37] Additional light is shed on the importance of ionic interactions in the double-helical structures by the fact that thermal denaturation of single-stranded polynucleotides is not too dependent upon ionic strength,[38] but that of double-stranded polynucleotides is very dependent upon it.[39] This is reasonable, as the interactions between phosphates in the same chain do not change much upon going from the stacked structure to the random coil form. This is not to say that the intrachain repulsions are unimportant; it has been shown that increased salt causes the helix to decrease in length as evidenced by a decrease in the viscosity of the DNA solution.[40] This is presumably due to the decreased repulsion resulting from shielding of intrachain phosphates from each other, though neutralization of interstrand repulsions could also play a part.

Electronic Effects

That the nucleic acid bases interact with each other electronically is quite well known. The exciton theory[41-43] unifies a number of experimental results and states that, for molecular crystals, energy is not absorbed by a single molecule but is distributed over many molecules instead. If the ordered polynucleotide is considered a one-dimensional crystal, the exciton theory is applicable.

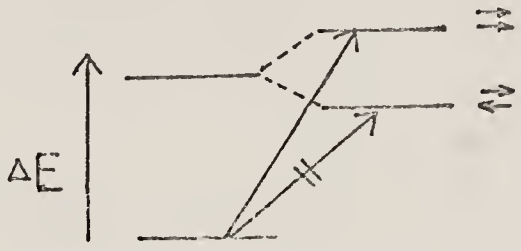

Figure 5. Exciton Coupling in DNA.

As seen in Figure 5, the excited state energy levels of the bases are considered to be split to produce two new levels. The lower energy transition has the electronic vectors of the bases antiparallel, while the higher energy transition has these vectors parallel. Quantum mechanical selection rules forbid the transition to the lower excited level, so the only transition seen is the one of higher energy than the original uncoupled transition. The absorption spectral maximum is thus shifted toward the blue end of the spectrum. Also seen is a hypochromic effect, with the intensity of the new transition being lower than that of the monomer. This fact is explained by the theory of intensity interchange of coupled transition moments and is illustrated in Figure 6.

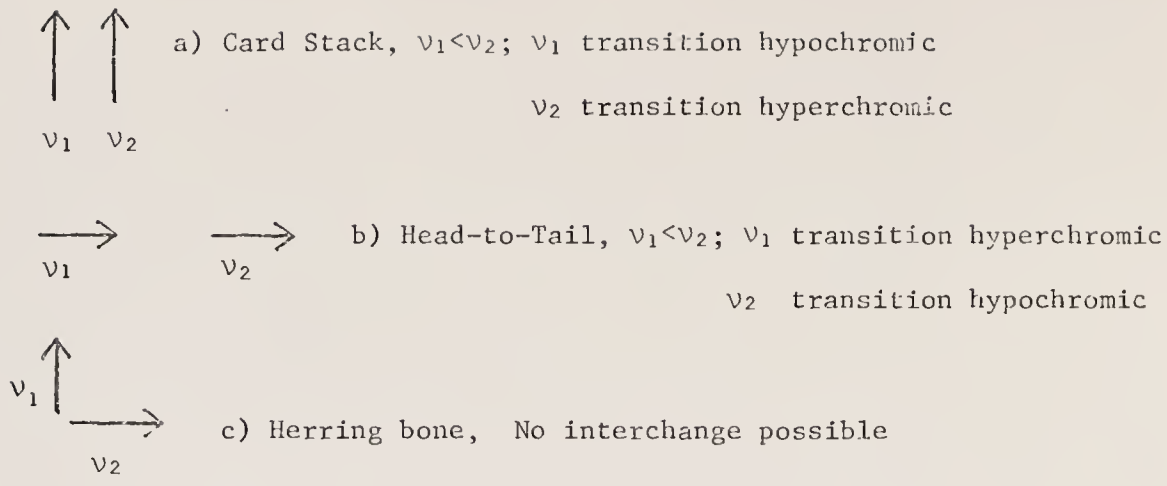

Figure 6. Intensity Interchange of Coupled Transition Moments.

If the transition moments are in a card stack orientation as put forth in the model, the higher energy transition is hyperchromic, and the lower energy transition is hypochromic. The technique of circular dichroism also demonstrates the theory to be true. Contrary to the situation in absorption spectroscopy, transitions to both the upper and the lower states are allowed by the pertinent selection rules. Thus, one sees both a red-shifted band and a blue-shifted band as compared to the absorption maximum of the monomer. The signs of the CD bands, however, cannot be predicted without the consideration of more complicated quantum mechanical arguments.[44] It may be stated, however, that the two transitions are found to be opposite in sign, thus yielding the very distinctive double Cotton effect for the polynucleotide.

Dynamic Structure of Nucleic Acids

Several lines of evidence point toward a rather remarkable quality associated with the double-helical polynucleotides. It appears

that the hydrogen-bonded base pairs are in a continual state of flux with respect to their non-hydrogen-bonded "open" forms. The work of von Hippel and coworkers,[45-47] utilizing the exchange-out of tritium label has established a firm basis for the existence of the "open" forms of the nucleic acids. Incubation of the nucleic acids in tritiated water and rapid separation of the labeled polynucleotide from excess radioactive solvent via gel filtration enabled these workers to show that the kinetics of exchange-out of the label were much faster than for protein systems. Further, it can be shown that the observable exchange is taking place with the protons involved in the base-base hydrogen bonding of the double helix. Three possible models were examined by McConnell and von Hippel.[46] These were (1) unstacking without hydrogen bond breakage, (2) hydrogen bond breakage without unstacking, and (3) hydrogen bond breakage with partial or complete unstacking and strand separation. These alternatives are shown in Figure 7.

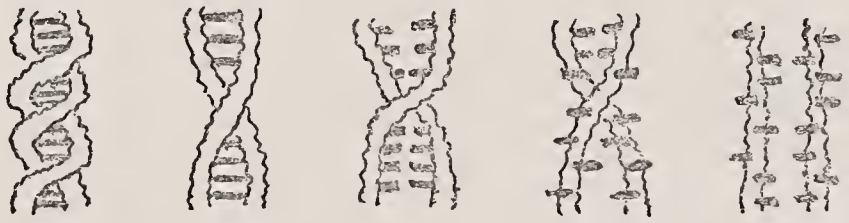

Figure 7. Possible Open Conformations of DNA.

a) Stacked and hydrogen-bonded double helix,

b) Unstacked without hydrogen bond breakage,

c) Hydrogen bond breakage without unstacking,

d) Hydrogen bond breakage and unstacking with partial strand separation,

e) Complete strand separation.

The evidence gathered from studies utilizing helix-destabilizing salts such as sodium perchlorate indicated that there exist two possible open states for the exchange reaction, a stacked one and an unstacked one. At temperatures far below the melting temperature of the double helix, the open state induced by thermally caused twisting and unwinding of the strands relative to each other provides the exchange intermediate. Since unstacking is minimized, little energy is required for this process. If, however, the difference between the melting temperature and the temperature used for the exchange is less than twenty Centigrade degrees, the stacked form appears to be rapidly and cooperatively formed and begins to dominate the exchange process. The use of large concentrations of destabilizing salts was found to have the same effect as raising the temperature at which the exchange was carried out. The implication of the destabilizing salts in the disruption of the stacking interactions between the bases is fairly well grounded. For example, Robinson and Grant[48] showed that the solubility of the bases in water was increased in the presence of these salts in direct proportion to their effect on the melting temperature of nucleic acids.

The form characterized by minimal unstacking also was shown to be in equilibrium with the "propped" form which owes its existence to mismatched hydrogen bonding sites caused by protonation or deprotonation in the presence of added acid or base. These propped forms are shown in Figure 8. Several studies[46,49,50] have shown that DNA can suffer extensive protonation without an accompanying increase in hyperchromism. This indicates that the unstacking is minimal.

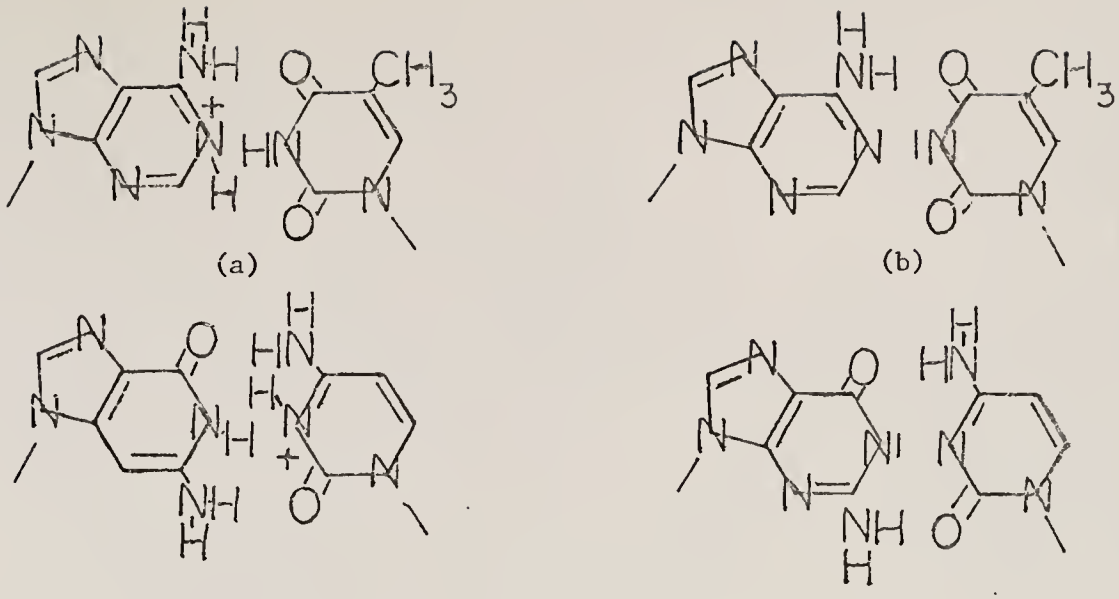

Figure 8. Propped Base Pairs at a) Low pH and b) High pH.

Another method of establishing the existence of open forms of the nucleic acids is based on the fact that formaldehyde reacts with the single strands at a much faster rate than with the native double helical form. Haselkorn and Doty[51] established that the activation energy of the reaction with the double helix was much greater than the energy needed for the formylation of the single strands of denatured DNA. They postulated that the helix had to be denatured before reaction could take place. Von Hippel and Wong[52] subsequently analyzed this reaction in detail and found that the comparison of reaction rates for native and denatured DNA enabled them to separate the reaction into a conformational alteration and a subsequent chemical reaction. The difference in activation energy between the two was attributed to the conformational alteration as denatured DNA does not have this added barrier to cross. Via this method, an estimate of nine base pairs was advanced as the size of the "opening unit."

Further studies which are not unrelated have to do with the mode of action of the antibiotic actinomycin. The structure of this drug is shown in Figure 9. In a very thorough study, Mueller and Crothers[53] used a host of different physical techniques to delineate the forces at work in the complex of actinomycin and DNA. It was found that the very bulky molecule was intercalated between base pairs of the nucleic acid. Further, the nucleic acid was postulated to be altered in conformation as a result of the complexation. It was shown that the kinetics scheme was very complex, with several rate constants observable in both the forward and reverse reactions. In addition, the possibility of specific electronic interactions was considered by investigation of the binding behavior with a number of different aromatic systems. It was found that such specificity does indeed exist, and very subtle alterations to the aromatic nucleus could drastically alter the affinity for the antibiotic.

The Small Molecule Approach

The question naturally arises as to how one goes about investigating the properties of a molecule as large and complex as DNA or a large protein. The technique of attaching an innocuous and easily monitored probe to these large molecules was pioneered by Koshland,[54,55] who attached a p-nitrophenol group to the enzyme chymotrypsin. He was able to draw conclusions regarding the enzyme conformation by monitoring the concomitant spectral changes of the p-nitrophenol chromophore. This technique has been applied to the problem of nucleic acid solution structure by Gabbay and coworkers.[56-59] Figure 10 illustrates the general type of molecules utilized in these studies. It is actually a diammonium salt substituted with a planar group capable of intercalation.

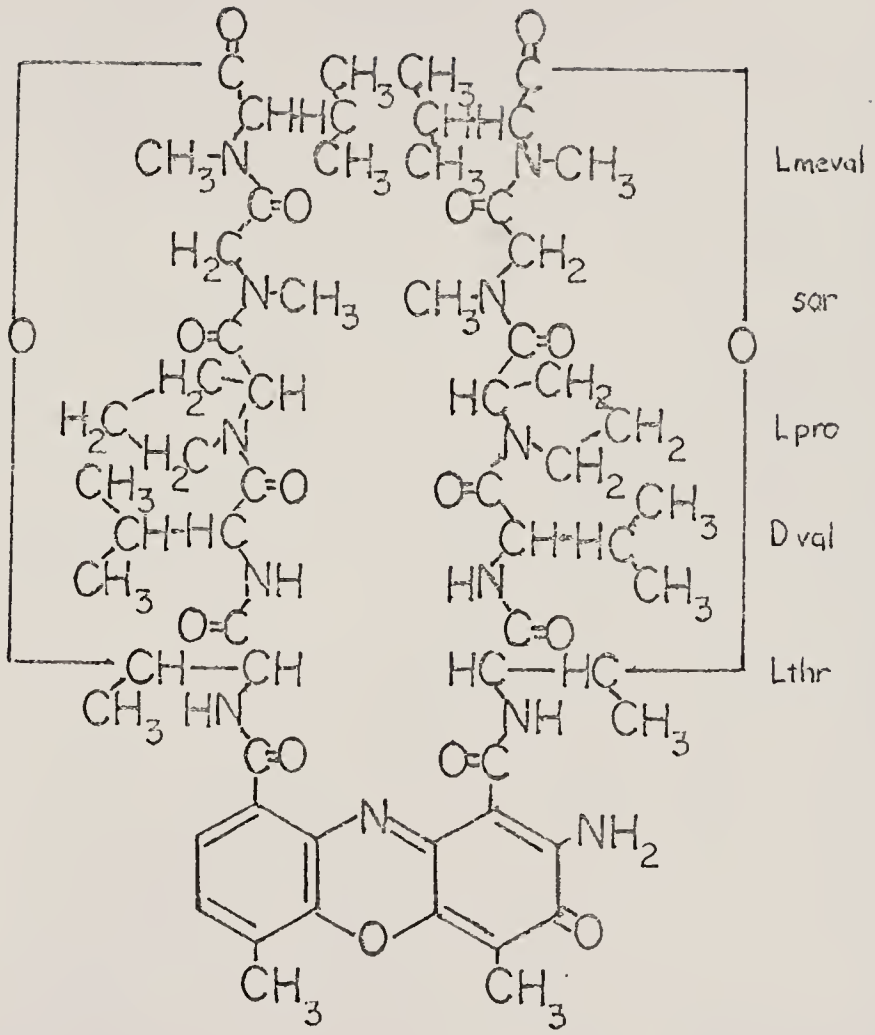

Figure 9. Structure of Actinomycin D.

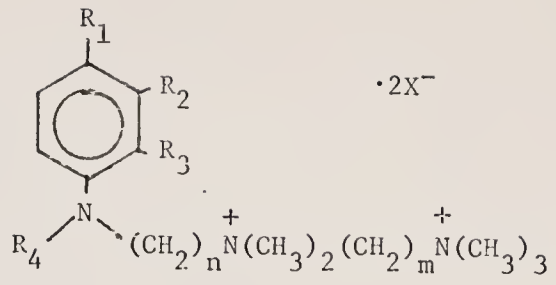

Figure 10. Intercalating Reporter Molecule.

This process will be discussed later in detail, but it essentially consists of inserting the planar aromatic system between the base pairs of the nucleic acid. The design of these molecules was based on the extensive investigations into the interactions of simple diammonium salts with nucleic acids. These simple salts were found[60] to stabilize the double helix with respect to the thermal melting into two separate strands. Gabbay [61,62] studied these interactions in detail and found that the salts were bound to adjacent phosphate anions on the same strand. This conclusion was based on several lines of evidence. First, maximum stabilization against thermal denaturation of the nucleic acid double helix is found at n = 3 for the salts $H_3\overset{+}{N}(CH_2)_n\overset{+}{N}H_3 \cdot 2\ Cl^-$. If, however, the ammonium protons are replaced by various alkyl groups, the maximum stabilization effect occurs at n = 2. In addition, both the simple diammonium salts and the alkylated derivatives were found to inhibit the RNAse-catalyzed hydrolysis of single-stranded polyribonucleotides. The effect was again maximized at n = 3 for the simple salts and at n = 2 for the alkylated derivatives. These results are consistent with binding to adjacent phosphates on the same strand. In the alkylated derivatives, the steric requirements introduced by the bulky groups on

each end would force the molecule to be fully extended, while the simple salts might be expected to be somewhat more compact. The fully extended distance between the two positive charges for the case where n = 2 agrees very closely with the intrastrand phosphate-phosphate distance, while the interstrand phosphate-phosphate distance is much too large for effective binding.

This type of molecule was further modified by Gabbay[56,57,59] to include the aromatic chromophore, and it was found to have very interesting properties. The added interactions were seen to be those typical of an intercalated system. Dyes such as acridine orange and proflavine have been postulated to bind to nucleic acids by an intercalation mechanism involving insertion of the planar dye molecule between the base pairs of the nucleic acid.[63] A number of observations suggested this mechanism. Flow dichroism and polarized fluorescence studies indicated that the dyes were lying at right angles to the helical axis. The viscosity of the complex solution might be expected to increase due to the expansion in the length of the nucleic acid required to accomodate the dye molecule, and this is found to be the case.[63,64] X-ray studies also show the mass per unit length of the complex is less than that of the nucleic acid alone.[65] Since the density of the intercalated molecule is greater than that of the solvent which may be displaced, the only possible explanation is that the polynucleotide has been extended.

In the case of the reporter molecules, the expected viscosity increase is also seen.[66] In addition, an abundance of other data also supports the intercalation model. First, the visible spectrum of the reporter is drastically altered in the presence of nucleic acids, with the expected red shift and hypochromic effect both being in evidence. The hypochromic effect is explained by the intensity interchange

theory discussed previously, with the transition moment of the reporter being coupled to the transition moments of the nucleic acid bases adjacent to it. The red shift is caused by the presence of nearby negatively charged phosphate groups of the nucleic acid. It was shown by Gabbay [56] that a positive charge placed near the aromatic system of the reporter molecule caused a blue shift in the spectrum, so the presence of a negative charge might be expected to counteract this effect and cause a red shift in the absorbance maximum. Pmr studies[67] show complete broadening of the ring protons of the reporter, but sharpening of the signals results upon raising the temperature. The resonances in the spectrum obtained at elevated temperatures remain shifted upfield, indicating that the reporter is still bound to the nucleic acid. The nucleic acids, being quite large, tumble very slowly, and the local magnetic fields about the protons of the small molecule are not effectively averaged. This behavior is well grounded in theory, and it was used by Fischer and Jardetsky[68] to determine the portions of the small molecule (penicillin G in their case) which were involved in the binding to the large molecule (bovine serum albumin). By noting the portions of the small molecule's pmr spectrum which were broadened the most by the presence of the larger molecule, the binding site could be established. Likewise, all the protons of the DNA molecule itself are broadened due to the very rigid structure.[69] The upfield shift is due to the ring current effect of the DNA bases above and below the reporter as shown in Figure 11.

By far the most detailed evidence on the reporter-nucleic acid interaction was the result of circular dichroism studies by Gabbay[56,59] The reporter molecules do not exhibit optical activity of

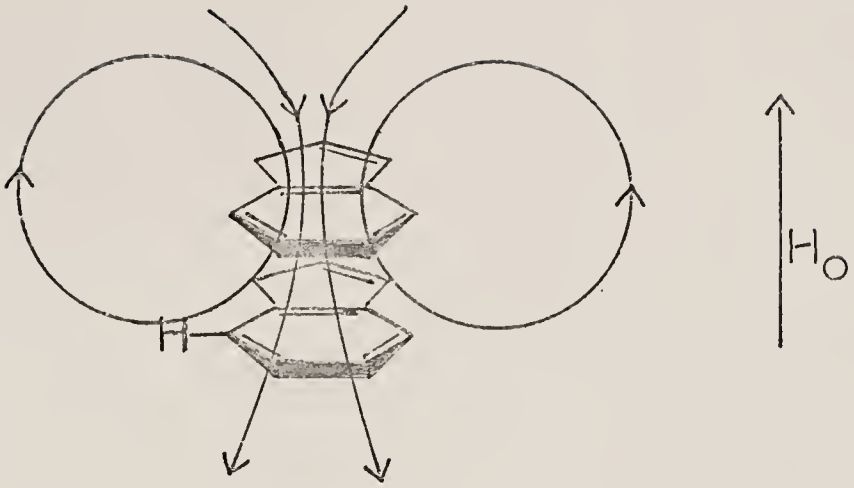

Figure 11. Ring Current Effect of Aromatic Systems.

their own, but the presence of the asymmetric binding site in nucleic acids causes an induced optical activity. Due to the fact that the sign of the induced CD effect differed between the DNA complex and the RNA complex, it was postulated that two different geometries were being seen. These are pictured below in Figure 12. The intercalation was postulated to take place from the minor groove of the nucleic acids

IN OUT

Figure 12. Schematic Representation of Intercalation Geometries.
$R=(CH_2)_2\overset{+}{N}(CH_3)_2(CH_2)_3\overset{+}{N}(CH_3)_3 \cdot 2Br^-$

for several reasons. The major groove of the DNA molecule contains the methyl groups of thymine, and the minor groove of RNA contains the

added 2'-hydroxyl group of the ribose sugar system. Thus, the in geometry could only logically be assumed to be in the minor groove of DNA, which is less hindered than the minor groove of RNA. Further evidence resulted from consideration of the molecule shown in Figure 13. This system possesses two distinct transitions, the 4-nitroaniline at 440 nm and the naphthylamine at 322 nm. With DNA, both transitions

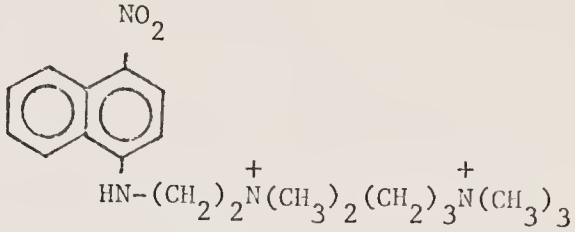

Figure 13. Reporter Molecule.

were made optically active and yielded a CD signal. With RNA, however, only the nitroaniline transition was made optically active, thus suggesting that the fused phenyl ring points in in the DNA complex and out in the RNA complex.

Some additional evidence regarding the intercalation model is of an intuitive nature and relies on the idea that only so "thick" a molecule can be expected to fit into the "niche" in the nucleic acid. Indeed, molecules 1 and 2 below in Figure 14 were made by Gabbay and coworkers[70,71] and found not to intercalate, though they were found to be bound to the nucleic acids.

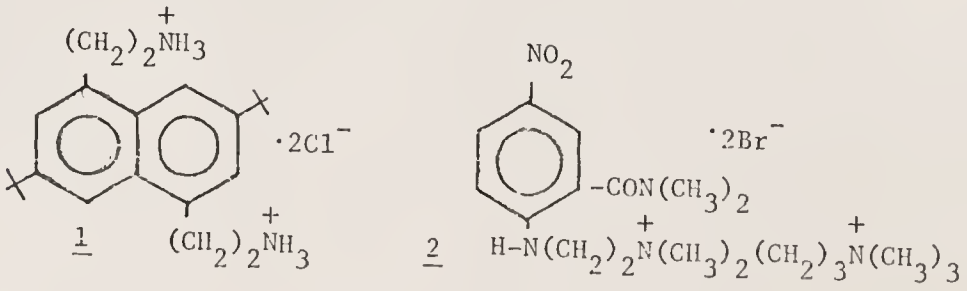

Figure 14. Molecules Incapable of Intercalation.

It has also been shown that the reporter molecules are capable of exhibiting a certain degree of specificity. Gabbay and Gaffney[59] were able to show that the magnitude of the induced CD signal was a function of the base content of the nucleic acid. While these results could be due to steric hindrance by the third hydrogen bond of the G-C rich DNA's, it is also possible to invoke more sophisticated interactions such as electronic energy differences among the different intercalating sites. Another case in point deals with the methods whereby proteins selectively interact with nucleic acids. It has been shown that aromatic amino acids are capable of intercalation between base pairs of the nucleic acids. Specifically, it has been shown that the aromatic amino acids cause destacking of the polyadenylic acid molecule as evidenced by downfield shifts for the protons of the adenine residues upon complexation.[72] Both pmr data and the fact that the 280 nm peak in the circular dichroism spectrum of the polynucleotide decreased in magnitude, indicating some destacking, were used to demonstrate intercalation by tyramine, tyrosine, and tryptamine.[73,74] That the intercalation of aromatic residues of a protein may contribute to the selectivity exhibited by such molecules in their interactions with nucleic acids is quite an intriguing suggestion. Indeed, detailed studies with a large number of di- and tripeptide systems have indicated that specificity may be influenced by the inclusion of aromatic amino acids in the peptide system.[75]

Statement of Problem I

As stated previously, several lines of evidence make it clear that "open" forms of the nucleic acids exist at temperatures far below the melting temperature. In addition, the studies on actinomycin point

to the fact that even very large aromatic systems with quite bulky substituents can be bound to nucleic acid systems via an intercalation mechanism. Further, the possibility of specificity derived from the stacking interactions in an intercalated complex has been demonstrated. From consideration of these facts, it is quite apparent that these open forms could be quite important for a number of biologically important processes. Since the bases of the nucleic acid are much more available to solvent, other small molecules may also be able to interact in a much more intimate and specific way with the macromolecule. Carrying this theme a bit farther, the open form could be very sequence dependent in its opening reaction or its geometry. Indeed, a very obvious way to study such forms is to use the small probe approach so successfully applied to other facets of the nucleic acid solution structure problem. Unfortunately, the open forms are expected to be present in very small amounts. Thus, methods which judge various structures only in proportion to their relative amounts are not too useful. Any effects due to the open structures will be swamped out by the very large excess of "normal" forms. All of the methods discussed previously fall into this class. One must use probes specific for the open forms alone. The molecules in Figure 15 were made by Gabbay and Baxter[76] and shown to behave in this manner. Due to the fact that the distance between the side chains of I is 11.2 angstroms, both side chains cannot fit into one groove of the nucleic acid. Any intercalated complex would necessitate having one side chain in each groove of the nucleic acid for this reason. Since it has already been mentioned that bulky groups prevent intercalation between the base pairs, it is concluded that local opening of the intact double helix must occur prior to intercalation. The molecule II serves as a

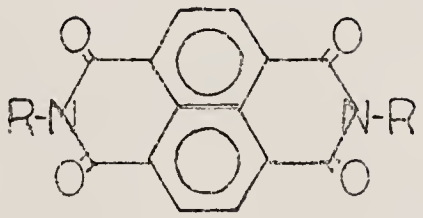

I

3 $R=(CH_2)_2\overset{+}{N}(CH_3)_2C_7H_7$

4 $R=(CH_2)_2\overset{+}{N}(CH_3)_2C_3H_7$

5 $R=(CH_2)_2\overset{+}{N}H(CH_3)_2$

6 $R=(CH_2)_2NH(C_2H_5)_2$

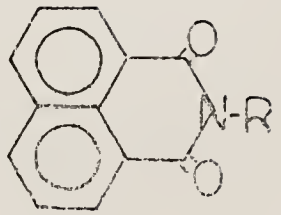

II

7 $R=(CH_2)_2\overset{+}{N}(CH_3)_2(CH_2)_3\overset{+}{N}(CH_3)_3$

Figure 15. Reporter Molecules Used in Kinetic Studies.

standard, as it has a very similar planar system; it can, however, be intercalated in the usual manner. A detailed kinetic investigation was undertaken to gain a better understanding of the possible specificity involved in the opening reaction of nucleic acids. To this end, both the reporter molecule and the nucleic acid component were perturbed in a number of ways to delineate the factors important in these interactions.

Statement of Problem II

Since little is known about what factors are responsible for intercalation specificity either in terms of the small molecule or the nucleic acid component, a detailed study of a large number of variously substituted reporters was launched. The molecules were all p-nitroanilines as shown in Figure 16, but R_1,R_2,R_3, and n were varied. The standard methods of investigation for such probes were utilized and included ultraviolet-visible spectroscopy, pmr, viscosity measurements, CD, melting curves, and direct binding studies. The nucleic acid component was also varied to investigate the possibility of specificity due to base sequence and base content.

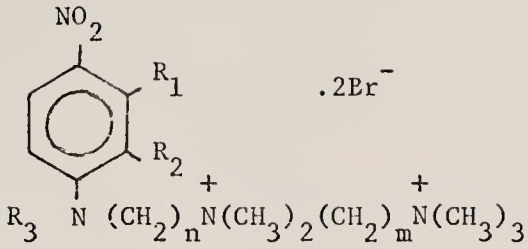

III

Reporter	R_1	R_2	R_3	n	m
8	H	NO_2	H	2	3
9	H	NO_2	CH_3	2	3
10	H	NO_2	C_2H_5	2	3
11	H	NO_2	C_6H_{11}	2	3
12	H	H	H	2	3
13	H	H	CH_3	2	3
14	H	CN	H	2	3
15	H	CH_3	H	2	3
16	CH_3	H	H	2	3
17	H	CF_3	H	2	3
18	H	CF_3	H	3	3
19	H	NO_2	H	2	3
20	H	H	C_6H_{11}	2	3

Figure 16. Substituted Reporter Molecules.

RESULTS AND DISCUSSION-PART I

A new class of reporter molecules has been utilized to probe the dynamic aspects of nucleic acid conformation in aqueous solution. These molecules are illustrated in Figure 15. Both the 1,8-napthylimide 7 and the 1,8,4,5-naphthyldiimides 3-6 were found to exhibit physical properties characteristic of an intercalated molecule in the presence of nucleic acids. Intercalation consists of inserting a planar aromatic system between the base pairs of a nucleic acid and has been shown to occur with a number of systems such as acridine orange, proflavine, and ethidium bromide.[40,63,64] Several lines of evidence in support of an intercalation mechanism for the binding of molecules 3-7 to nucleic acids are discussed below.

Proton Magnetic Resonance Studies (Pmr)

The pmr spectra for complexes of both 3 and 7 with salmon sperm DNA were found to be completely broadened and indistinguishable from baseline noise.[76] Raising the temperature as high as 90°C did not cause the signals to reappear. This broadening effect is explained as being due to the very slow tumbling rates of the reporters bound to the large nucleic acid molecule.[77] If the rate of tumbling of molecules in solution is lower than the typical Larmor frequencies W_0 (of the order of 10^8-10^9 radians sec^{-1} for protons in the conventional magnetic field), then T_2, the transverse relaxation time, is considerably diminished, leading to substantial line broadening of the proton signal. This situation is obtained if the proton is contained in a

rigid macromolecule, e.g., DNA, or if the proton is contained in a slowly tumbling small molecule bound to a macromolecule.

Simple external ionic binding of the reporters to the nucleic acid phosphates would not explain the broadened signals, as the tumbling rate would not be sufficiently lowered.[71] Only binding of a type causing very restricted tumbling, such as an intercalation process, can account for the results.

Circular Dichroism Studies

Both molecule 3 and molecule 7 exhibit pronounced induced circular dichroism effects in the presence of nucleic acids. Table 1 shows the results of circular dichroism studies on the complexes of both 3 and 7 with several nucleic acids, and Figure 17 shows the entire induced circular dichroism spectrum for salmon sperm DNA complexes of 3 and 7. Since these molecules have no optical activity of their own, the induced CD effect is attributed to the highly asymmetric binding site in the nucleic acid double helix.

The data shown in Table 1 indicate that the induced CD in the absorption band of 7 is not as sensitive to changes in the nucleic acid used as the induced CD in the absorption band of 3. The shape of the CD curve remains the same for complexes of 7 with salmon sperm DNA, poly rI-poly rC, and poly rA-poly rU and consists of a trough at 312-325 nm and a peak at 355-360 nm. The molar ellipticity value, however, seems to be somewhat higher for the poly rA-poly rU complex than for the other complexes. With the complexes involving 3, however, the CD spectrum depends to a much greater degree upon the identity of the nucleic acid used. For example, the induced CD of salmon sperm DNA·3 complex exhibits two troughs, one at 355 nm ($[\theta]_M = -5.47 \times 10^3$) and

Table 1

Summary of Induced Circular Dichroism Spectra for Nucleic Acid Complexes of 3 and 7.[a]

Complex[b]	λ^t	$[\theta]^t_M \times 10^{-3}$	λ^p	$[\theta]^p_M \times 10^{-3}$
poly rI-poly rC·3	408	-1.63	319	6.25
poly rA-poly rU·3	365	-8.50		
salmon sperm DNA·3	355 407	-5.47 -0.83		
poly rI-poly rC·7	325	-1.63	360	3.25
poly rA-poly rU·7	321	-7.25	355	2.25
salmon sperm DNA·7	312	-1.50	357	1.83

[a] Experiments were carried out in 0.01 M MES (pH 6.2, 0.005 M in Na^+) at ambient temperature.

[b] Experiments with poly rI-poly rC and poly rA-poly rU were carried out at base pair to reporter concentration ratios and nucleic acid concentrations of 15.6 and 1.0 x 10^{-3} M P/1, and those with salmon sperm DNA were carried out at a base pair to reporter concentration ratio of 16.4 and a nucleic acid concentration of 1.9 x 10^{-3} M P/1.

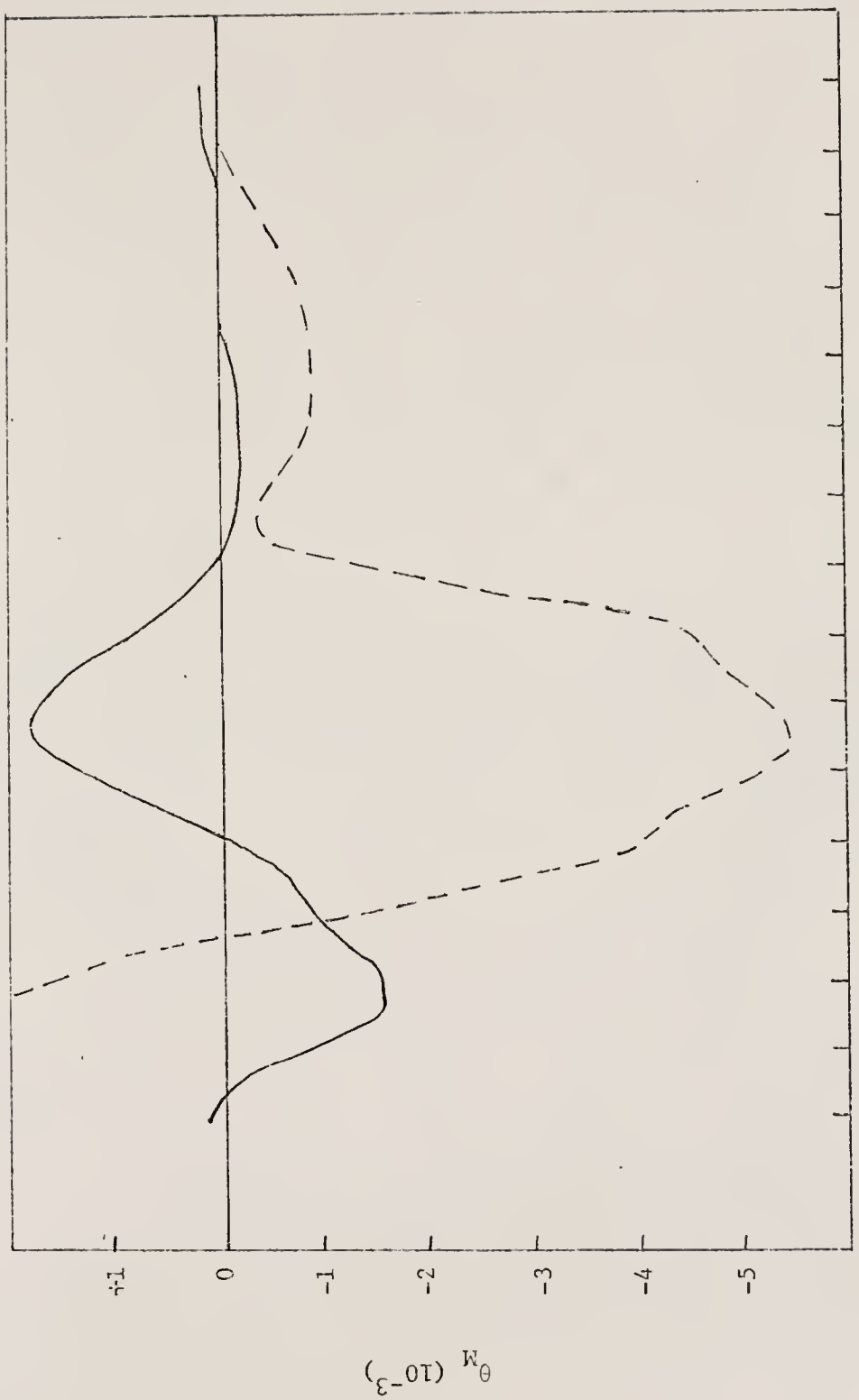

Figure 17. Circular Dichroism Spectra of Salmon Sperm DNA Complexes of 3 (---) and 7 (——). Experiments were done in 0.01 M MES (pH 6.2, 0.005 M in Na^+) at a base pair to reporter ratio of 16.4 and a DNA concentration of 1.92×10^{-3} M P/l.

another at 407 nm ($[\theta]_M = -0.83 \times 10^3$), while the poly rA-poly rU·3 complex exhibits a single trough at 365 nm ($[\theta]_M = -8.50 \times 10^3$) and the poly rI-poly rC·3 complex exhibits a peak at 319 nm ($[\theta]_M = 6.25 \times 10^3$) and a trough at 365 nm ($[\theta]_M = -1.63 \times -10^3$). The detailed interpretation of these results is rather difficult due to the fact that the CD effect depends on both the magnitude of the interacting transition moments and their relative directions. The only conclusions possible are that intercalation is strongly suggested and molecule 3 may be more able to discriminate among nucleic acids than is molecule 7.

Viscosity Studies

Viscosity studies also support an intercalation model for the complexes of molecules 3 and 7 with nucleic acids. DNA is a long rigid rod-like molecule, and the viscosity of a DNA solution is a function of the length of the molecule. Since intercalation involves the insertion of an aromatic residue between base pairs, the helix must unwind and increase in length for this process to take place. Passero et al.[66] showed that this effect was present in the formation of a number of nucleic acid-reporter complexes and used this as partial proof for intercalation.

The effect on the viscosity of a salmon sperm DNA solution observed upon adding increments of either 3 or 7 was studied, and the results are shown in Figure 18. The relative specific viscosity ($\eta_{sp}^{complex}/\eta_{sp}^{DNA}$) increases with increasing concentration of the reporters and levels off at base pair to reporter concentration ratios of 2.30 and 1.74 for reporters 7 and 3, respectively.

Visible Spectral Studies

The visible spectra of molecules 3 and 7 were determined in both the presence and the absence of a number of nucleic acids. Figures

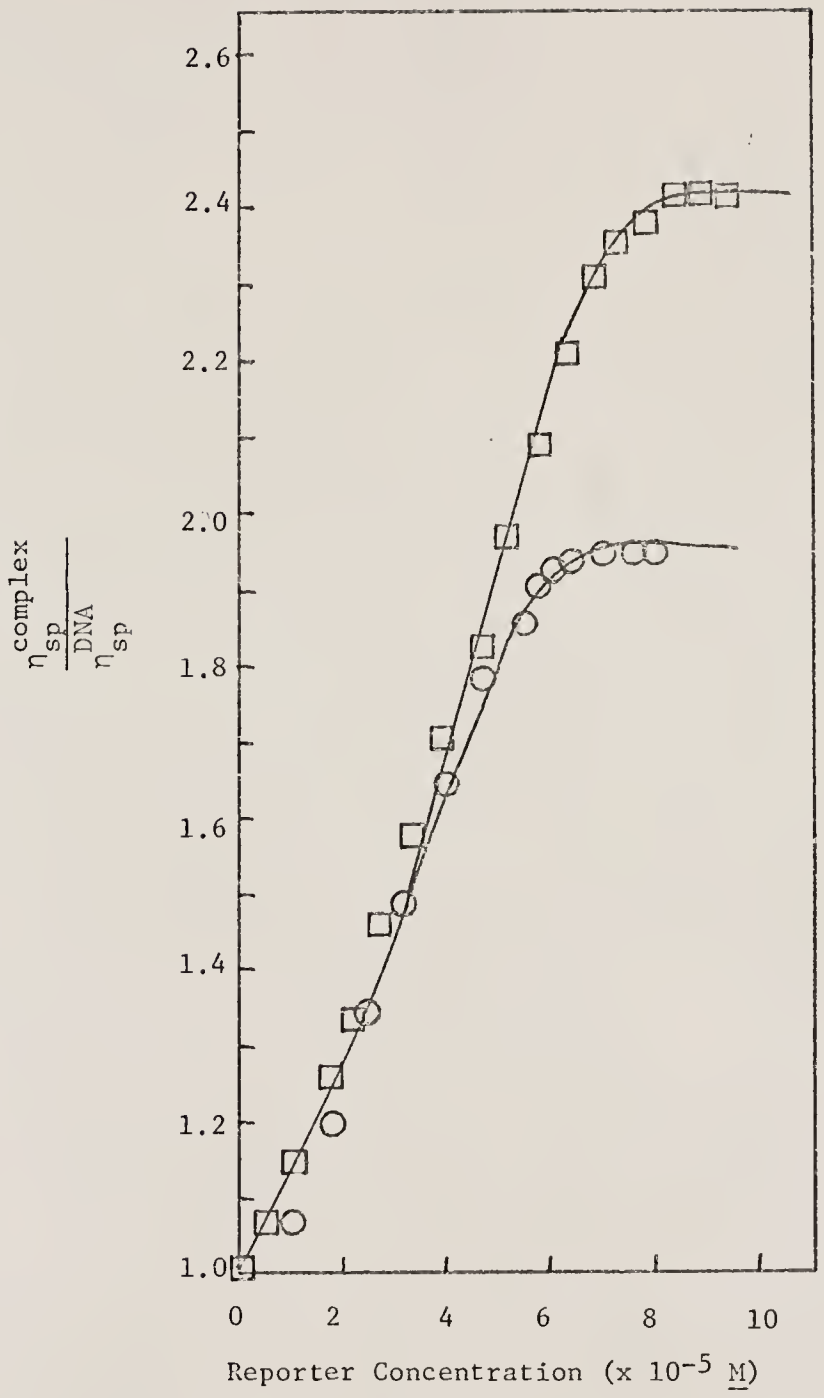

Figure 18. Viscometric Titrations of Salmon Sperm DNA with 3 (□—□) and 7 (○—○). Experiments were done in 0.01 M MES (pH 6.2, 0.005 M in Na^+) at 37°C. DNA concentration was 2.65×10^{-4} M P/l.

19 and 20 show the results for salmon sperm DNA complexes of 3 and 7, respectively, and Table 2 shows the absorption maxima and molar absorptivities for all systems studied. It is seen (Figures 19 and 20) that the presence of the nucleic acid causes a dramatic decrease in the intensity of the observed transition for both 3 and 7. The percent hypochromicity (%H = $[\varepsilon_{max}^{buffer}/\varepsilon_{max}^{DNA} - 1]100\%$) varies from 110-171% for the complexes of 3, while the values for the complexes of 7 vary over a wider range. The values for the complexes of 7 with poly rI-poly rC and poly rA-poly rU are 36% and 42%, respectively, while the values obtained with other nucleic acids are approximately the same as those for the corresponding complexes of 3. The lower intensities for the transition of the complexes as compared to that of the free reporter are predicted by the intensity interchange theory discussed previously. Since the reporter transitions are of lower energy than those of the nucleic acid bases to which they are coupled, the card stack geometry postulated for the intercalated complex implies that the reporter transition will be decreased in intensity upon formation of the complex.[41-43]

Another point worthy of note is the charge transfer band at the low energy end of the spectra shown in Figures 19 and 20. This type of band may be due to electron transfer between the pi system of the reporter and that of the nucleic acid bases.[78] The stacked geometry postulated for the intercalated complex would allow for this kind of interaction between the closely stacked pi systems of the two molecules involved.

Equilibrium Dialysis Studies

Equilibrium dialysis binding studies were performed on molecules 3-7 with a number of different nucleic acid systems, and the results are shown in Table 3. This method does not yield information on the

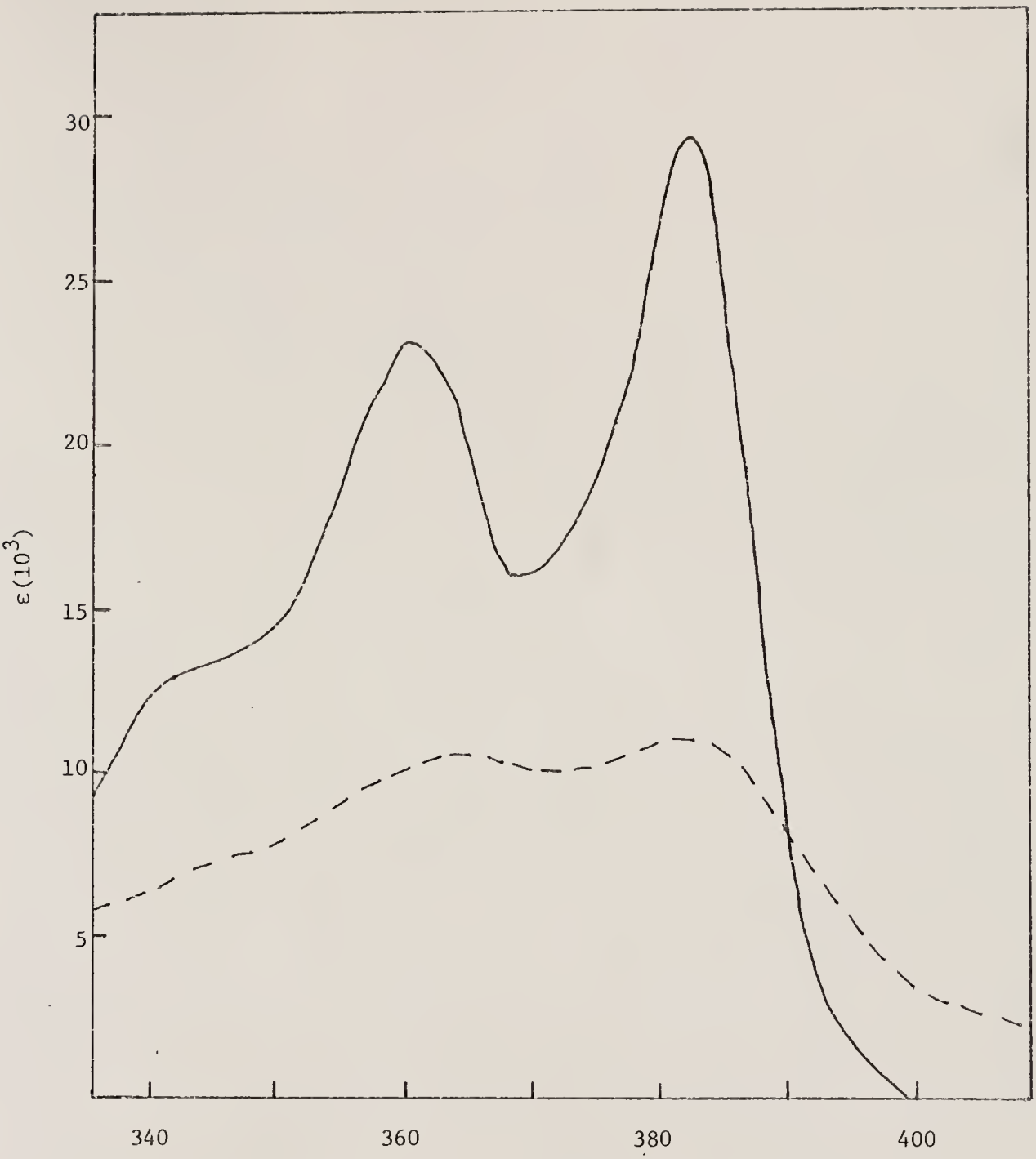

Figure 19. The Effect of DNA on the Absorption Spectrum of 3. Studies were done using 3.2×10^{-5} M 3 in 0.01 M MES (pH 6.2, 0.005 M in Na^+) in the presence (---) and absence (___) of 1.8×10^{-3} M P/1 salmon sperm DNA.

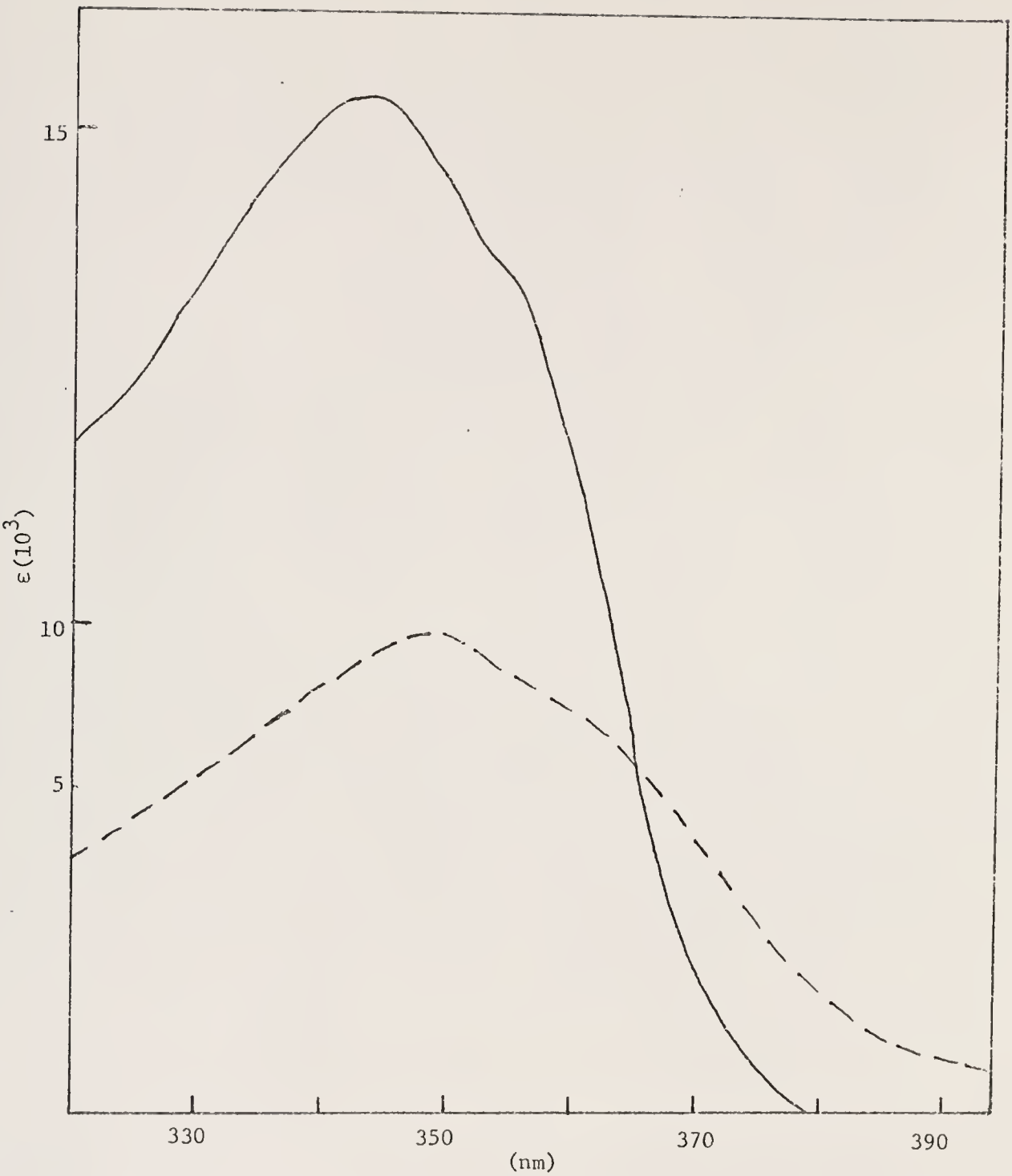

Figure 20. The Effect of DNA on the Absorption Spectrum of 7. Studies were done using 6.7×10^{-5} M & in 0.01 M MES (pH 6.2, 0.005 M in Na^+) in the presence (---) and absence (___) of 1.8×10^{-3} M P/1 salmon sperm DNA.

Table 2

Summary of Absorption Spectra of 3 and 7 in Buffer, 95% Ethanol, and Nucleic Acid Solutions[a]

Reporter	H_2O-Buffer		95% Ethanol		Salmon Sperm DNA[b]		
	λ^{max} (nm)	ε^{max}	λ^{max} (nm)	ε^{max}	λ^{max} (nm)	ε^{max}	%H
3	381	29700	381	22500	381	10950	159
7	344	12480	342	12100	348	5670	120

	Poly dAT-poly dAT[c]			Poly dG-poly dC[d]			Poly rA-poly rU[e]		
	λ^{max} (nm)	ε^{max}	%H	λ^{max} (nm)	ε^{max}	%H	λ^{max} (nm)	ε^{max}	%H
3	381	11700	149	384	12040	144	382	12610	130
7	347	6360	114	347	7610	78	353	11790	42

	Poly rI-poly rC[e]		
	λ^{max} (nm)	ε^{max}	%H
3	382	13750	110
7	353	12320	36

[a]Spectra were determined at ambient temperature in 0.01 M MES (pH 6.2, 0.005 M in Na^+). [b]Experiments done at a base pair to reporter ratio of 28 and a nucleic acid concentration of 1.8×10^{-3} M P/l. [c]Experiments done at a base pair to reporter ratio of 9.6 and a nucleic acid concentration of 7.6×10^{-5} M P/l. [d]Experiments done at a base pair to reporter ratio of 6.8 and a nucleic acid concentration of 1.1×10^{-4} M P/l. [e]Experiments done at a base pair to reporter ratio of 89 and a nucleic acid concentration of 1.0×10^{-3} M P/l.

Table 3

Equilibrium Dialysis Binding Studies for Molecules 3-7 with Nucleic Acids of Varying Base Constent.[a]

Nucleic Acid (conc. x 10^{-4} M P/l)	Reporter	Binding Constant[b]
Salmon Sperm DNA (3.02)	3	10240
	4	6520
	5	6670
	6	5460
	7	2510
Poly dAT-poly dAT (2.99)	3	8480
	4	2610
	5	4920
	6	3800
	7	4130
Poly dG-poly dC (2.69)	3	11810

[a]Studies were carried out at initial reporter concentrations of 5 x 10^{-5} M in BPES buffer (0.08 M Na_2HPO_4, 0.02 M NaH_2PO_4, 0.18 M NaCl, and 0.01 M Na_2EDTA, pH 6.90).

[b]Binding constants were reproducible within ±10%.

type of binding in the complex but does give an indication of the strength of binding. A semi-permeable membrane was used for these studies and allowed the selective passage of small molecules. When reporter molecule was placed on one side of this membrane and nucleic acid was placed on the other side, the reporter molecule could pass through the membrane to the DNA side until the concentration of unbound reporter was the same on both sides. After equilibration was achieved, the reporter concentration in the side free from DNA was determined via absorption spectroscopy. From mass balance considerations, the amount of reporter bound to the DNA was calculated and the equilibrium constant for the complex determined. The pertinent calculations are shown below in equations (1)-(3), where K_a is the equilibrium constant for formation of the complex and O. D.$^{\lambda max}$ is the optical density (measured at the absorption maximum of the reporter) of the solution in the DNA-free side of the dialysis vessel.

$$K_a = [R]_{bound}/[R]_{free}\,[DNA] \tag{1}$$

$$[R]_{free} = O.\,D.^{\lambda max}/_{\varepsilon max} \tag{2}$$

$$[R]_{bound} = 2([R]_{total} - [R]_{free}) \tag{3}$$

The results indicate that the binding constants are a function of the base content of the nucleic acid used. For instance, 3 has binding constants of 11,810, 10,240, and 8,480 to poly dG-poly dC, salmon sperm DNA, and poly dAT-poly dAT, respectively. The molecules 4-6 are also found to bind more strongly to salmon sperm DNA than to poly dAT-poly dAT. In all cases, 3 shows a higher binding constant than any of the other molecules examined. It therefore seems that these molecules are

specific for nucleic acids, rich in G-C base pairs, and the binding is sensitive to the substitution pattern of the reporter. The relationship between the binding constant and the substitution pattern does not seem to be straightforward, however.

Consequences of Intercalation

It is noted that the 1,8-naphthylimide ring of 7 may intercalate readily between base pairs without the necessity of breaking hydrogen bonds. However, in order to intercalate the 1,8,4,5-naphthyldiimide ring system of 3 between base pairs of DNA, unstacking of adjacent base pairs and local melting (hydrogen bond breakage) of the helix appear to be necessary. If the 1,8,4,5-naphthyldiimide ring of 3 intercalates, the N-benzyl, N,N-dimethyl side chains must occupy opposite grooves in DNA (i.e., one side chain in the minor, the other in the major groove), since the distance between side chains is about 11.2 angstroms in 3. This argument is illustrated in Figure 21 below.

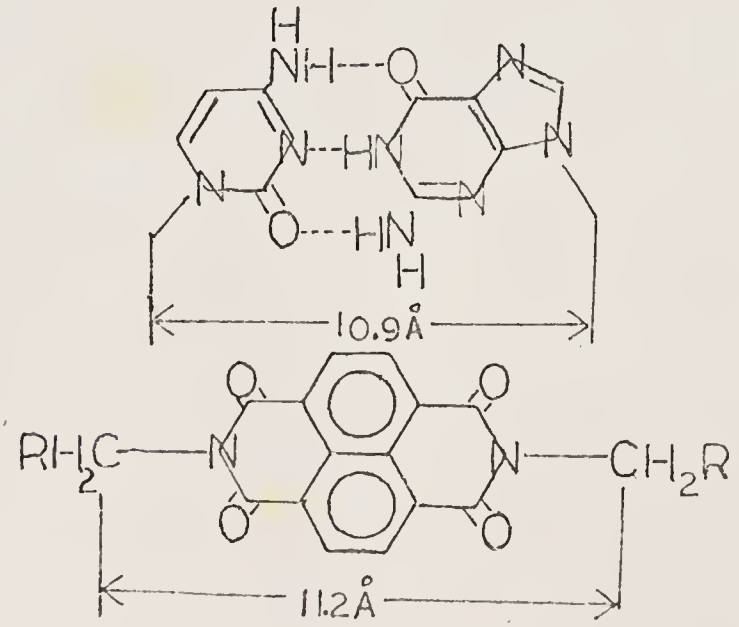

Figure 21. Relative Dimensions of 3 and the DNA Double Helix.

Moreover, it has already been mentioned that molecules 1 and 2 (Figure 14) do not intercalate due to the bulky substituents on their aromatic ring systems. Since the N-benzyl, N,N-dimethyl group of 3 is larger than the substituents employed in the molecules 1 and 2, it is concluded that intercalation of the aromatic ring system of 3 must be preceeded by local opening, i.e., melting of the helix.

As stated previously, existence of the open forms of the nucleic acid double helix has been indicated by several lines of investigation. The rates of exchange-out of tritium label from intact nucleic acid double helices are unexpectedly fast compared to protein systems.[45-47] These results were explained as being due to the existence of transient open forms which exposed the nucleic acid bases to the bulk solvent normally excluded from the hydrophobic interior of the helix. A comparison of the rates of formylation of denatured and native DNA also indicated the presence of the open forms.[52]

The Experimental Approach

The reason that the hydrogen exchange and formylation reactions are able to delineate the open forms of the nucleic acid conformation is that they do not measure an average conformation as the spectral methods do. Instead, these reactions take place specifically with the open forms. It was found that the reaction of molecule 7 with nucleic acids was faster than the capability of the instrumentation employed (1 msec), while the reactions of molecules 3-6 under the same conditions were significantly slower.[76] This fact indicated that these molecules might be useful for investigating the dynamic aspects of the nucleic acid conformation in aqueous solution. Detailed kinetic investigations on the interaction of 3 with a number of different nucleic acid systems

were therefore carried out. The reaction was studied in both the forward and the reverse directions, the latter involving dissociating premade nucleic acid·3 complexes with low concentrations of the detergent sodium dodecyl sulfate (SDS). The SDS acts by sequestering the free reporter molecule and does not take an active part in the reaction, as shown by the fact that varying the concentration of SDS used by a factor of five did not influence the kinetics of the dissociation reaction. Since the time scale of the reactions was too fast for conventional methods, a stopped-flow method was used and is described in the experimental section. It consisted of following the reactions by observing either the hypochromic effect on the reporter's absorption spectrum at 383 nm or the development of a charge transfer band at 410 nm (see Figure 19) as a function of time.

It should be noted that there is an assumption made in the analysis of the kinetic results. While the concentration of the reporter or complex as a function of time is the desired quantity, the apparatus used yields only a measure of the change in transmittance. This difficulty is circumvented by using concentrations of reporter or complex which have very low absorbances (0.08 or less). For absorbances in this range, the changes in transmittance are linearly related to the changes in absorbance. In turn, the absorbance change is directly proportional to the concentration change.

The photograph of the oscilloscope trace is used in a very direct fashion to calculate the rate constants. The distances (D) from the line representing the equilibrium value for the transmittance to the points on the curves associated with the various time spans examined are simply measured with a ruler and plotted as a logarithmic function

of time. Figure 22 shows a typical trace labeled with the appropriate parameters.

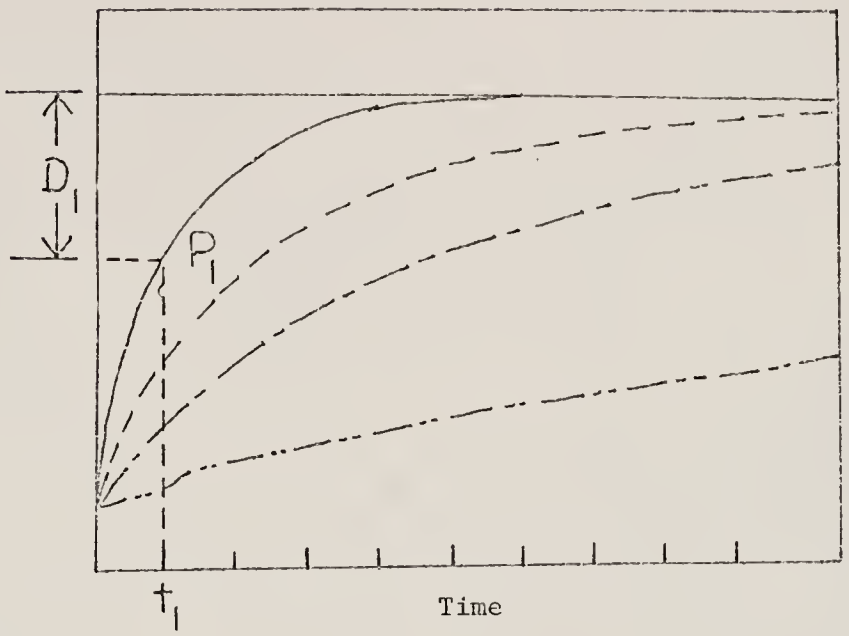

Figure 22. Oscilliscope Trace Obtained for Dissociation of C. perfringens DNA·3 Complex. The curves correspond to time scales of 0.5 sec/div. (——), 0.2 sec/div. (----), 0.1 sec/div. (—–—), and 0.02 sec/div. (————).

The corresponding rate plot is shown in Figure 23. The method of obtaining the observed rate constant from the slope of the plot is summarized by equation (4) below,

$$k_{obs} = 2.3/(t_2 - t_1) \log (D_2/D_1) \qquad (4)$$

where D_2 and D_1 are displacements from the equilibrium line on the oscilliscope trace to points 1 and 2 on a particular reaction curve. The times corresponding to points 1 and 2 are t_1 and t_2, respectively.

The Association Reaction

Order with respect to reporter molecule

Synthetic DNA of repeating sequence.--A number of lines of evidence indicate that the association reaction is first order with respect to the

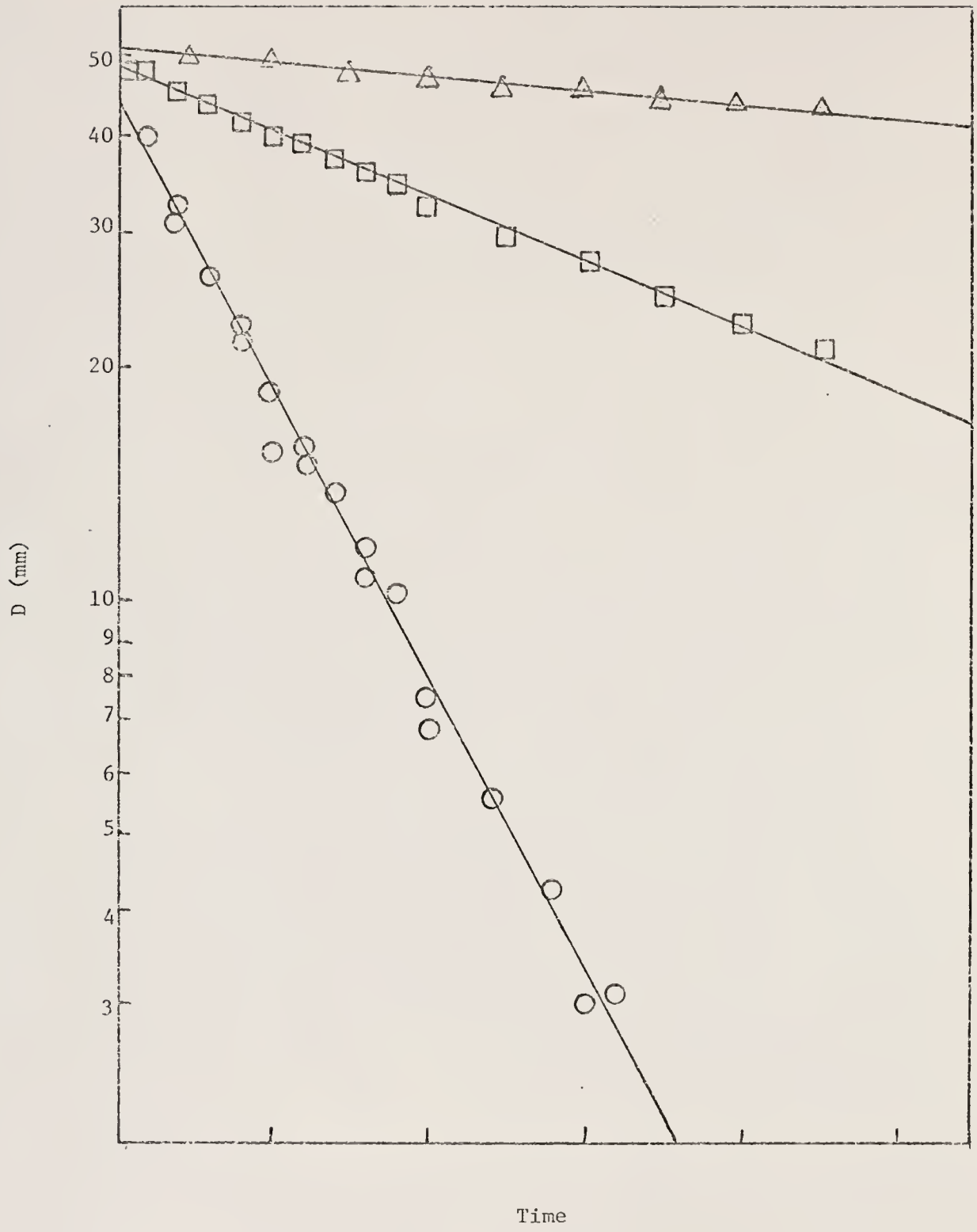

Figure 23. First Order Rate Plot for Dissociation of C. perfringens DNA·3 Complex. The time scale is 0.5 sec/div. (○—○), 0.1 sec/div. (□—□), or 0.02 sec/div. (△—△), and the reaction was followed at 410 nm.

concentration of 3 when DNA of repeating sequence is used. For a first order reaction such as A→B, the rate of loss of A is given by equation (5).[79] Dividing both sides by the concentration of A

$$-dA/dt = kA \tag{5}$$

and integrating yields the result shown in equation (6). A plot of

$$-\ln A = kt + \text{constant} \tag{6}$$

the natural logarithm of the concentration of A as a function of time therefore yields the first order rate constant in a direct manner. In the case at hand, the nucleic acid concentration does not enter into the rate equation because it is present in excess at all times during the course of the reaction and is included in the observed first order rate constant. This result (equation (6)) implies that the first order plot of the concentration of the reacting species will not depend on the initial value for the concentration of this species. Further, the reaction should not be influenced by the nucleotide concentration as long as the nucleic acid is present in sufficient excess.

With the synthetic polymer duplexes poly dAT-poly dAT and poly dG-poly dC, the reaction appears to be first order with respect to the reporter molecule 3 for the following reasons. (1) The observed rate constant does not depend upon the concentration of the reporter used. For example, as seen in Table 4, the observed rate constant for reaction of 2.50×10^{-6} M 3 with 1.29×10^{-4} M P/1 of poly dAT-poly dAT is 11.95 sec^{-1}, while the observed rate constant for association of 1.25×10^{-6} M 3

Table 4

Observed First Order Rate Constants for Association of 3 and 7 with Nucleic Acids.[a]

R (conc. x 10^{-6} M P/l)	k_{obs}, sec^{-1}[b] Poly dAT-poly dAT (conc. x 10^{-6} M P/l)					Poly dG-poly dC (conc. x 10^{-6} M P/l)
	129.0	69.3	34.7	17.3	8.7	58.1
3 (2.50)	11.95	9.15	7.30	5.40	4.40	3.48
3 (1.25)	12.40	8.85	6.80	-	-	3.57
7 (2.50)			c			c

[a] Experiments performed by Gabbay.[80]

[b] Stopped-flow kinetics were carried out on a Durrum stopped-flow apparatus thermostatted with a Lauda K-2/R circulating bath. The reaction was followed at 383 and 347 nm for reporters 3 and 7, respectively, in BPES (0.08 M Na_2HPO_4, 0.02 M NaH_2PO_4, 0.18 M NaCl, 0.01 M Na_2EOTA, pH 6.9).

[c] The kinetics of binding of 7 to nucleic acids were found to be faster than the capability limit of the instrument (1 M sec).

with the same concentration of poly dAT-poly dAT is 12.40 sec^{-1}. The difference in rate constants is within the experimental error of the method. (2) The first order plots of the reaction of 3 with poly dAT-poly dAT are linear over a range of phosphate to reporter ratios from 3.5/1 to 103/1 (Figure 24).

Synthetic RNA of repeating sequence.--The kinetics of binding of 3 to the ribopolymers poly rI-poly rC and poly rA-poly rU were also examined (Table 5).

Table 5

Observed First Order Rate Constants for Association of 3 with Synthetic RNA of Repeating Sequence.[a]

Nucleic Acid (conc. x 10^{-4} M P/$_{\ell}$)	k_{obs}, sec^{-1}
poly rI-poly rC (0.25)	31.45
(0.75)	50.07
(1.50)	57.30
(2.50)	77.60
poly rA-poly rU (0.25)	78.80
(0.75)	94.65
(1.50)	169.50
(2.50)	200.00

[a]Experiments were carried out using 5 x 10^{-6} M of 3 at a temperature of 20.5°C in 0.01 M MES(pH 6.2, 0.025 M in Na^{+}). The reaction was followed at 383 nm.

Linear first order plots were obtained over a range of phosphate to reporter concentration ratios from 5/1 to 50/1. It is important to note that these studies were carried out at a much lower salt concentration than were the studies with the synthetic DNA previously discussed. This was necessary due to the fact that the binding was essentially eliminated in the presence of salt concentrations on the order of those used in the DNA studies, as shown by the observation that no hypochromic effect on the absorption spectrum of the reporter

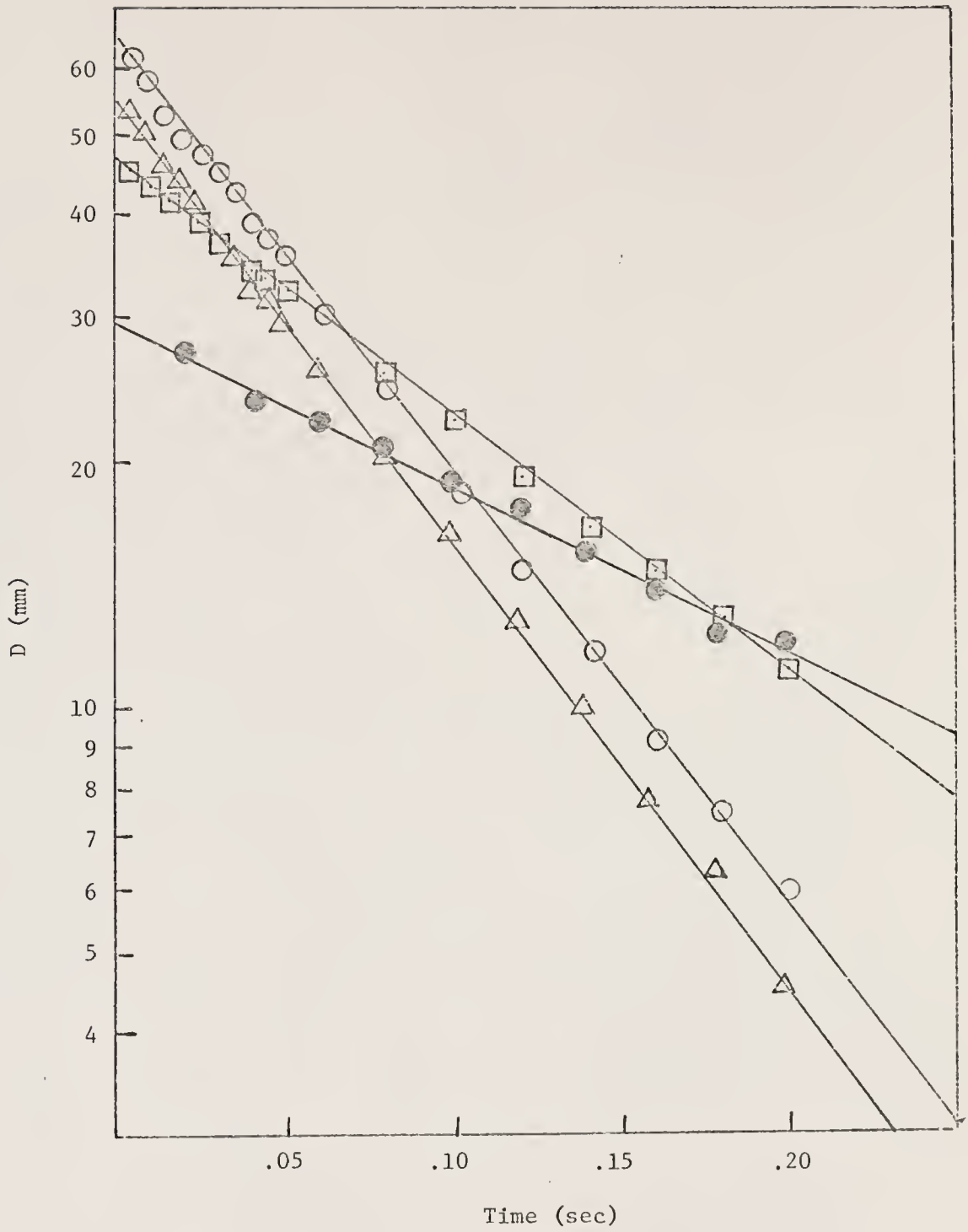

Figure 24. Rate Plots for Formation of Poly dAT-poly dAT·3 Complex at Varying Phosphate/3 Ratios. Experiments were carried out in BPES (0.08 M Na_2HPO_4, 0.02 M NaH_2PO_4. 0.18 M NaCl, 0.01 M Na_2EDTA), pH 6.9, at 20°C and 410 nm. Phosphate/3 ratios and poly dAT-poly dAT concentrations were respectively 103 and 12.9 x 10^{-5} M P/l (△), 52 and 12.9 x 10^{-5} M P/l (○), 14 and 3.47 x 10^{-5} M P/l (□), or 3.5 and 8.7 x 10^{-6} M P/l (●).

molecule is noted in the presence of high salt concentrations. An interesting fact seen in the data included in Table 5 is the much faster reaction rate of poly rA-poly rU as compared to poly rI-poly rC. The reporter 3 therefore appears to be able to discriminate between the two polynucleotides.

Salmon sperm DNA.--The kinetics of binding of reporter 3 to salmon sperm DNA were investigated and found to be complex, i.e., several linear regions of different slopes were observed in the first order rate plots. This finding is consistent with the presence of several different classes of binding sites in the DNA molecule. The results of kinetic experiments with poly dAT-poly dAT and poly dG-poly dC are also compatible with the presence of different classes of binding sites (Table 4). For example, the observed first order rate constant with 6.93×10^{-5} M P/1 poly dAT-poly dAT is found to be 9.00 ± 0.15 sec^{-1}, while the observed first order rate constant with 5.81×10^{-5} M P/1 poly dG-poly dC under identical conditions is only 3.53 ± 0.04 sec^{-1}.

In line with the postulate that reporter 3 is reacting with several different classes of binding sites is the fact that the kinetic plots may be simplified by increasing the ratio of the concentration of nucleic acid base pairs to the concentration of reporter 3. Under conditions where the intercalating sites are in huge excess, the reporter 3 might be expected to seek out the most favorable sites. Indeed, as shown by Figures 25 and 26, this appears to be the case. Figure 25 shows the association reaction of salmon sperm DNA with 3 at a base pair to reporter ratio of 15/1, under which conditions the reaction gives linear first order kinetics for at least three half-lives of reaction. Figure 26 shows the same reaction done at a base pair to

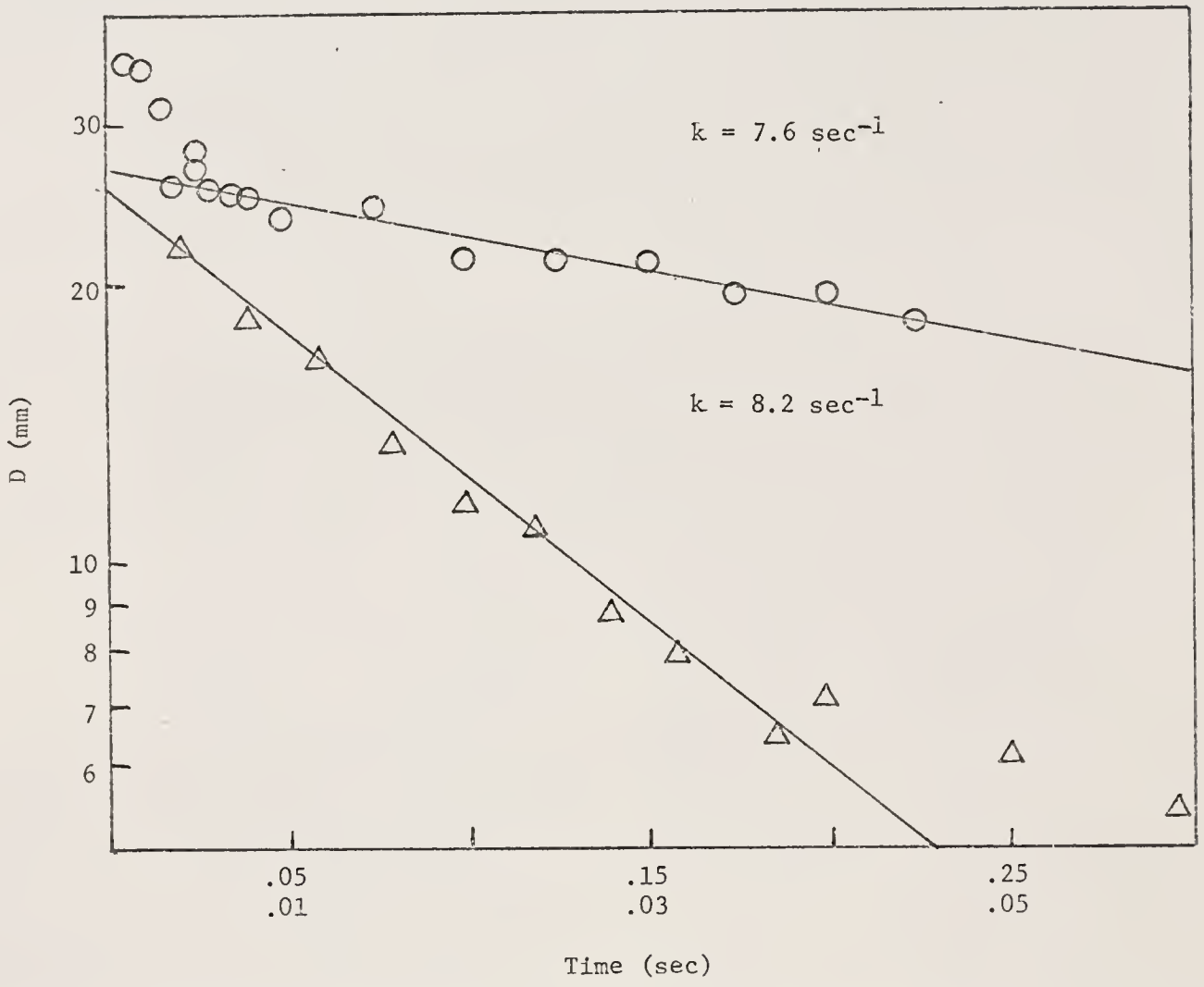

Figure 25. First Order Rate Plot for Association of 3 and Salmon Sperm DNA. Reaction was followed at 410 nm at a temperature of 19.5°C in 0.05 M MES (pH 6.2, 0.30 M in Na^+). The base pair to reporter ratio was 15/1, and the nucleic acid concentration was 3.0×10^{-4} M P/1. Time scales are 0.05 sec/div. (Δ) or 0.01 sec/div. (○).

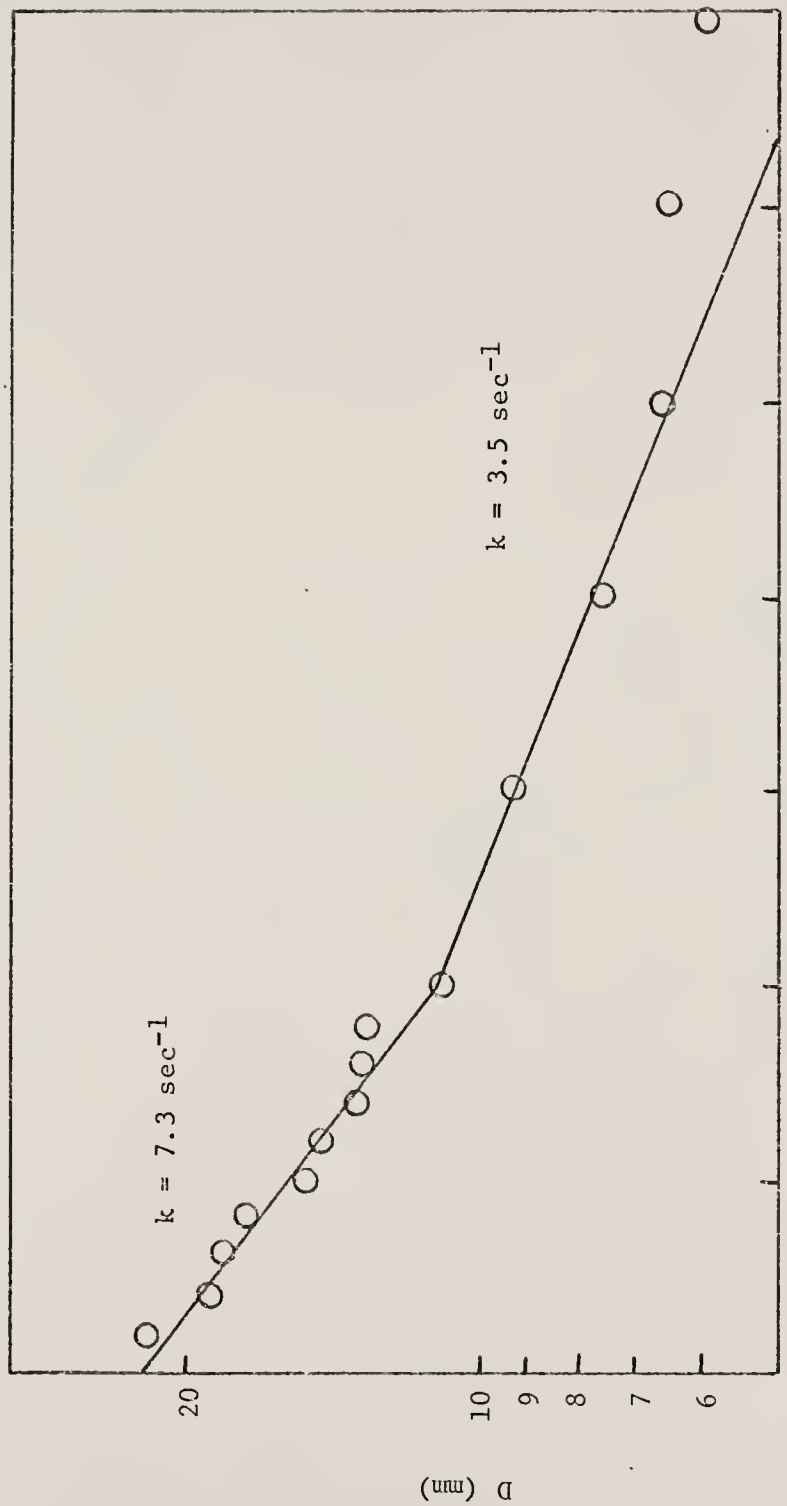

Figure 26. First Order Rate Plot for Association of 3 and Salmon Sperm DNA. Reaction was followed at 410 nm at a temperature of 19.5°C in 0.05 M MES (pH 6.2, 0.30 M in Na^+). The base pair to reporter ratio was 7.5/1, and the nucleic acid concentration was 1.5×10^{-4} M P/l.

reporter ratio of only 7.5/1. Under these conditions, it is possible to see at least two processes which contribute substantially to the reaction. In fact, there are also traces of both faster and slower processes in the experiment using a high base pair to reporter concentration ratio, though the deviation from the straight line is more certain at the very early times than at the very late times due to the inaccuracy involved in measuring very short distances on the oscilliscope trace.

A comparison of the kinetics at two different wavelengths (383 nm and 410 nm) was also carried out. The first wavelength is the absorption maximum for the reporter, while the second is in the area of the spectrum due to the charge transfer band of the complex. It was found that identical kinetics were obtained regardless of whether the development of the hypochromic effect at the absorption maximum of the reporter or the development of the charge transfer band for the complex was followed (Table 6).

Table 6

Observed First Order Rate Constants for the Formation of Salmon Sperm DNA·3 Complex at 383 nm and 410 nm.[a]

Wavelength (nm)	k_{obs}, sec^{-1}		
	k_1	k_2	k_3
383	36.05	17.23	9.74
410	44.50	18.21	-

[a] Studies were done at 19.5°C in 0.05 M MES (pH 6.2, 0.10 M in Na^+) using DNA and 3 concentrations of 1.5×10^{-4} M P/1 and 1.0×10^{-5} M, respectively.

Order with respect to nucleic acid

Since the concentration of the nucleic acid is included in the pseudofirst order rate constant, varying this concentration and following the resultant change in the rate constant provides a measure of the kinetic order with respect to the nucleic acid. Since the pseudofirst order rate constant is actually the product of the true rate constant and the nucleic acid to some power (equation (7)), a plot of the

$$k_{obs} = k' \text{ (nucleic acid)}^{n} \qquad (7)$$

logarithm of the observed rate constant versus the logarithm of the nucleic acid concentration should yield a line with a slope equal to the true kinetic order with respect to the nucleic acid.[81] Such studies were done with poly dAT-poly dAT, poly rI-poly rC, poly rA-poly rU, and salmon sperm DNA, and the resulting log-log plots are shown in Figure 27. The most surprising point evident from a consideration of these data is the fact that the order with respect to the nucleic acid may vary depending upon the polynucleotide examined. It was established that the order was 0.4 with poly dAT-poly dAT, 0.5 with poly rI-poly rC and poly rA-poly rU, and 1.0 with salmon sperm DNA. In the case of the latter, the rate constants used were those obtained from portions of the rate plots which were linear over at least three half-lives of reaction (Table 7). The varying order with respect to the nucleic acid may be explained by assuming that the same concentrations of nucleic acids may yield different concentrations of reactive sites for interaction with the reporter 3.

Kinetic Models

The main points considered in the formulation of a model to explain the kinetic data were the first order dependence on the reporter

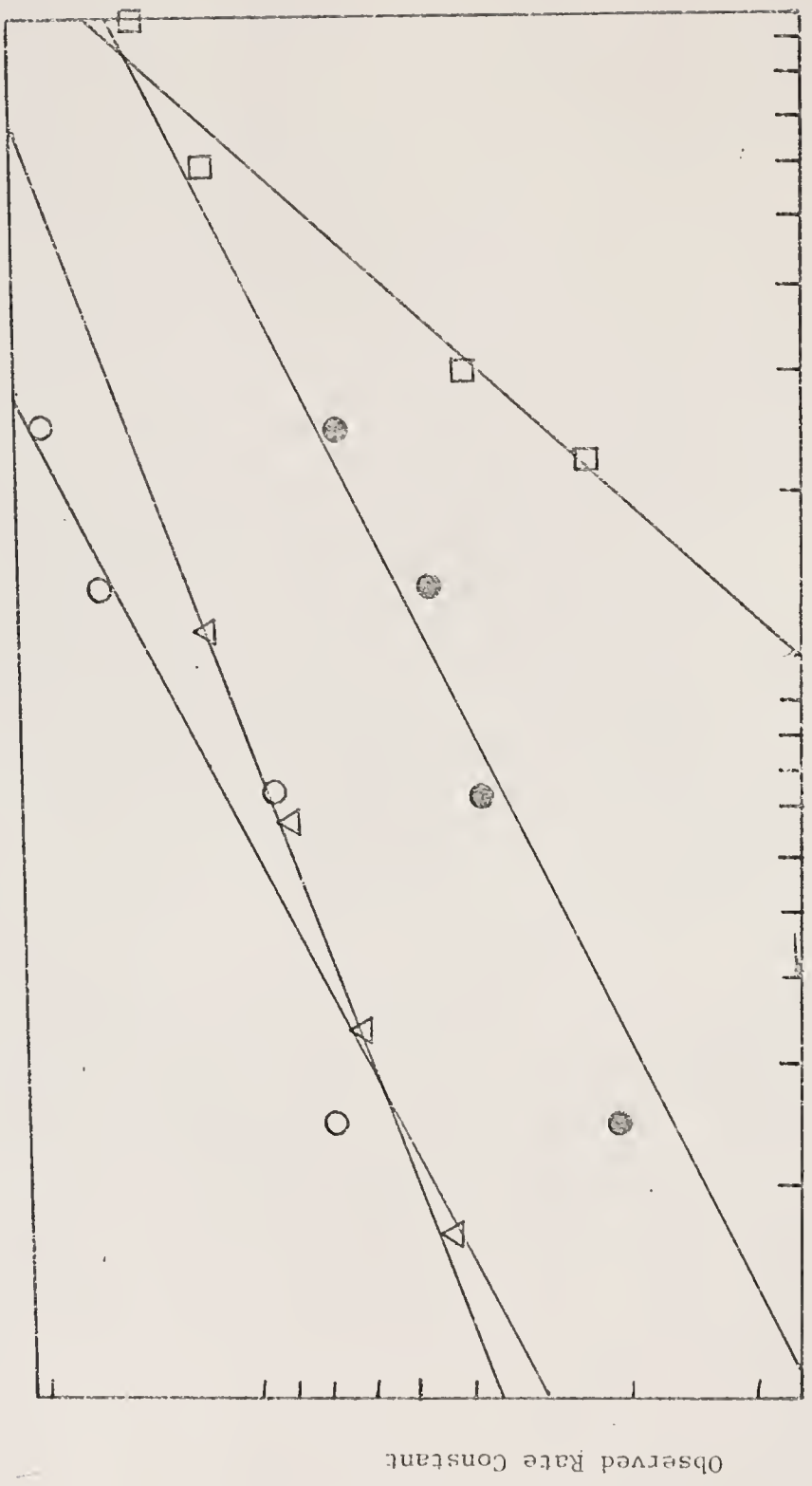

Figure 27. Log-log Plots for the Determination of Order with Respect to Nucleic Acid. Data points for poly dAT-poly dAT (Δ), ribopolymers poly rI-poly rC (●) and poly rA-poly rU (○), and salmon sperm DNA (□) are shown in Tables 4, 5, and 7, respectively.

Table 7

Observed First Order Rate Constants for Formation of Salmon Sperm DNA·3 Complexes at Different Nucleic Acid Concentrations.[a]

Nucleic Acid Concentration (x 10^{-4} M P/1)	k_{obs}, sec^{-1}
2.25	3.38
3.00	5.12
6.00	12.30
10.00	15.50

[a]Experiments were carried out using 5 x 10^{-6} M of 3 at a temperature of 20.5°C in 0.05 M MES (pH 6.2, 0.375 M in Na^{+}). The reaction was followed at 410 nm.

concentration, the varying order with respect to the nucleic acids, and the nonlinear nature of the rate plots obtained with salmon sperm DNA. A number of reaction schemes were considered. The detailed kinetic equations are presented in Appendix 1, but the salient features of the models are presented in simplified form in Figure 28. Model 1 (Rate-Determining Preequilibrium) is ruled out on the grounds that the reaction is expected to be slower in its initial stages than in its later stages; this is contrary to the observed results. Model 2 (Product Inhibition) was found to be in qualitative agreement with the results, but it predicts a smooth decrease in the observed rate of reaction as the product concentration increases. The observed kinetics, however, consist of several rather extended linear regions of different slopes. Model 3 (Catalysis by an Intermediate Complex) again predicts a smoothly decreasing rate of reaction and is ruled out on this basis. Model 4 (Rate-Determining Formation of Intermediate Complex) is not in agreement with the data since it predicts a slower rate at the onset of the reaction rather than a faster rate. Model 5 (Multiple Sites) was the best explanation for the results and is shown in Figure 29 along with a detailed derivation of the first order rate equation. It is assumed that the reaction involves a conformational equilibrium between closed and open forms of the nucleic acid double helix. Transient twisting of one strand relative to the other is postulated to open the double helix and expose a segment several base pairs long. This process partially decouples the opened segment from the rest of the structure and allows for dynamic properties depending upon the sequence and base content of the opened segment. These open but still stacked segments may then react with the reporter molecule by unstacking and

Model 1 - Rate-Determining Nucleic Acid Preequilibrium

$$(CH) \underset{-1}{\overset{1\,(slow)}{\rightleftharpoons}} n(OH)$$

$$(OH) + (R) \underset{-2}{\overset{2}{\rightleftharpoons}} (OH\cdot R) \xrightarrow{3} (CH\cdot R)$$

Model 2 - Product Inhibition

$$(CH) \underset{-1}{\overset{1}{\rightleftharpoons}} n(OH)$$

$$(OH) + (R) \underset{-2}{\overset{2}{\rightleftharpoons}} (OH\cdot R) \xrightarrow{3\,(slow)} (CH\cdot R)$$

$$(CH\cdot R) + n(OH) \xrightarrow{4} (CH\cdot R) + (CH)$$

Model 3 - Catalysis by an Intermediate Complex

$$(CH) \underset{-1}{\overset{1}{\rightleftharpoons}} n(OH)$$

$$(OH) + (R) \underset{-2}{\overset{2}{\rightleftharpoons}} (OH\cdot R) \xrightarrow{3\,(slow)} (CH\cdot R)$$

$$(OH\cdot R) + (CH) \xrightarrow{4} (OH\cdot R) + n(OH)$$

Model 4 - Rate-Determining Formation of Intermediate Complex

$$(CH) \underset{-1}{\overset{1}{\rightleftharpoons}} n(OH)$$

$$(OH) + (R) \xrightarrow[(slow)]{2} (OH\cdot R) \underset{-3}{\overset{3}{\rightleftharpoons}} (CH\cdot R)$$

Figure 28. Possible Models for the Association Reaction of 3 with Nucleic Acids. (CH) and (OH) are the closed and open intercalating sites, (R) is the reporter.

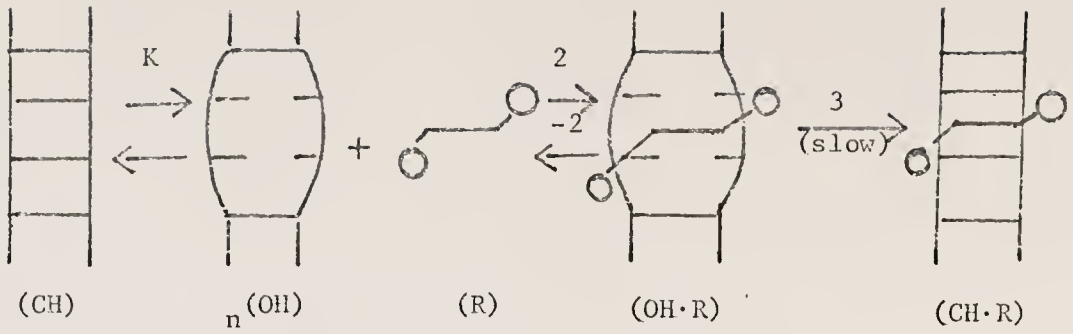

$$\frac{d(CH\cdot R)}{dt} = \frac{-dR}{dt} = k_3(OH\cdot R)$$

$$\frac{d(OH\cdot R)}{dt} = 0 = -k_3(OH\cdot R) + k_2(OH)(R) - k_{-2}(OH\cdot R)$$

$$(OH\cdot R) = \frac{k_2(OH)(R)}{k_{-2}+k_3}$$

$$K = \frac{(OH)^n}{CH} \quad \text{and} \quad (OH) = (K)^{1/n}(CH)^{1/n}$$

$$(OH\cdot R) = \frac{k_2(K)^{1/n}(CH)^{1/n}(R)}{k_{-2}+k_3}$$

$$\text{and} \quad \frac{-dR}{dt} = \frac{k_2k_3(K)^{1/n}(CH)^{1/n}(R)}{k_2+k_3}$$

$$\frac{-dR}{R} = \frac{k_2k_3K^{1/n}}{k_{-2}+k_3}(CH)^{1/n}dt$$

$$-\ln R + \text{const.} = k'(CH)^{1/n}t$$

$$-\ln R + \text{const.} = k_{obs}t$$

$$k_{obs} = k'(CH)^{1/n}$$

$$\log k_{obs} = \log k' + 1/n \log(CH)$$

Figure 29. The Multiple Sites Model for the Association of 3 with Nucleic Acids. (CH) and (OH) refer to closed and open variants of the double helix, respectively while (R) refers to the reporter molecule.

then reclosing over the planar portion of the reporter system in the slow rate-determining step.

It is worth noting that evidence exists for both the stacked and the unstacked open variants of the nucleic acid conformation. The main evidence comes from the formylation studies[52] cited previously. This investigation indicated that the unstacked conformation required a much higher energy of activation for formation than did the stacked open conformation utilized in the hydrogen exchange reaction.

The precise nature of the unstacking and intercalation events may obviously differ from one nucleic acid to another or even from one segment to another. This is indicated by the observation that complex first order plots are observed for association of 3 with nucleic acids of heterogeneous base sequence, while the association with synthetic nucleic acids of repeating sequence yields only one first order rate constant. Likewise, the results indicating that the order with respect to the nucleic acid may differ from one nucleic acid to another are also accomodated by this model. The opening segments may either be of different length or of different capacities with regard to the number of reporter molecules which may be intercalated in a given stretch of the helix. In either case, the value for n in the rate equation implied by this model indicates the number of reactive sites yielded by the opening of a nucleic acid segment of a given size. For example, the order with respect to poly dAT-poly dAT was found to be 0.4, and this implies that the opening reaction with this polynucleotide supplies open segments capable of intercalating 2.5 molecules of 3 on the average. Poly rI-poly rC and poly rA-poly rU both need a value of 0.5 for the order and can apparently intercalate 2.0 molecules of 3

into an average opened segment. Salmon sperm DNA gives a value of 1.0 for the order and can therefore only intercalate one molecule of 3 in the average opened segment. These findings indicate that a certain degree of specificity dependent on the nature of the nucleic acid is possible in the intercalation reactions.

Influence of ionic strength

A series of experiments was carried out to assess the effects of varying ionic strength on the formation of the salmon sperm DNA·3 complex. The observed rate constants for the association reaction are found to be lower at high ionic strength (Figure 30). There are at least two explanations for these results. (1) The reaction may be slowed due to a shift in the equilibrium between closed and open forms of the nucleic acid double helix, i.e., K may be decreased at high ionic strength. It has already been stated that the intact double helix is favored by high ionic strength due to the decreased phosphate-phosphate ionic repulsions. (2) The reaction may be slowed due to the lesser importance of ionic interactions in solutions of high ionic strength. Since the ionic attraction between the reporter and the opened nucleic acid conformer is expected to be of some importance on intuitive grounds, the lesser importance of these interactions at higher ionic strength, i.e., the decreased value of k_2/k_{-2}, would also explain the results. It is not possible to rule out either of these possibilities, but both are in general agreement with the model discussed in the previous section.

Experiments with polylysine-DNA complexes

To get further information on the interactions between reporter 3 and nucleic acids, the kinetics of the binding of 3 to salmon sperm DNA-polylysine complexes were investigated. The observed first order

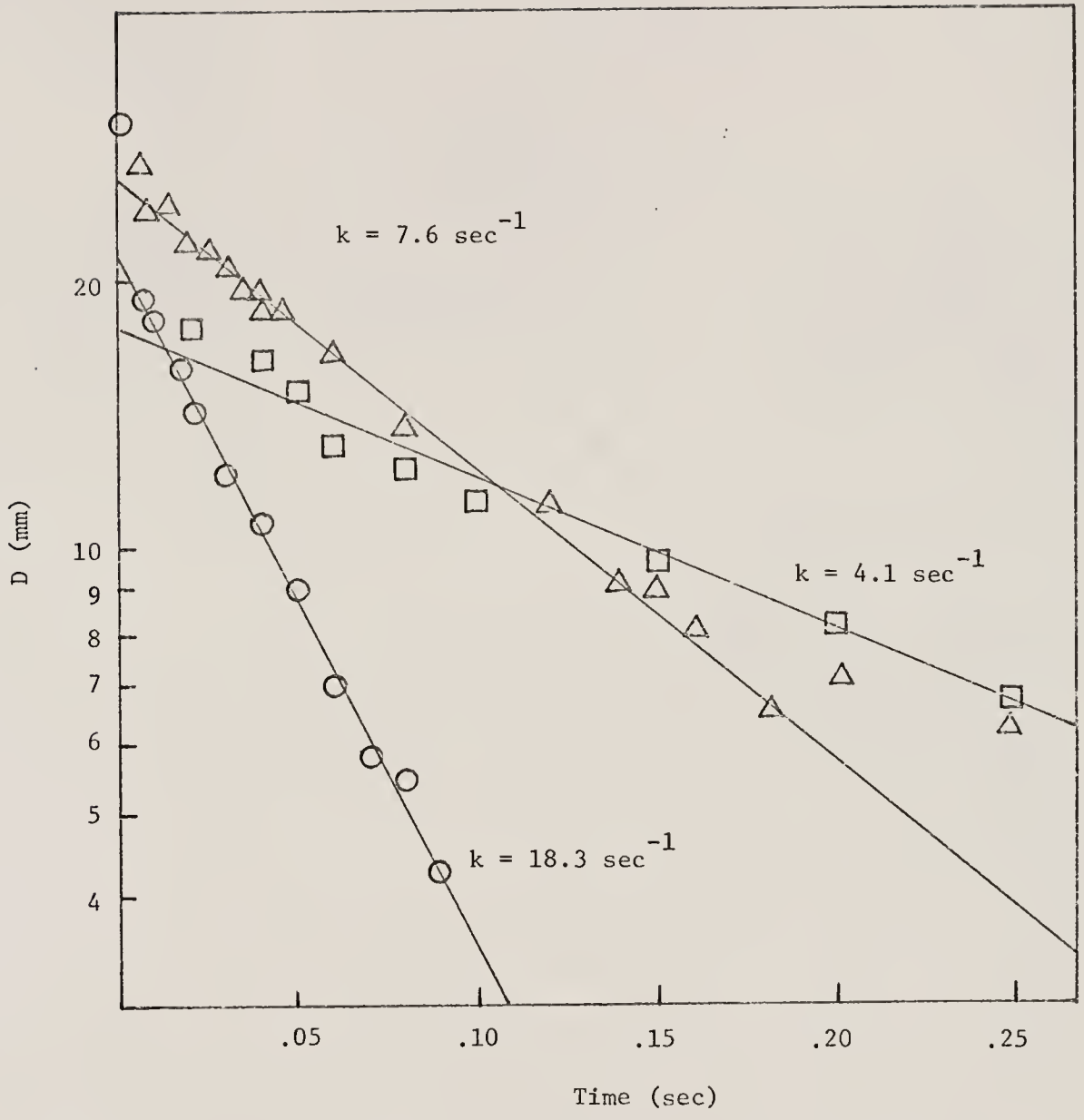

Figure 30. Effect of Varying Ionic Strength on the Association of Salmon Sperm DNA and 3. Experiments were done in 0.05 M MES, pH 6.2 at 19.5°C. Total Na^+ was 0.2 M (○), 0.3 M (△), or 0.4 M (□). The base pair to reporter ratio was 15/1, and the nucleic acid concentration was 3.0×10^{-4} M P/l in all cases.

rate constants for this reaction as a function of polylysine concentration are shown in Table 8. As with DNA alone, the rate plots exhibit

Table 8

Observed Rate Constants for Association of 3 with DNA-Polylysine Complexes[a]

Polylysine (μg/ml)	Lysine/Phosphate	k_{obs}, sec^{-1}			
		k_1	k_2	k_3	k_4
0	0	44.50	18.21	-	-
5	.15	19.40	8.68	-	-
10	.29	22.80	6.24	0.42	-
15	.44	24.60	3.99	0.90	0.48
20	.59	19.30	2.37	0.62	0.32

[a]Experiments were done at 410 nm in 0.05 M MES (pH 6.2, 0.10 M in Na^+) at a temperature of 19.5°C. Salmon Sperm DNA and 3 were used at concentrations of 1.5×10^{-4} M P/l and 5×10^{-6} M, respectively.

several linear regions of different slopes. The effect of increasing the polylysine concentration was twofold. (1) The various rates were all slower than the rates shown with DNA alone. (2) There appear to be more rate processes observed as the amount of protein increases. While there were only two rate processes for the complex containing 5μg/ml of polylysine, the complex containing 10μg/ml showed three rate processes, and the complexes containing 15μg/ml and 20μg/ml showed four rate processes. There are several ways to explain these results, but all would be rather speculative due to the lack of detailed information on the structure of the DNA-polylysine complexes.

The Dissociation Reaction

Order with respect to nucleic acid·3 complex

The kinetics of dissociation of nucleic acid·3 complexes were followed at 410 nm using the SDS technique discussed previously. Low concentrations of the detergent SDS were mixed with the complex, and the resulting decrease in absorbance due to the freeing of the reporter molecule from the nucleic acid double helix was followed as a function of time. Two lines of evidence indicate that the dissociation is first order with respect to the complexes. (1) The experiments using a nucleic acid of repeating sequence yield only one rate constant, in agreement with the model for the association reaction. Since the repeating sequence of poly dAT-poly dAT provides only two very similar intercalating sites and that of poly dG-poly dC provides only one intercalating site, one might expect to see only one dissociation rate process with complexes involving these nucleic acids. It is found that the first order rate plots are linear over at least four half-lives of reaction in the case of poly dAT-poly dAT·3 complexes (Figure 31). The typical first order plots showing several long linear regions with different slopes are obtained when natural DNA is used for the reaction. The more complicated cases seen when using the complexes of 3 with C. perfringens DNA and M. luteus DNA are shown in Figures 32 and 33, respectively. (2) The rate constant does not depend upon the initial concentration of complex used. Table 9 shows the results obtained by varying the concentrations of calf thymus DNA·3 and salmon sperm DNA·3 complexes. It is seen that the observed first order rate constants do not change over as much as a fourfold increase in the concentration of the complex. For example, a complex containing salmon sperm DNA at a concentration of 6.0×10^{-4} M P/1

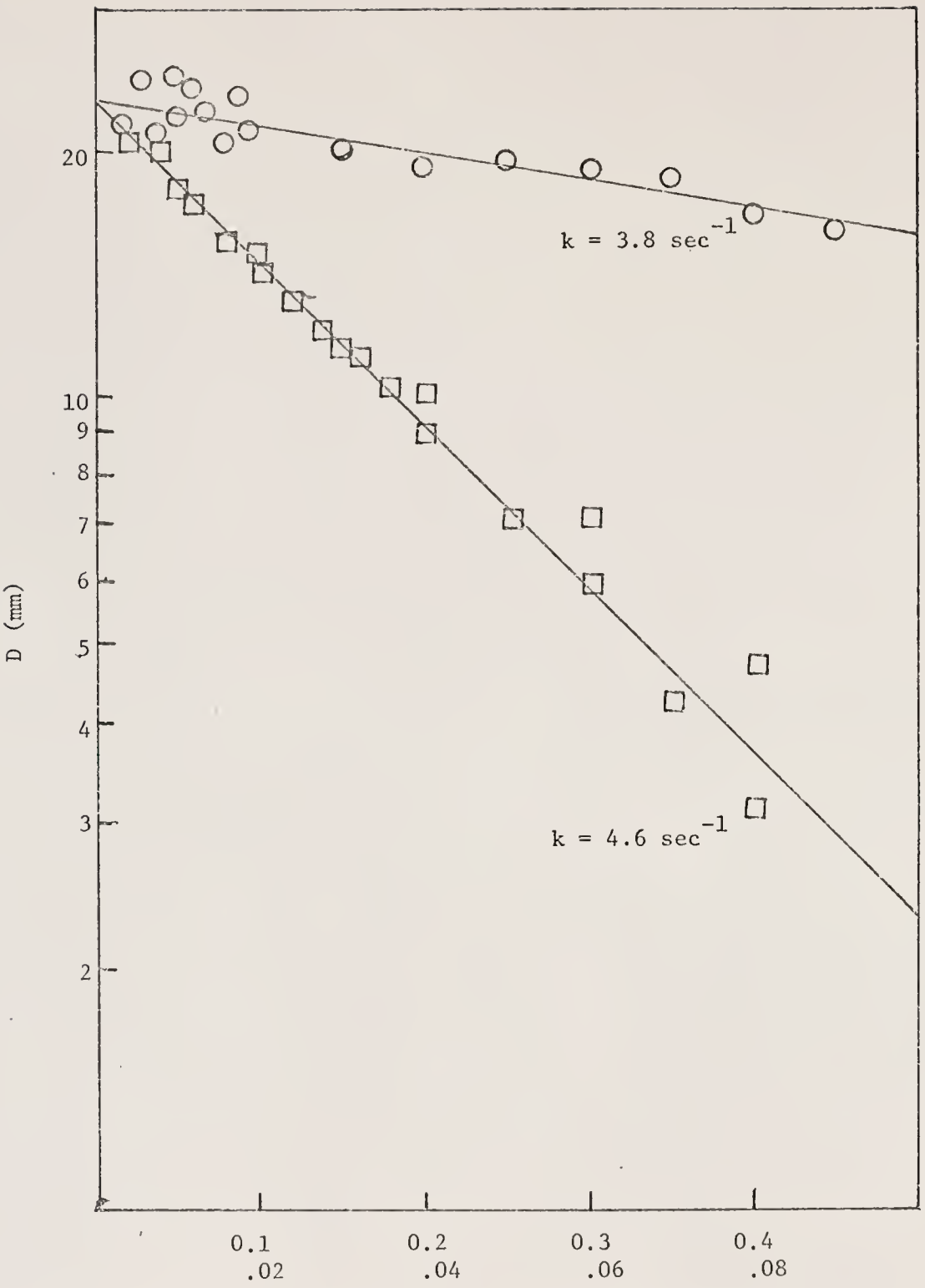

Figure 31. Rate Plot for Dissociation of poly dAT-poly dAT·3 Complex at 410 nm. Time scale is either 0.02 sec/div. (Ō) or 0.1 sec/div. (□).

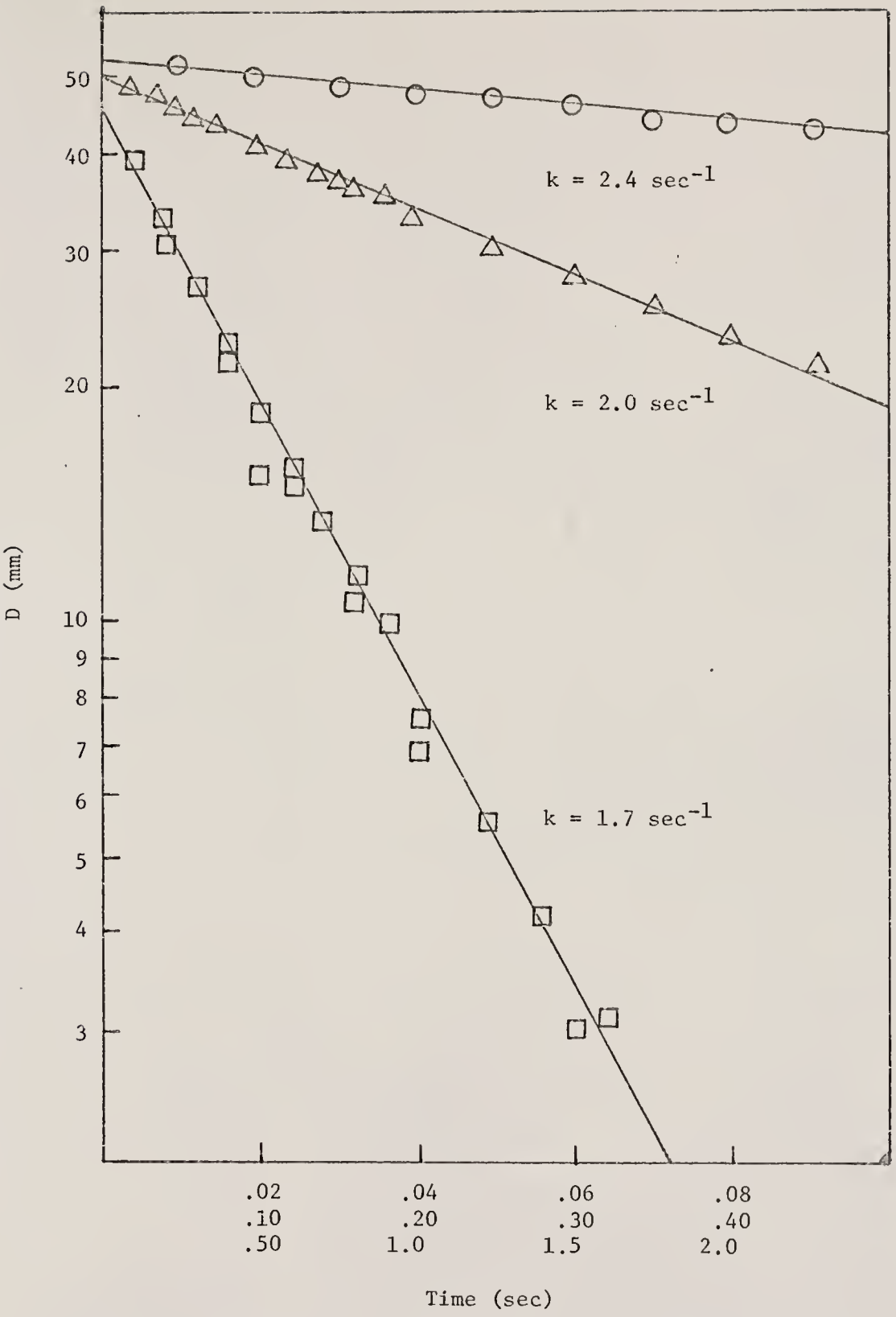

Figure 32. Rate Plot for Dissociation of C. perfringens DNA . 3 Complex at 410 nm. Time scale is 0.02 sec/div. (○—○), 0.10 sec/div. (△—△), or 0.50 sec/div. (□—□).

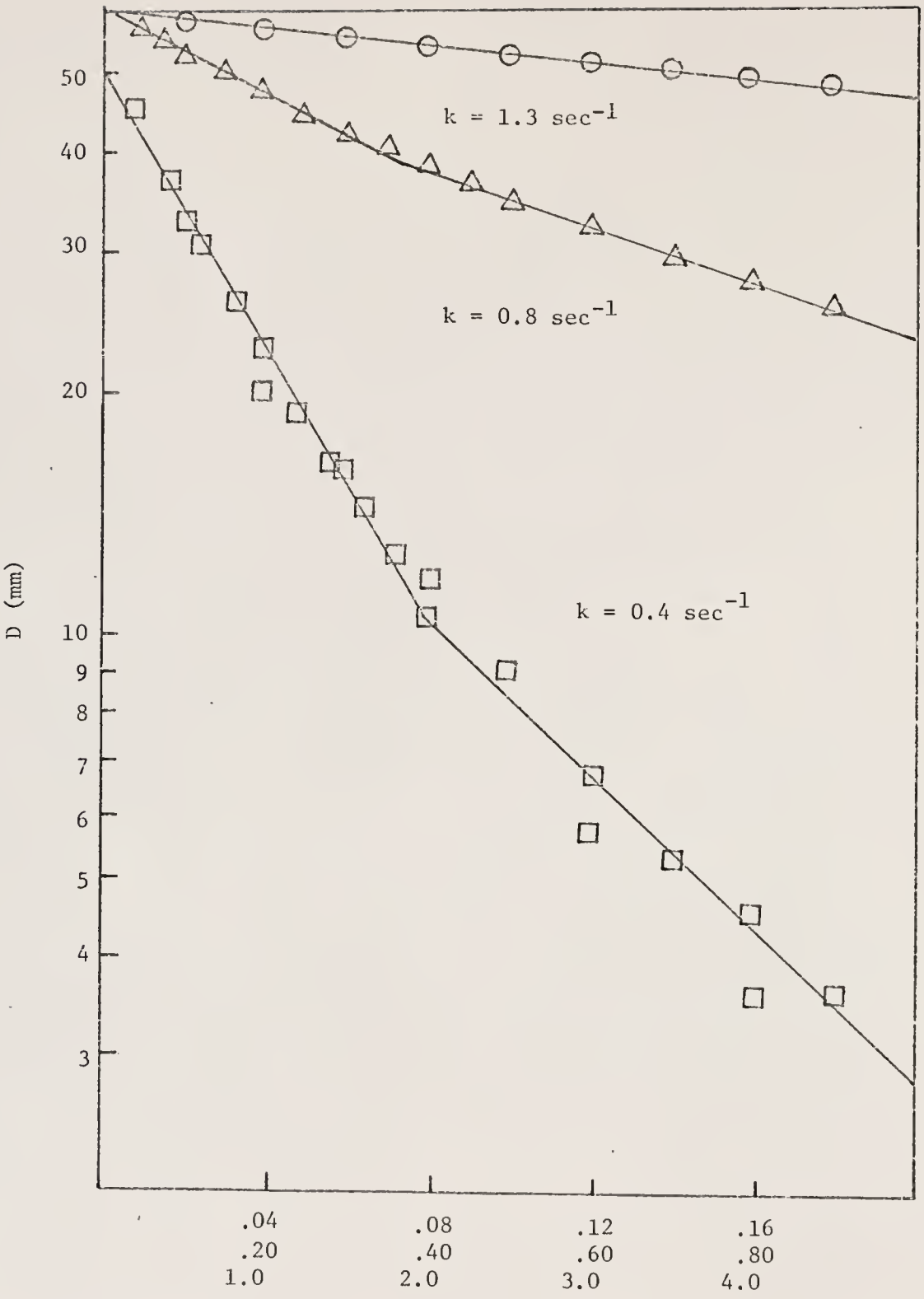

Figure 33. Rate Plot for Dissociation of M. luteus DNA · $\overline{3}$ Complex at 410 nm. Time scale is 0.04 sec/div. (○—○), 0.20 sec/div. (△—△), or 1.0 sec/div. (□—□).

Table 9

Dependence of Dissociation Rates on the Concentration of the Nucleic Acid·3 Complex[a]

Nucleic Acid (conc. x 10^{-4} M P/1)	[3]	k_{obs}, sec^{-1}		
		k_1	k_2	k_3
Salmon Sperm (9.0)	4 x 10^{-5} M	1.61	1.48	1.23
(6.0)	4 x 10^{-5} M	1.86	1.65	1.05
(3.0)	2 x 10^{-5} M	1.63	1.54	1.13
(1.5)	1 x 10^{-5} M	1.65	1.54	-
Calf Thymus (6.0)	4 x 10^{-5} M	2.02	1.53	1.17
(3.0)	4 x 10^{-5} M	1.93	1.51	1.38
(3.0)	2 x 10^{-5} M	1.67	1.54	1.13

[a]Studies were done at 410 nm in 0.05 M MES (pH 6.2, 0.0 M in Na^+) at 20°C.

and 3 at a concentration of 4.0×10^{-5} M showed rate constants of 1.86, 1.55, and 1.05 sec^{-1}, while a complex containing salmon sperm DNA at a concentration of 3.0×10^{-4} M P/l and 3 at a concentration of 2.0×10^{-5} M showed rate constants of 1.63, 1.54, and 1.13 sec^{-1}.

Kinetic model

The model for the dissociation reaction parallels the model presented for the association reaction in Figure 29. The mechanism involves the same type of sequence-dependent opening reaction as that shown for the association reaction, and this is followed by the release of the reporter into the solution where it is rapidly sequestered by the SDS. Since the reaction is followed at 410 nm where the free reporter has no absorption (Figure 19), the effect seen is due to the time-dependent decrease in absorbance due to the complex alone. Figure 34 shows the model in schematic form along with the detailed derivation of the first order rate equation. This model assumes that the opening of the complex involving the double helix is the rate-determining step.

Experiments with sonicated and heat-denatured DNA

Kinetic studies were also done on complexes of 3 with both sonicated low molecular weight DNA and heat-denatured DNA. While the sonication had little effect on the observed rates of dissociation measured by the SDS method, the denaturation of the DNA proved to have a very marked effect (Table 10). It was found that the rate constants were much faster for the denatured DNA than for the native DNA. On the basis of the very small effect caused by sonication of the DNA, it may be concluded that the opening event is not dependent upon proximity to a chain end. To thoroughly understand the significance of the results with denatured DNA, the details of the structure of this system must be

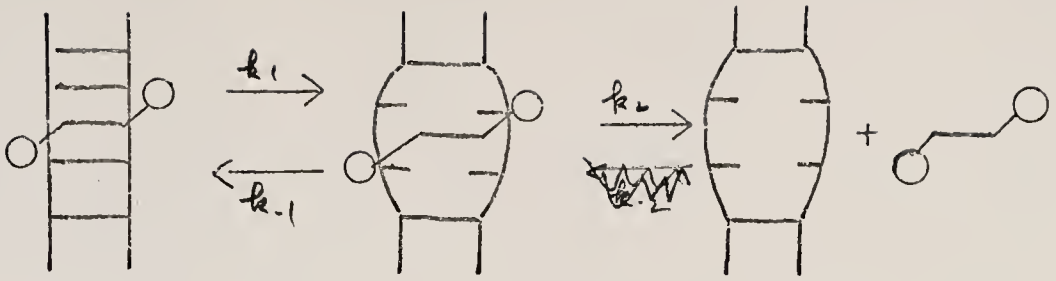

(CH·R) (OH·R) (OH) (R)

$$dR/dt = k_2\ (OH\cdot R) = \frac{-d\ (CH\cdot R)}{dt}$$

$$\frac{d(OH\cdot R)}{dt} = 0 = -k_2(OH\cdot R) - k_{-1}\ (OH\cdot R) + k_1\ (CH\cdot R)$$

$$\therefore\ (OH\cdot R) = \frac{k_1\ (CH\cdot R)}{k_2+k_{-1}}$$

$$\therefore\ \frac{-d(CH\cdot R)}{dt} = \frac{k_1k_2(CH\cdot R)}{k_2+k_{-1}} \quad \text{or} \quad \frac{-d(CH\cdot R)}{(CH\cdot R)} = \frac{k_1k_2}{k_2+k_{-1}}\ dt$$

$$\therefore\ -\ln(CH\cdot R) = \frac{k_1k_2}{k_2+k_{-1}}\ t + \text{constant} = k_{obs}t + \text{constant}$$

Figure 34. Kinetic Model for the Dissociation of Nucleic Acid·3 Complexes. (CH) and (OH) refer to the closed and open conformations of the nucleic acid double helix; (R) refers to the reporter molecule.

Table 10

Observed First Order Rate Constants for the Dissociation of Complexes of 3 with Native, Denatured, and Sonicated Salmon Sperm DNA.[a]

Nucleic Acid	k_{obs}, sec^{-1}		
	k_1	k_2	k_3
Salmon Sperm (Native)	1.95	1.70	1.46
Salmon Sperm (Sonicated)	2.12	1.86	1.63
Salmon Sperm (Denatured)	32.2	17.9	10.5

[a]The reactions were followed at 410 nm in 0.05 M MES (pH 6.2, 0.10 M in Na^+) at a temperature of 20°C. Nucleic acids and 3 were used at concentrations of 3.0×10^{-4} M P/1 and 4×10^{-5} M, respectively.

considered. Printz and von Hippel have found that denatured DNA contains a large amount of short double helical segments of widely different stabilities.[82] They also found that the hydrogen exchange rates of native and denatured DNA were strikingly similar, indicating that the two preparations are similar in conformational motility. An apparent contradiction exists between these results and our own, since our results indicate that the conformational properties of the two DNA preparations are quite different. As stated previously, the hydrogen exchange reaction is thought to utilize a stacked open state of the nucleic acid conformation under mild experimental conditions. If it is assumed that the reporter is not using the stacked open state but is using the unstacked open state, the literature results may be reconciled with our own. The denatured DNA must evidently give rise to a higher steady state concentration of the unstacked open form than does the native preparation. Another possibility considered was that the structure of the denatured DNA was different enough to radically alter the types of binding sites

available. Three lines of evidence argue against this possibility. (1) It was found that the absorption spectra of denatured and native DNA·3 complexes are very similar (Table 11).

Table 11

Summary of Absorption Spectra of 3 in Buffer and in Native and Denatured Salmon Sperm DNA Solutions.[a]

Buffer		Native DNA			Denatured DNA		
λ^{max} (nm)	ε^{max}	λ^{max} (nm)	ε^{max}	%H	λ^{max} (nm)	ε^{max}	%H
381	31400	381	14330	119	381	15270	97

[a]Experiments were carried out in 0.05 M MES (pH 6.2, 0.10 M in Na^+) at ambient temperature. The base pair to reporter ratio was 5.0 and the nucleic acid concentration was 1.5×10^{-4} M P/l.

Since the percent hypochromicity is a crude measure of the closeness of contact between the reporter and the nucleic acid bases in the complex, it seems that the two types of complexes cannot be drastically different. (2) The rates of dissociation of the two types of complexes were also investigated as a function of temperature to get a measure of the activation energies involved. The Arrhenius relationship shown in equation (8) states that the derivative of the natural logarithm of the

$$d\ln k/d(1/T) = -E_a/R \qquad (8)$$

rate constant with respect to the reciprocal of the absolute temperature is equal to the activation energy for the reaction multiplied by a constant.[83] This relationship indicates that a plot of the observed rate constant for the dissociation reaction versus the reciprocal of the absolute experimental temperature should yield a straight line with a slope that gives a measure of the activation energy for the reaction. The results of such studies on complexes of 3 with denatured and native DNA are shown in Figures 35 and 36, respectively. The activation

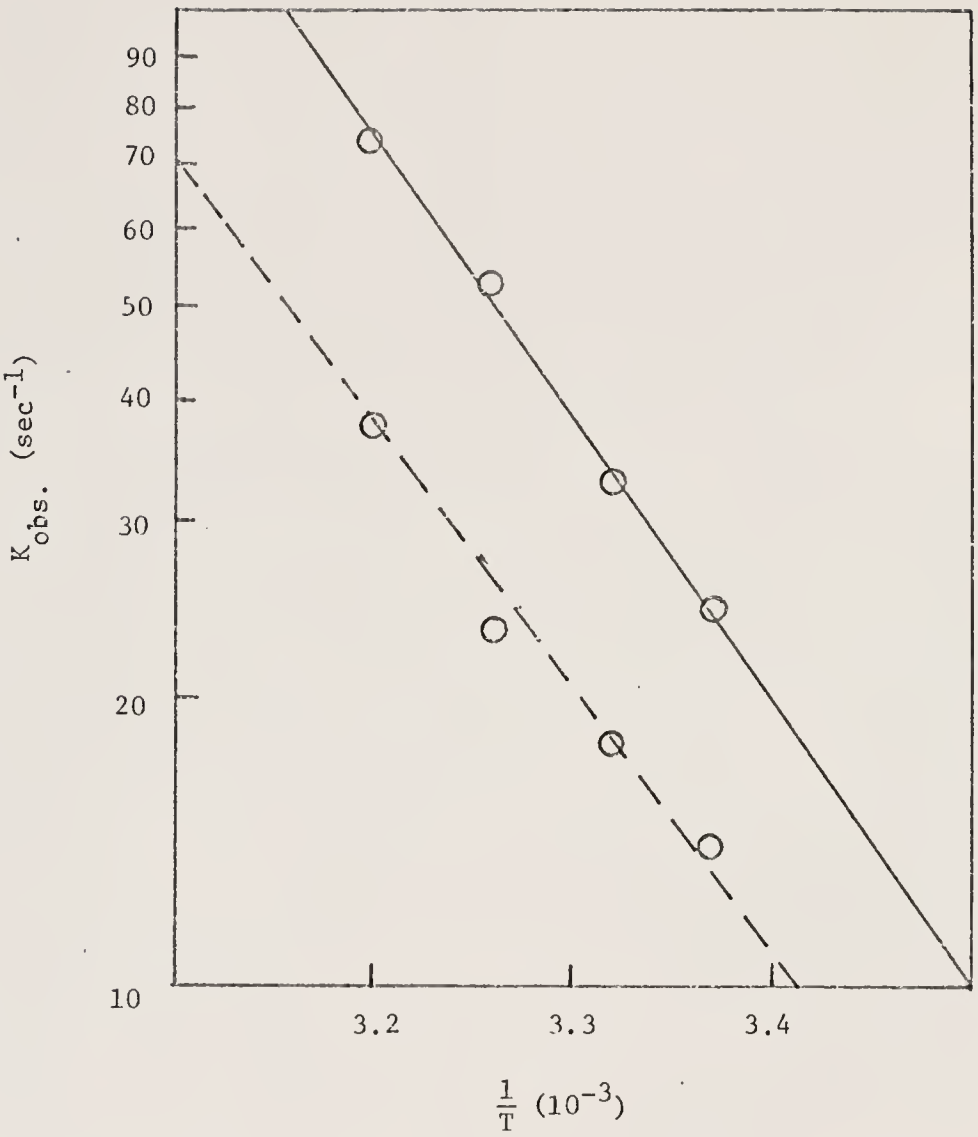

Figure 35. Van't Hoff Plot for k_1 (——) and k_2 (---) Rate Processes in the Dissociation of Denatured Salmon Sperm DNA·3 Complex. Experiments were done at DNA and 3 concentrations of 3.0×10^{-4} M P/1 and 4.0×10^{-5} M, respectively, in 0.05 M MES (pH 6.2, 0.10 M in Na^+).

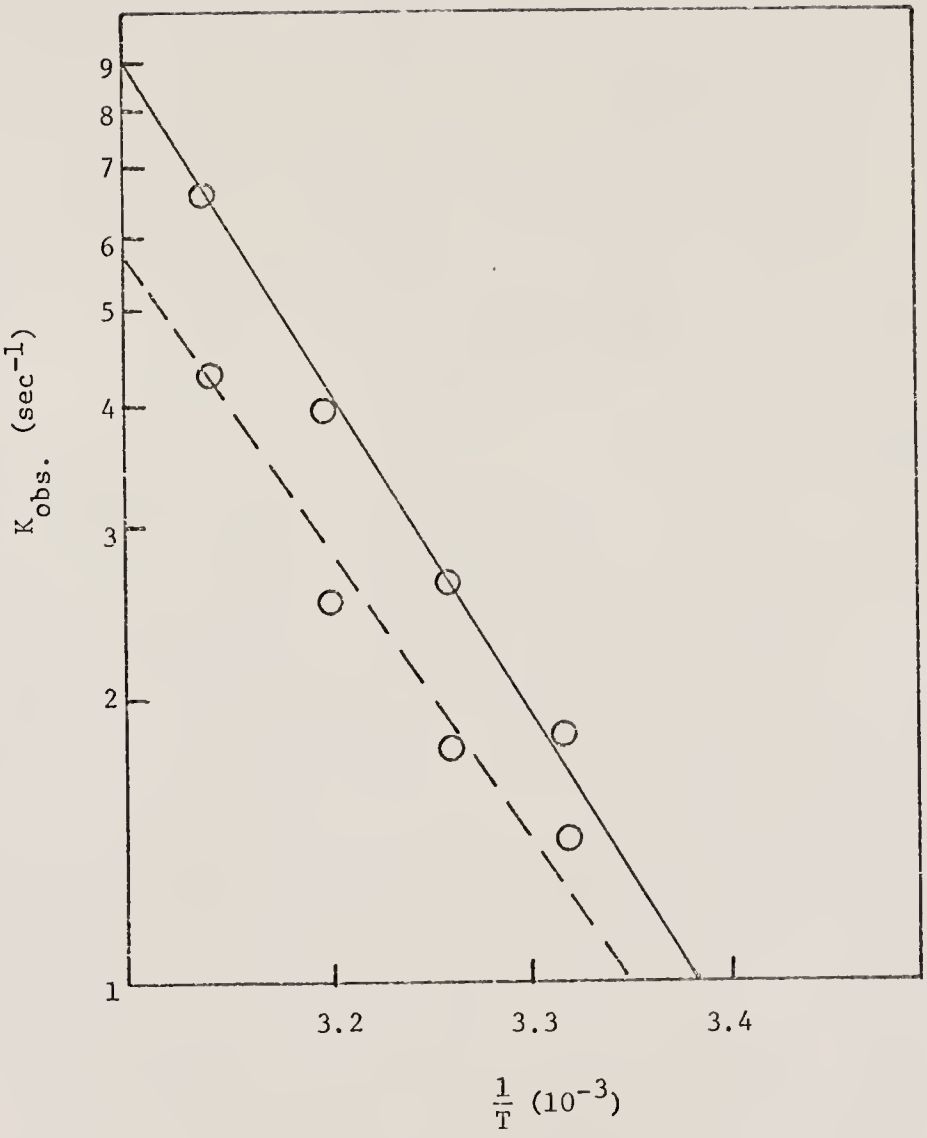

Figure 36. Van't Hoff Plot for k_1 (___) and k_2 (---) Rate Processes in the Dissociation of Native Salmon Sperm DNA·3 Complex. Experiments were done at DNA and 3 concentrations of 3.0 x 10^{-8} M P/e and 4.0 x 10^{-5} M, respectively, in 0.05 M MES (pH (.2, 0.10 M in Na^+).

energies determined from these plots are all in the range 13-16 kilocalories per mole and indicate that the two types of DNA may be quite similar. (3) The two types of complexes were also compared by equilibrium dialysis techniques. A number of different concentrations of reporter molecule are dialyzed against a single concentration of nucleic acid, and the position of the equilibrium is assessed according to the methods outlined previously. The concentration of the unbound reporter is determined via measurement of the absorbance of the solution in the side of the dialysis vessel containing no DNA and is inserted into the Scatchard equation (9), where $\bar{n}$ is the number of moles of reporter bound

$$\bar{n} = \bar{n}_{max} - (1/K_a)\ (\bar{n}/R_f) \qquad (9)$$

per mole of phosphates, $\bar{n}_{max}$ represents maximum binding, K_a is the association constant for the DNA·3 complex, and R_f is the concentration of free reporter molecules.[84] A plot of $\bar{n}$ versus $\bar{n}/R_f$ then gives the values for $\bar{n}_{max}$ (x-axis intercept) and $\bar{n}_{max}K_a$ (y-axis intercept). Table 12 shows the results of these studies for complexes of 3 and 7 with both native and denatured salmon sperm DNA, and the data plots are reproduced in Figures 37 and 38 for complexes of 3 and 7, respectively. The calculated values for the minimum number of base pairs required to provide one strong binding site for the reporter ($1/2\bar{n}_{max}$) are also shown in Table 12. These data indicate still another similarity between the two types of complexes. Both types yield the same value for the maximum number of reporters able to be bound to the nucleic acid on a per phosphate basis ($1/2n_{max}$), although the binding constants (K_a) are quite different. For example, 3 binds to both types of DNA to the extent of 0.166-0.167 molecules per nucleic acid phosphate, while the binding constants are 26.7×10^4 and 12.6×10^4 for reaction with native and denatured DNA, respectively.

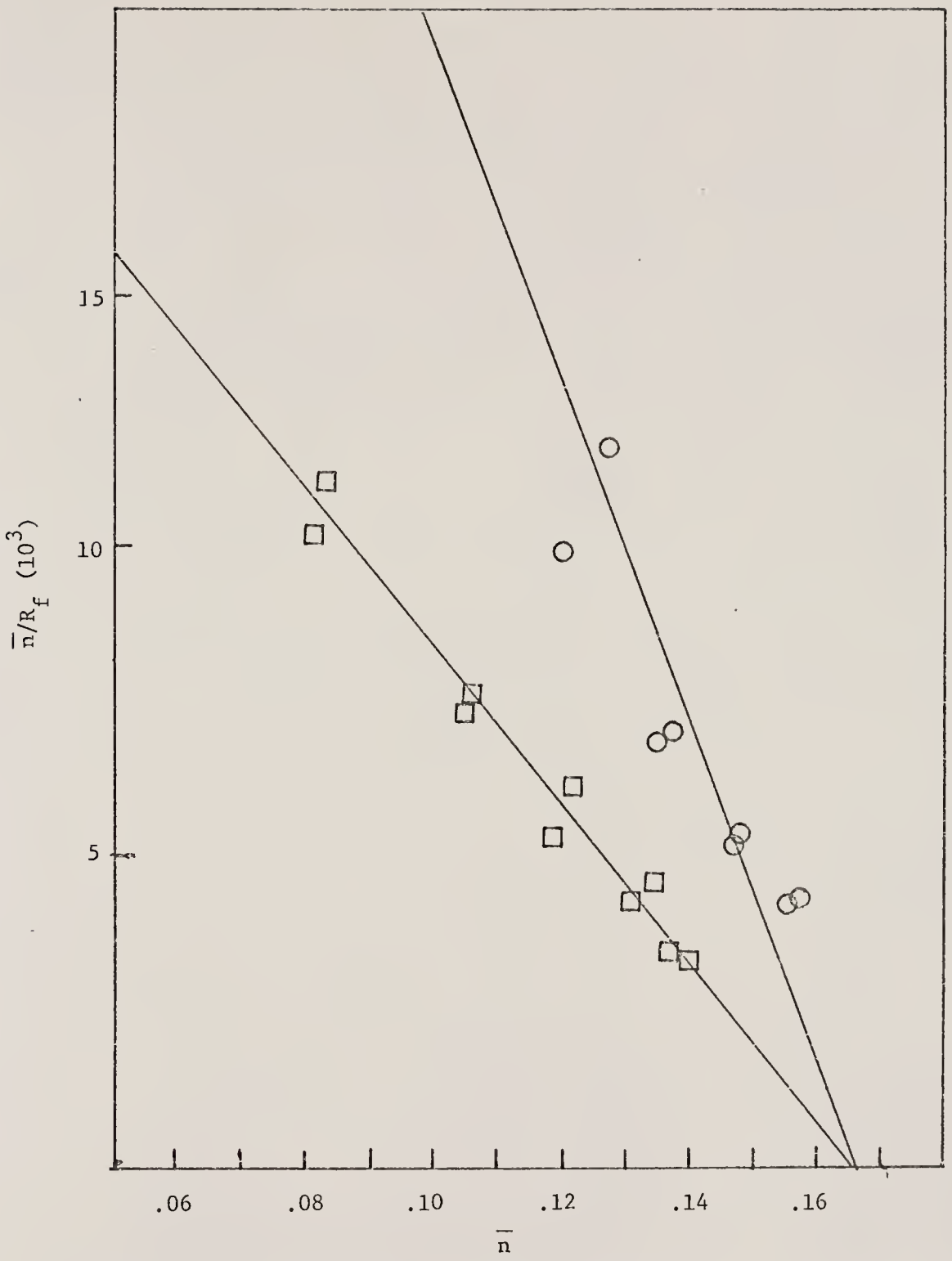

Figure 37. Scatchard Plot for Equilibrium Dialysis of 3 with Native (O—O) and Denatured (□—□) Salmon Sperm DNA.

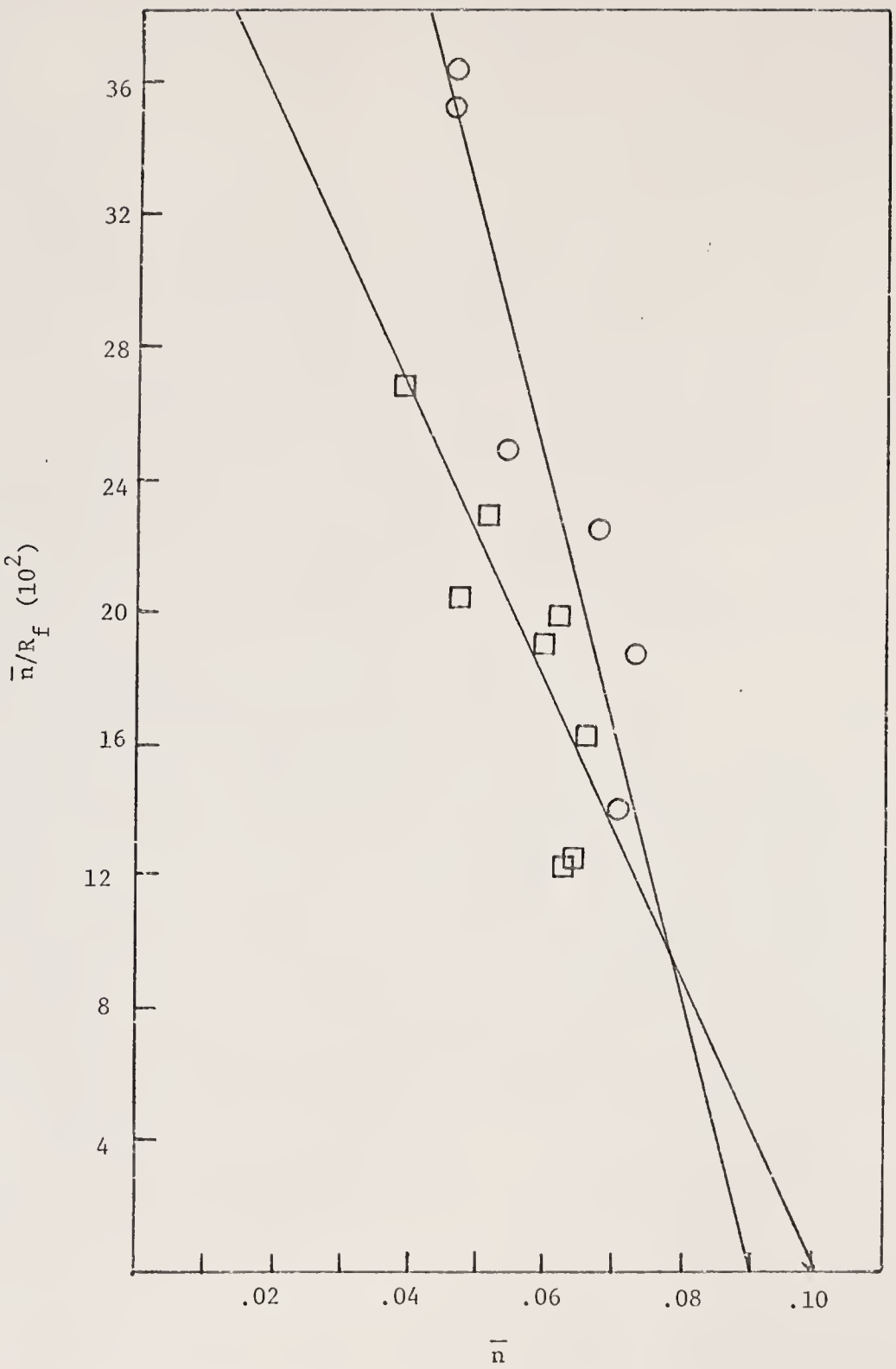

Figure 38. Scatchard Plot for Equilibrium Dialysis of 7 with Native (○—○) and Denatured (□—□) Salmon Sperm DNA.

Table 12

Equilibrium Dialysis Results for Native and Denatured Salmon Sperm DNA Complexes of 3 and 7.[a]

Reporter	DNA	$K_a (10^4)$	$\bar{n}_{max}$	$1/2\bar{n}_{max}$
3	native	26.7	0.167	3.00
3	denatured	12.6	0.166	3.00
7	native	4.4	0.100	5.00
7	denatured	7.9	0.090	5.56

[a]Experiments were carried out in BPES (0.08 M Na_2HPO_4, 0.02 M NaH_2PO_4, 0.18 M NaCl, 0.01 M Na_2EDTA, pH 6,9) at ambient temperature. The DNA concentration was 3.0×10^{-4} M P/l, and the reporters were used at initial concentrations of 2,3,4,5, and 6×10^{-5} M.

Experiments with nucleic acids of differing base content

Still further experiments showed that the dissociation rates were a function of the base content of the nucleic acid used to form the complex (Table 13). It can be seen that the rates of dissociation are fastest for those nucleic acids which are richest in adenine and thymine. This implies that the AT base pairs cause a higher steady state concentration of the reactive open forms under the experimental conditions. The fact that poly dAT-poly dAT associated with the reporter 3 about three times as fast as did poly dG-poly dC also fits in quite well with these data.

Table 13

Observed First Order Rate Constants for Dissociation of Complexes of 3 with Nucleic Acids of Differing Base Content.[a]

Nucleic Acid	%A+T	k_{obs}, sec^{-1}		
		k_1	k_2	k_3
Poly dAT-poly dAT	100	4.22	-	-
C. perfringens	76	2.35	1.99	1.74
Calf Thymus	58	1.93	1.45	1.15
Salmon Sperm	58	1.74	1.56	1.19
M. luteus	24	1.25	0.81	0.44

[a]Kinetic measurements were carried out at 20°C in 0.05 M MES (pH 6.2, 0.10 M in Na^+) and followed at 410 nm. Nucleic acids and 3 were used at 3.0×10^{-4} M P/l and 4.0×10^{-5} M, respectively, except in the experiments with poly dAT-poly dAT, where the concentrations were 2.2×10^{-5} M P/l and 2.0×10^{-5} M, respectively.

In summary, the results indicate that the dynamic aspects of nucleic acid conformation depend upon the particular bases involved in the opening segment. This finding is quite significant, as it is easy to imagine the role of such open structures in the many important biological processes where open single strand conformations have been indicated to be necessary. Two examples are genetic recombination and nucleic acid replication. The fact that the formation of the open segment has been indicated to be base content-dependent presents an obvious method for the introduction of specificity into these processes.

RESULTS AND DISCUSSION-PART II

The second part of the dissertation deals with the investigation of precisely which features of the p-nitroanilines (Figure 39) are

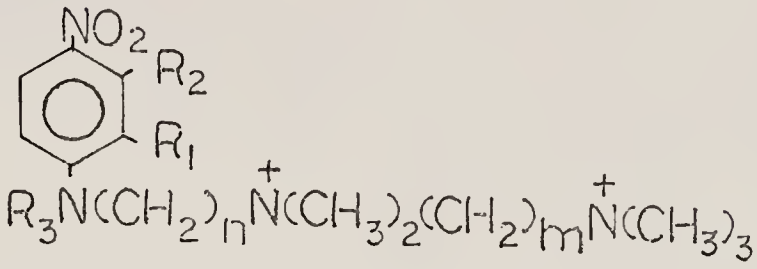

Figure 39. The p-Nitroaniline Reporter Molecule.

responsible for specificity in their interactions with nucleic acids. That such specificity may exist is indicated by the results of Gabbay and Gaffney.[59] Circular dichroism studies showed that the reporter molecules exhibited a more negative induced CD effect in the presence of those nucleic acids richest in adenine-thymine base pairs. Further, as stated previously, the drug actinomycin has been shown to exhibit selectivity for those nucleic acids richest in guanine. This behavior has been postulated to involve specificity in the stacking forces present in the complex.[53]

A number of experimental methods including pmr, ultraviolet-visible spectroscopy, melting temperature profiles, viscosity measurements, circular dichroism studies, and equilibrium dialysis binding studies were used to investigate the intercalation reactions of a number of different p-nitroaniline reporter molecules in the presence of nucleic acids. The results of these studies will be presented and

discussed in order.

Ultraviolet-Visible Spectral Studies

The results of comprehensive ultraviolet-visible spectral studies show several points worthy of note (Table 14). (1) The hypochromicity value ($\%H = [\varepsilon^{max}_{H_2O}/\varepsilon^{max}_{p} - 1]\ 100$) is most pronounced with those compounds bearing only planar substituents. For example, 8 (2-NO_2) and 14 (2-CN) show percent hypochromicity values of 75% and 68%, respectively, in the presence of salmon sperm DNA. These results suggest that the planarity of the aromatic system of the reporter molecule is important for a close contact of the reporter and the nucleic acid bases in the complex. The hypochromic effect in the absorption spectrum of the reporters is due to intensity interchange between the electronic transitions of the latter and those of the nucleic acid bases and is probably a good indicator of the contact distance in the complexes. (2) The percent hypochromicity values for the 4-nitroaniline series and those for the 2,4-dinitroaniline series are affected differently by increases in the size of the N-alkyl substituent. The percent hypochromicity values for the 2,4-dinitroaniline series are 75% for 8 (2-NO_2), 47% for 9 (2-NO_2, N-CH_3), 31% for 10 (2-NO_2, N-C_2H_5), and 29% for 11 (2-NO_2, N-C_6H_{11}). On the other hand, the values for the 4-nitroaniline series are 33% for 12 (unsubstituted), 30% for 13 (N-CH_3), 45% for 20 (N-C_6H_{11}), and 35% for 21 (N-C_7H_7). The results indicate that the presence of progressively larger N-alkyl substituents in the 2,4-dinitroaniline series causes a progressive increase in the contact distance between the reporter and the nucleic acid bases in the complex, although little effect is observed in the 4-nitroaniline series. The most obvious explanation for the results is increasing steric interference

Table 14

Summary of the Absorption Spectra of Reporter Molecules in Buffer, 95% Ethanol, and Salmon Sperm DNA Solution.[a]

Reporter	H_2O-Buffer		95% Ethanol		Salmon Sperm DNA		%H[b]
	λ^{max} (nm)	ε^{max}	λ^{max} (nm)	ε^{max}	λ^{max} (nm)	ε^{max}	
8	350	15600	341	14680	356	8700	75
9	367	12750	352	13050	374	8700	47
10	368	11290	353	10970	378	8600	31
11	369	9250	353	9160	381	7180	29
12	382	15700	369	16600	392	11800	33
13	399	14150	378	13700	402	13400	30
14[c]	352	14900	341	17500	367	8890	68
15[c]	387	14440	371	14840	399	10440	38
16[c]	381	13600	366	13600	392	10700	27
17[c]	360	15300	346	16700	367	10200	50
19[c]	356	16160	343	16050	362	10340	56
20	403	13500	381	13100	407	9400	45
21[c]	390	17500	367	16900	395	12200	35

[a]Absorption spectra were taken at ambient temperature in 0.01 M MES (pH 6.2, 0.005 M in Na^+) at base

Table 14. continued.....

pair to reporter ratios of 50-75 and reporter concentrations of 1×10^{-4} M; under these conditions, the reporters are fully bound.

[b] Percent hypochromicity (%H) = $[\varepsilon_{H_2O}^{max}/\varepsilon_{P}^{max} - 1]$ 100%, where $\varepsilon_{H_2O}^{max}$ and ε_{P}^{max} are the extinction coefficients in the absence and presence of nucleic acid, respectively.

[c] Experiments done by Gabbay and Gaffney.[59]

between the 2-nitro group and the N-alkyl group, resulting in increasing nonplanarity of the aromatic system of the reporter. Consideration of the molar absorptivity values (ε^{max}) for the reporters in buffer solution lends further support to this explanation. Increasing the size of the N-alkyl substituent in the 2,4-dinitroaniline series causes a steady decrease in the molar absorptivity from 15600 for 8 (2-NO_2) to 9250 for 11 (2-NO_2, N-C_6H_{11}), while no such effect is seen in the 4-nitroaniline series. Twisting of the alkyl-substituted aniline nitrogen atom with respect to the rest of the aromatic system of the reporter would decrease the resonance interaction between the nonbonded electrons of the former and the rest of the aromatic system due to poor orbital overlap. Since a charge transfer transition contributes to the intensity of the absorption spectra for systems of this kind, the overall intensity will decrease upon partial removal of the delocalization capability of the aniline nitrogen.[85] (3) Compounds 13 (N-CH_3), 15 (2-CH_3), and 16 (3-CH_3) have percent hypochromicity values of 30%, 38%, and 27%, respectively, in the presence of nucleic acid. The results indicate that the position of the methyl substituent may influence the contact distance between the reporter and the nucleic acid bases in the complex.

Proton Magnetic Resonance Studies (Pmr)

Pmr spectra were obtained for a number of p-nitroaniline reporter molecules in both the absence and the presence of salmon sperm DNA (Table 15). It is observed that the signals for the protons of the reporters are both broadened and shifted upfield in the presence of DNA (Figure 40). As discussed previously, the broadening is attributed to the slow tumbling rate of the large nucleic acid molecule,

Table 15

Chemical Shifts (δ) in Hz from the Internal Standard Sodium 2,2-dimethyl-2-silapentanesulfonate (DSS) of Free and DNA-bound Reporters at Various Temperatures.[a,b]

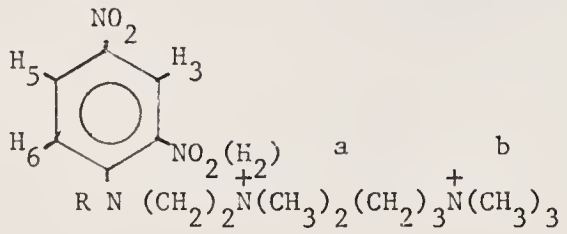

Sample	Temperature (C°)	$\delta(H_3)$				
		H_3	H_5	H_6	$H_a + H_b$	
8·DNA	37	-	-	-	321.5 bs	
	50	-	-	-	316.5 bs	
	90	-	-	-	313 s	318 s
	Q	-	-	-	318 bs	
8	37	904d(2.5)	831dd(9.5, 2.5)	717d(9.5)	318 s	
	90	902d(2.5)	886dd(10, 2.5)	720d(9.5)	319.5 s	318 s
9·DNA	37	-	797bm	-	320.5 bs	
	50	796bm	-	-	317 bs	
	90	847d(3)	801dd(11, 1)	721d(10)	321.5 s	318.5 s
	Q	-	782bm	-	321 bs	
9	37	879d(3)	836dd(9.5, 2.5)	741d(9.5)	325 s	320 s
	90	828.5d(2.5)	840dd(9.5, 2.5)	745d(9.5)	325 s	321 s
10·DNA	37	-	788bm	-	317 bs	
	50	801d(2)	-	-	318 bs	
	90	850d(2.5)	817dd(10, 3)	737d(10	318 s	316 s
	Q	-	-	-	318 bs	
10	37	881d(2.5)	842dd(10, 3)	749d(9.5)	375 s	322 s
	90	876d(3)	842dd(9.5, 3)	751d(9)	322.5 s	320 s

Table 15 Continued

Sample	Temperature (C°)	δ(H_3) H_3	H_5	H_6	$H_a + H_b$	
11-DNA	37	-	-	-	320 bs	
	50	-	-	-	317 bs	
	90	847d(3)	828dd$\binom{8}{2.5}$	747d(9)	320 s	318 s
	Q	-	-	-	321 bs	
11	37	876d(2.5)	842dd$\binom{9.5}{2.5}$	753d(9.5)	322 s	319 s
	90	907d(2.5)	886dd$\binom{10}{2.5}$	720d(9.5)	321.5 s	319 s
		$H_{3,5}$	$H_{3,6}$			
12·DNA	37	751bm	618bm		316.5 bs	
	50	754bm	619bm		318 bs	314 s
	90	786d(9)	557d(9.5)		324 s	314.5 s
	Q	-	-		318.5 bs	
12	37	814d(9)	628d(9)		323.5 s	310 s
	90	818d(9)	683d(9)		327 s	314 s
13·DNA	37	-	-		317 bs	
	50	748bs	-		318 bs	
	90	784d(10)	654d(9.5)		324.5 s	317.5 s
	Q	-	-		324 bs	
13	37	813d(9)	684d(9.5)		326 s	316 s
	90	820.5d(9)	689.5d(9.5)		329 s	320.5 s
20·DNA	37	-	-		324 bs	
20·DNA	50	-	-		319.5 bs	
	90	786.5d(9)	663.5d(9)		331 s	322.5 s
	Q	-	-		323 bs	
20	37	814.5d(9)	691.5d(9)		333.5 s	323 s
	90	818.5d(9.5)	694d(9)		331.5 s	321.5 s

[a] Sonicated low molecular weight (<500,000) salmon sperm DNA was used at 0.16 M P/1 in D_2O. Reporters were 0.02 M.

[b] Multiplicity of signals is as follows: s, singlet; bs, broad singlet; d, doublet; dd, doublet of doublets; bm, broad multiplet. The coupling constnats are shown as follows: $\binom{J_{AB}}{J_{BC}}$.

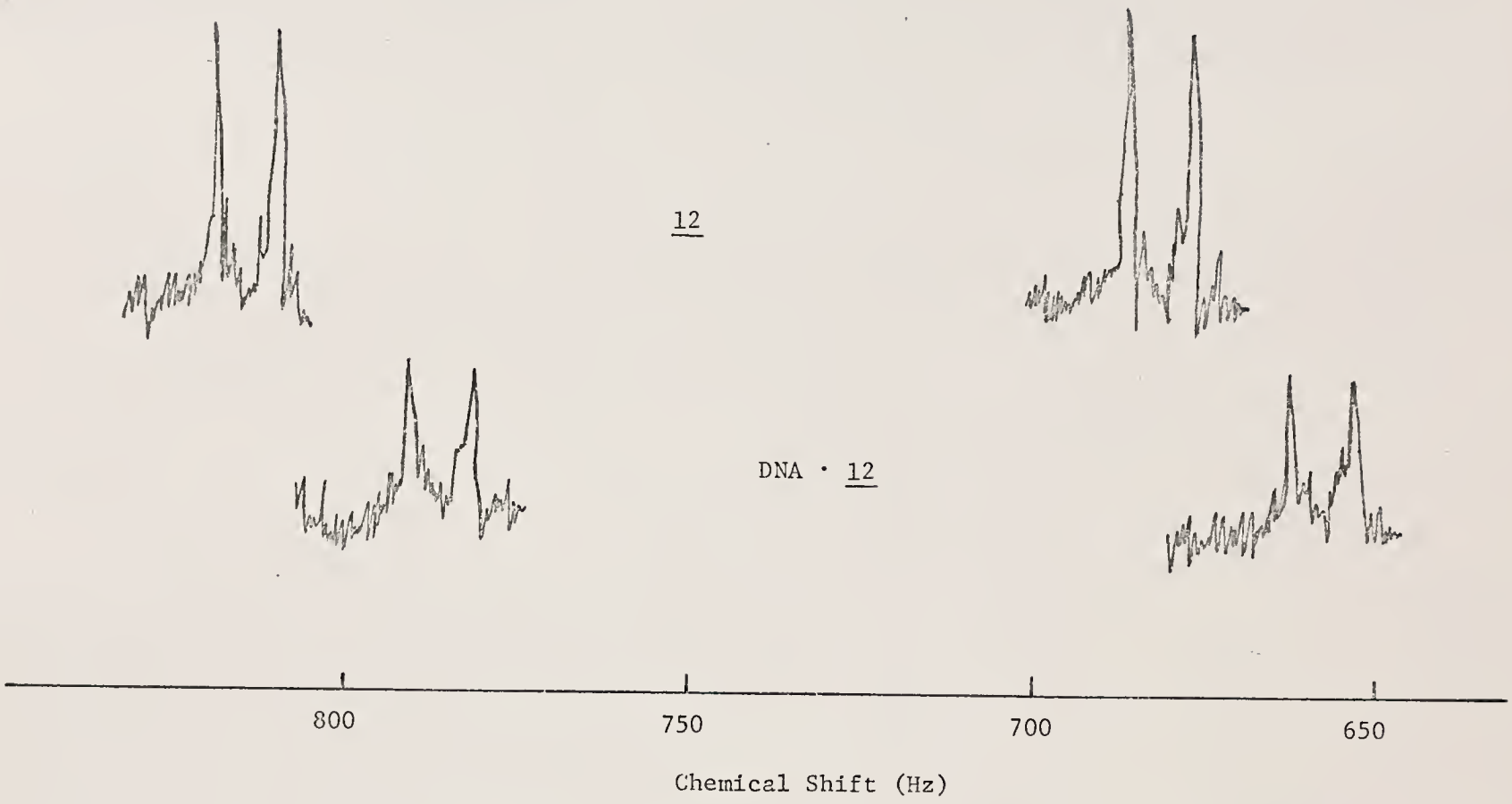

Figure 40. Partial Pmr Spectra for 12 and Salmon Sperm DNA·12 Complex at 90°C. Chemical Shifts are Measured from the Internal Standard DSS.

and the upfield shifts are due to the ring current effect of the aromatic nucleic acid bases. Both observations are compatible with an intercalation mechanism for binding of the reporters to the nucleic acid.

In a manner analogous to that used by Jardetsky and Fischer to determine the portions of the penicillin G molecule involved in binding to the protein bovine serum albumin,[68] a comparison of the upfield shifts observed for the pmr signals of the different aromatic protons of the reporter molecule in the presence of the nucleic acid can be used to determine the geometry of the small molecule in the complex (Table 16) The upfield shifts ($\Delta\delta$) are calculated according to equation (10), where δ_{free} is the chemical shift for a particular proton at 90°C in the absence of DNA and δ_{bound} is the chemical shift for the proton at 90°C in the presence of DNA. Comparisons of chemical shifts determined at

$$\Delta\delta = \delta_{free} - \delta_{bound} \qquad (10)$$

lower temperatures are not meaningful due to the extensive line broadening observed in the spectra of the DNA-reporter complexes under such conditions. Due to the temperature conditions, the relevant DNA species is the single strand, and the conclusions reached may or may not apply to the native DNA-reporter complexes present at ambient temperature.

The "in" geometry postulated previously for the intercalated reporter molecule is in agreement with the pmr evidence, as it would explain the greater ring current effect experienced by the H-3 proton in the 2,4-dinitroaniline series as compared to the H-6 proton (Figure 41). The H-6 proton is located on the outside perimeter of the nucleic acid structure and would be expected to experience less of the ring current effect than does the H-3 proton located deep inside the nucleic acid. The manner in which the upfield shifts for the various protons depend on

Table 16

Upfield Shifts in the Pmr Signals of the Aromatic Protons of Reporter Molecules in the Presence of Salmon Sperm DNA.[a]

Reporter	Upfield Shift ($\Delta\delta$) in Hz[b]		
	H_3	H_5	H_6
8	c	c	c
9	32	35	20
10	31	35	17
11	27	14	8
	$H_{3,5}$	$H_{2,6}$	
12	21	28	
13	30	29	
20	28	28	

[a]Sonicated salmon sperm DNA (MW 5 x 10^5) was used at 0.16 M P/1 in D_2O, and reporters were 0.02 M.

[b]$\Delta\delta = \delta_{free} - \delta_{bound}$, where δ_{free} is the chemical shift for a proton in the absence of DNA and δ_{bound} is the chemical shift for this proton in in the presence of DNA.

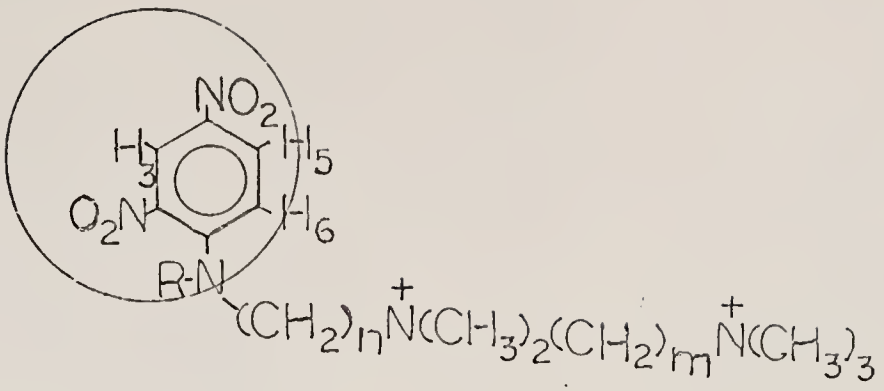

Figure 41. Reporter-DNA Complex in the "In" Geometry.

the N-alkyl substituent also agrees with the preceding analysis. If larger N-alkyl substituents increase the contact distance between the reporter and the nucleic acid bases in the complex, the effect would be expected to be more noticeable in the upfield shifts of the perimeter protons than in those of the H-3 proton located deep inside the nucleic acid structure. This is exactly what is observed, i. e., the upfield shifts for the H-3 protons of 9 (2-NO_2, N-CH_3), 10 (2-NO_2, N-C_2H_5), and 11 (2-NO_2, N-C_6H_{11}) in the presence of DNA are 32 Hz, 31 Hz, and 27 Hz, respectively, while the upfield shifts for the H-6 protons of these compounds are 20 Hz, 17 Hz, and 8 Hz, respectively. The upfield shifts for the H-5 protons of 9 (2-NO_2, N-CH_3) and 10 (2-NO_2, N-C_2H_5) in the presence of DNA are both 35 Hz, while that for the H-5 proton of 11 (2-NO_2, N-C_6H_{11}) is only 14 Hz. The large decreases in ring current effect experienced by the H-5 and H-6 protons of 11 as compared to the corresponding protons of 9 and 10 indicate that the large N-cyclohexyl substituent in the former causes a rather drastic increase in the contact distance between the reporter and the nucleic acid bases in the complex.

The 4-nitroaniline series exhibits a completely different trend. Slight increases in the upfield shifts observed in the presence of DNA are seen for the protons of the N-alkylated compounds 13 ($N-CH_3$) and 20 ($N-C_6H_{11}$) as compared to those of the unsubstituted compound 12. The data indicate that steric interference between the 2-nitro group and the N-alkyl substituents in the 2,4-dinitroaniline series may be masking a hydrophobic effect which favors the formation of a complex in which the reporters are in close contact with the nucleic acid bases. The DNA double helix possesses two hydrophobic regions, one in the grooves[86] and another between adjacent stacked bases, i. e., in the intercalation site. The hydrophobic nature of the N-alkyl substituents may increase the affinity of the reporter molecules for the nucleic acid by interacting with one of these regions of the DNA structure, though this effect is overcome by the steric problems inherent in the N-alkylated 2,4-dinitroanilines.

Melting Temperature Studies

All of the reporters examined cause an increase in the T_m of the helix-coil transition of DNA (Table 17). The added stability of the double helix with respect to thermal melting seen in the presence of the positively charged reporters is expected due to the decreased interstand phosphate-phosphate ionic repulsions. Further, a detailed consideration of the data reveals some interesting points. (1) Increasing the size of the N-alkyl substituent in the 2,4-dinitroaniline series results in progressively decreased stabilization of the DNA double helix against thermal melting. Salmon sperm DNA in the presence of 1×10^{-5} M concentrations of 8 ($2-NO_2$), 9 ($2-NO_2$, $N-CH_3$), 10 ($2-NO_2$, $N-C_2H_5$), and 11 ($2-NO_2$, $N-C_6H_{11}$) has melting temperatures which are 13.9C°, 5.4C°,

Table 17

The Effect of Reporter Molecules on the Temperature of the Helix-Coil Transition of Salmon Sperm DNA.[a]

Reporter	T_m^b (°C)	T_m^c (°C)
NONE	61.3	61.3
8	75.2	79.5
9	66.8	70.2
10	64.4	67.0
11	62.8	65.9
12	64.4	66.0
13	65.6	69.5
20	67.4	69.9

[a]Studies carried out in 0.01 M MES (pH 6.2, 0.005 M in Na^+) at a DNA concentration of 9.8×10^{-5} M P/1.

[b]Reporter concentration was 1×10^{-5} M.

[c]Reporter concentration was 2×10^{-5} M.

3.1C°, and 1.5C°, respectively, above that of DNA alone. (2) The effect of increasing the size of the N-alkyl group in the 4-nitroaniline series is quite different. Salmon sperm DNA in the presence of 1×10^{-5} M concentrations of 12 (unsubst.), 13 (N-CH_3), and 20 (N-C_6H_{11}) has melting temperatures that are 3.1C°, 4.3C°, and 6.1C°, respectively, above that of DNA alone. The trend in the 4-nitroaniline series indicates that progressively increasing the size of the N-alkyl substituent causes slight increases in the stabilization of the DNA double helix. The trend is reversed in the 2,4-dinitroaniline series due to the presence of the 2-nitro group and the consequent steric interference with the N-alkyl substituents.

Viscosity Studies

It has already been mentioned that the viscosity of a nucleic acid solution increases upon addition of a molecule possessing a planar aromatic system capable of intercalation. Further, it has been shown that this effect may be used to titrate the intercalating sites present in the nucleic acid. For example, a saturation curve is obtained from a plot of the relative specific viscosity versus the concentration of reporter molecule added (Figure 42). An interesting feature of such plots is the decrease in viscosity at high reporter concentration, i. e., after the DNA has been saturated. This effect is expected due to electrostatic constriction of the nucleic acid structure. Since all intercalating sites have been filled, the only effect exerted by additional increases in reporter concentration is increased shielding of the DNA phosphate-phosphate ionic repulsions. This allows the adjacent phosphates to move closer together, thereby compressing the structure, and the viscosity of the solution decreases. Experimental proof for this explanation was obtained by substituting a non-intercalating 1,3-diammonium salt for the reporter molecule after the DNA was saturated with intercalating molecules. It was found that equal increments of the reporter 8 and the 1,3-diammonium salt caused approximately equal decreases in the viscosity of the solution (Figure 42). Since the 1,3-diammonium salt has no intercalating moiety, the effect is probably due to electrostatic constriction of the DNA structure.

Viscometric titrations of salmon sperm DNA with a number of different reporters indicate that the saturation value for the base pair to reporter concentration ratio is a function of the substitution pattern of the reporter. The data shown in Table 18 are interesting in

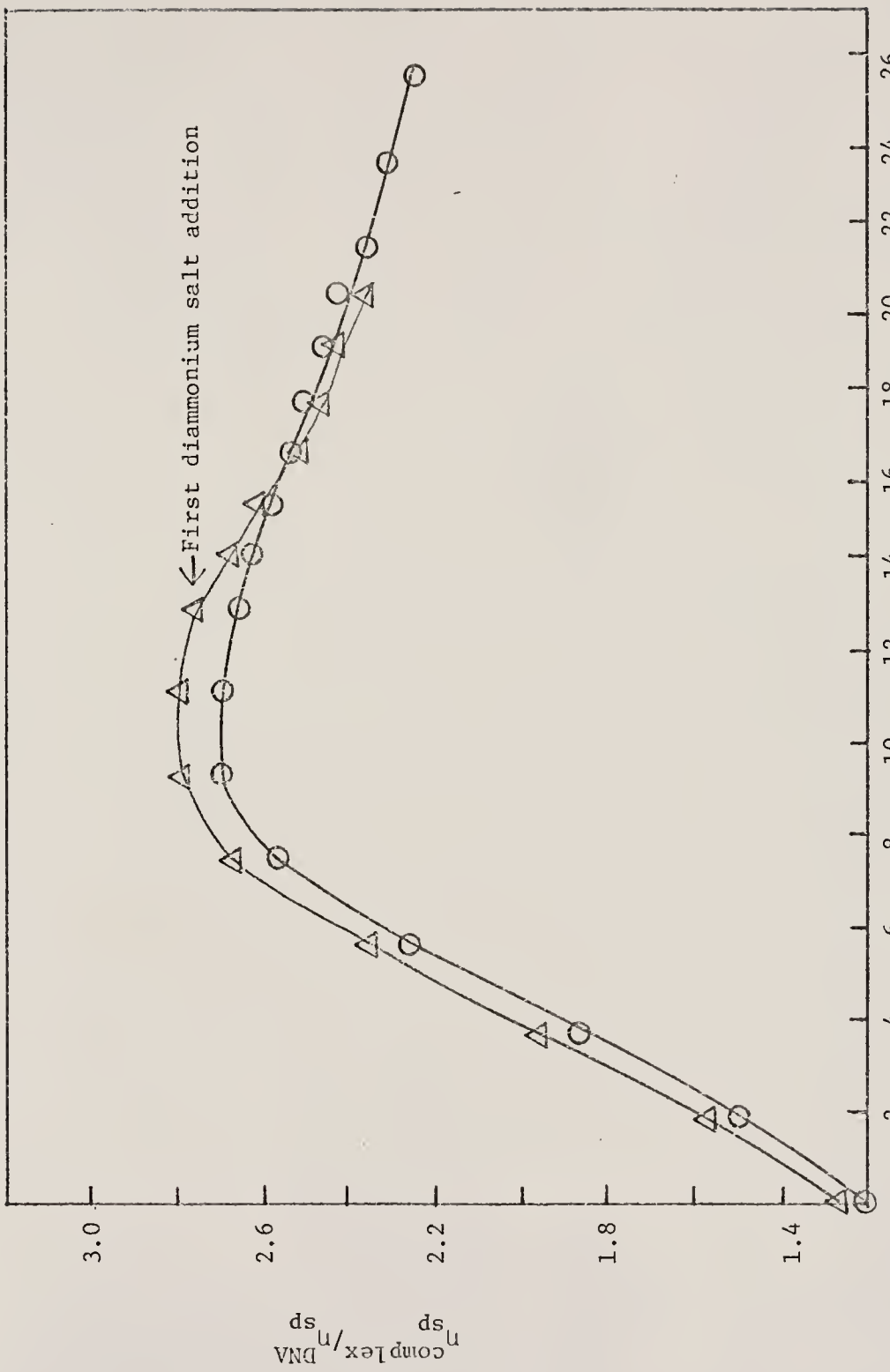

Figure 42. Viscometric Titrations of Salmon Sperm DNA with 8 (O) and 8 followed by trimethylene bis(trimethylammonium bromide) (Δ). The experiments were carried out in 0.01 M MES (pH 6.2, 0.005 M in Na^+) at 37°C using a DNA concentration of 6 x 10^{-4} M P/1.

Table 18

Results of Viscometric Titrations of Salmon Sperm DNA with Reporter Molecules.[a]

Reporter	Base Pairs/Reporter at Saturation
8	3.03
9	4.50
10	4.50
11	3.68
12	2.87
13	3.07
14	3.76
15	4.70
16	2.89
17	6.27

[a]Experiments were done at 37°C in 0.01 M MES (pH 6.2, 0.005 M in Na^+) at a DNA concentration of 4-6 x 10^{-4} M P/l; under these conditions, the reporters are at least 90% bound. The values for the base pair to reporter concentration ratio at saturation are reproducible within ±0.30.

several regards. (1) The effect of the N-alkyl substituents in the 2,4-dinitroaniline series is substantial. While 8 (2-NO_2) can intercalate to the extent of one reporter per 3.03 base pairs, the N-alkylated reporters 9 (2-NO_2, N-CH_3), 10 (2-NO_2, N-C_2H_5), and 11 (2-NO_2, N-C_6H_{11}) require 4.50, 4.50 and 3.68 base pairs, respectively, to provide one intercalation site. This result is in agreement with the other lines of evidence discussed which indicate that the N-alkyl substituents in this system cause increased steric requirements for the intercalation reaction. It should be noted, however, that the values for the base pair to reporter ratio at saturation (Table 18) do not correspond exactly to the number of base pairs required to provide one strong binding site. The reporter DNA complexes have finite association constants, and the ratio of free reporter to bound reporter in solution depends on the association constant. For this reason, the values for the base pair to reporter-concentration ratio at saturation may be somewhat lower than the true value calculated using the concentration of bound reporter. (2) The effects of substituting a methyl group at various positions in the 4-nitroaniline molecule appear to be rather different. Compounds 13 (N-CH_3), 15 (2-CH_3), and 16 (3-CH_3) can intercalate to the extent of one reporter per 3.07, 4.70, and 2.89 base pairs, respectively. The results show that the 2-methyl substituted reporter 15 is the most selective of the three. Further, substituting an even larger group at the 2-position causes increased selectivity, as shown by the fact that 17 (2-CF_3) only intercalates to the extent of one reporter per 6.27 base pairs.

Equilibrium Dialysis Studies

Extensive equilibrium dialysis studies on a number of p-nitro-

aniline reporter molecules were carried out by Sharpe[87] and analyzed by the Scatchard plot method already discussed. A typical Scatchard plot obtained for the binding of 14 (2-CN) to salmon sperm DNA is reproduced in Figure 43. Several points are evident from consideration of the data (Table 19). (1) Several reporters exhibit quite different binding behavior with the two nucleic acids used, though the base content of both is 58% AT and 42% GC. For example, 8 (2-NO_2) has binding constants of 1.12×10^5 and 2.53×10^5 with calf thymus DNA and salmon sperm DNA, respectively. (2) Molecules with a planar substituent on the aromatic system bind more strongly than do those without such a substituent. For example, 8 (2-NO_2), 14 (2-CN), and 19 (2-NO_2) have binding constants of 2.53×10^5, 2.02×10^5, and 2.35×10^5, respectively, with salmon sperm DNA, while the remaining molecules studied exhibit binding constants ranging from 2.6×10^4 for 16 (3-CH_3) to 5.7×10^4 for 13 (N-CH_3). (3) The binding constants are also sensitive to the substitution pattern. Reporters 13 (N-CH_3), 15 (2-CH_3), and 16 (3-CH_3) have binding constants of 5.7×10^4, 4.8×10^4, and 2.6×10^4, respectively, with calf thymus DNA. (4) The reporters with the highest binding constants invariably prefer salmon sperm to calf thymus DNA. Compounds 8, 14, and 19 have binding constants with salmon sperm DNA which are larger than those with calf thymus DNA by factors of 2.48, 1.62, and 1.78, respectively. This indicates that the salmon sperm DNA may have more intercalating sites suitable for forming a very strong complex than does calf thymus DNA. Studies by Sanford[88] showed that the affinity of 8 for poly dAT-poly dAT is about 2.6 times that for poly dG-poly dC. Taken together, these two observations indicate that salmon sperm DNA may have more regions rich in AT base pairs than does calf thymus DNA. These results

Table 19

Summary of Equilibrium Dialysis Studies on the Binding of Reporters to Calf Thymus and Salmon Sperm DNA.[a]

Reporter[b]	Calf Thymus[c]			Salmon Sperm[c]		
	$K_a (10^4)$	$\bar{N}_{max}$	$1/2\bar{N}_{max}$	$k_a (10^4)$	$\bar{N}_{max}$	$1/2\bar{N}_{max}$
8	11.2	.16	3.13	25.3	.14	3.57
9	4.6	.11	4.55	3.0	.19	2.63
10	2.1	.13	3.85	3.0	.13	3.85
11	9.8	.08	6.25	4.5	.12	4.17
12	3.9	.14	3.57	2.4	.14	3.57
13	3.2	.19	2.63	5.7	.19	2.63
14	12.5	.14	3.57	20.2	.14	3.57
15	6.5	.17	2.94	4.8	.16	3.13
16	2.5	.23	2.17	2.6	.22	2.17
17	4.7	.09	5.56	3.0	.11	4.55
18	3.1	.13	3.85	3.7	.12	4.17
19	13.2	.47	1.06	23.5	.37	1.28

[a] Results were obtained from Scatchard plots and are reproducible to within ± 10%.

[b] Reporter concentrations were 2,3,4,5 and 6 x 10^{-5} M in 0.01 M MES (pH 6.2, 0.020 M in Na^+).

[c] DNA concentrations were 2.5-3.0 x 10^{-4} M P/l in 0.01 M MES (pH 6.2, 0.020 M in Na^+).

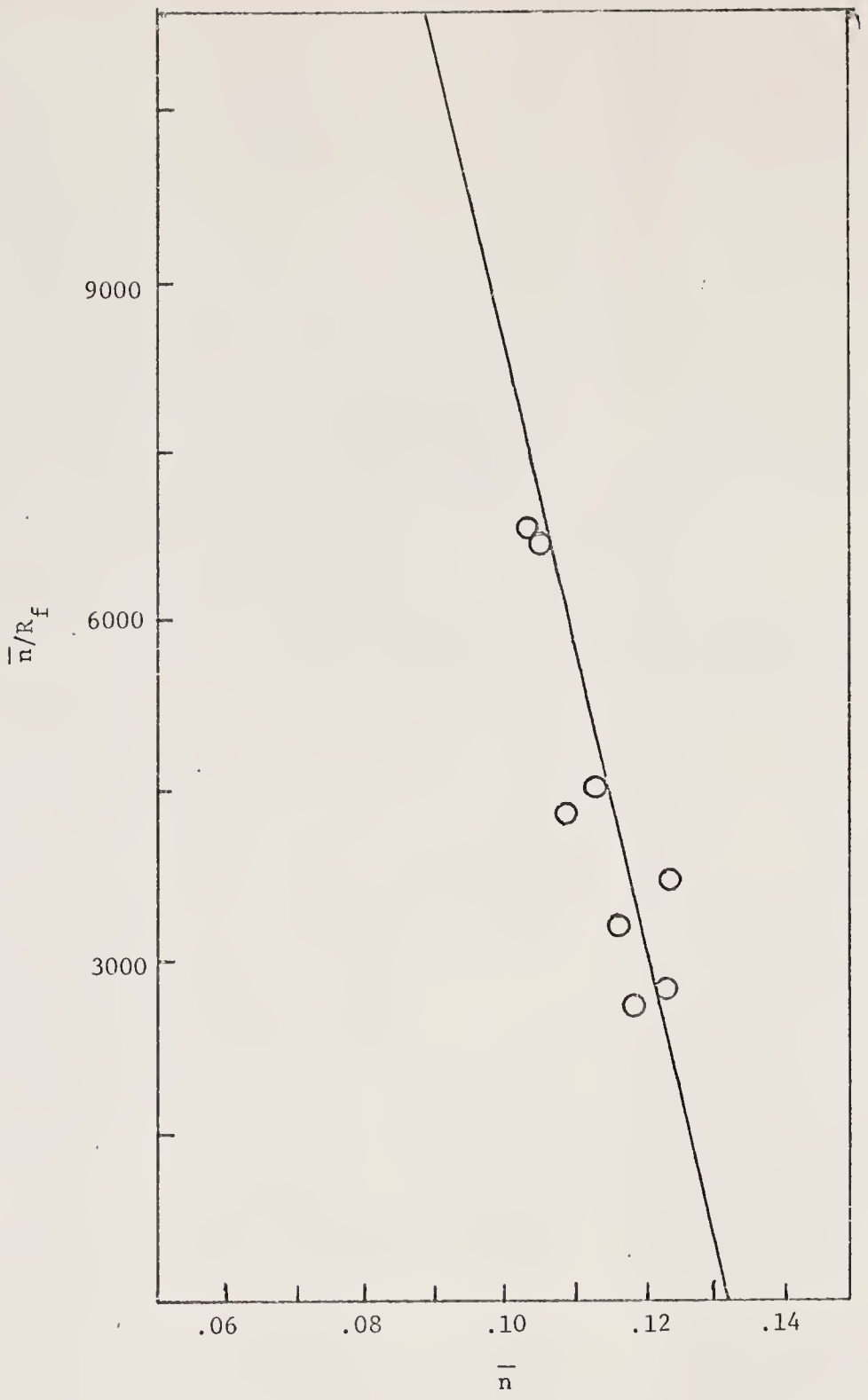

Figure 43. Scatchard Plot for Binding of 14 to Salmon Sperm DNA. Experiment was done in 0.01 MES (pH 6.2, 0.020 M in Na^+) at ambient temperature.

therefore indicate that the reporter molecules may be able to distinguish differences in the nucleic acid sequence.

Circular Dichroism Studies

The reporter molecules also exhibit an induced circular dichroism effect in the presence of DNA. While it is difficult to interpret the induced circular dichroism data from first principles, it is possible to note some interesting points (Table 20). (1) In the presence of DNA, the reporters with planar substituents on the aromatic ring exhibit induced CD effects which are much more marked than those observed with compounds having nonplanar substituents. For example, the induced CD spectra of 8 (2-NO_2) and 14 (2-CN) exhibit troughs at 361 nm ($[\theta]_M$ = -9200), respectively, while that of 15 (2-CH_3) has a trough of 410 nm ($[\theta]_M$ = -4560). These results again indicate the importance of steric considerations in the formation of the DNA-reporter complex. (2) Substituting the same group at different positions in the p-nitroaniline reporter molecule results in rather different induced CD spectra in the presence of DNA. Compounds 13 (N-CH_3), 15 (2-CH_3), and 16 (3-CH_3) have induced CD spectra exhibiting a peak at 410 nm ($[\theta]_M$ = 2600), a trough at 410 nm ($[\theta]_M$ = -4560), and a trough at 400 nm ($[\theta]_M$ = -3230), respectively. Since the CD effect is dependent on both the magnitudes of the interacting transition moments and their relative directions, the results could indicate either different positioning of 13, 15, and 16 in the complex or differences in the contact distances between the reporter and the nucleic acid bases in their respective complexes. (3) The induced circular dichroism spectrum of the DNA-reporter complexes was found to be dependent on the relative concentrations of DNA and reporter in solution. The induced CD spectra obtained at high DNA to reporter

Table 20

Summary of Induced Circular Dichroism Spectra of Salmon Sperm DNA-Reporter Complexes.[a]

Reporter	λ^t (nm)	$[\theta]_M^{t\,b} \times 10^{-3}$	λ^p (nm)	$[\theta]_M^{p\,b} \times 10^{-3}$
8	361	-10.50	-	-
9	418	- 2.70	365	1.40
10	426	- 3.20	374	2.10
11	438	- 3.20	377	5.90
12	421	- 1.80	374	1.90
13	-	-	410	2.60
14[c]	376	- 9.20	-	-
15[c]	410	- 4.56	-	-
16[c]	400	- 3.23	-	-
17[c]	388	- 2.84	-	-
18	365	- 6.24	-	-
19[c]	395 (443)	- 4.8 (-0.70)	-	-
20	-	-	395	12.20

[a] Experiments were carried out at a base pair to reporter ratio of 20-25 and a reporter concentration of 1 x 10^{-4} M at ambient temperature in either 0.01 M MES (pH 6.2, 0.005 M in Na^+) or 0.01 M phosphate buffer (0.01 M in Na^+, pH 6.5).

[b] $[\theta]_M = [\theta]_{obs} \cdot 10^2/dC$, where C is the reporter concentration and d is the path length in cm.

[c] Results of Gabbay and Gaffney.

concentration ratio (P/R = 70) and low DNA to reporter concentration ratio (P/R = 5.7) are quite different in each of the four cases examined (Figure 44). One possible explanation hinges upon the fact that there

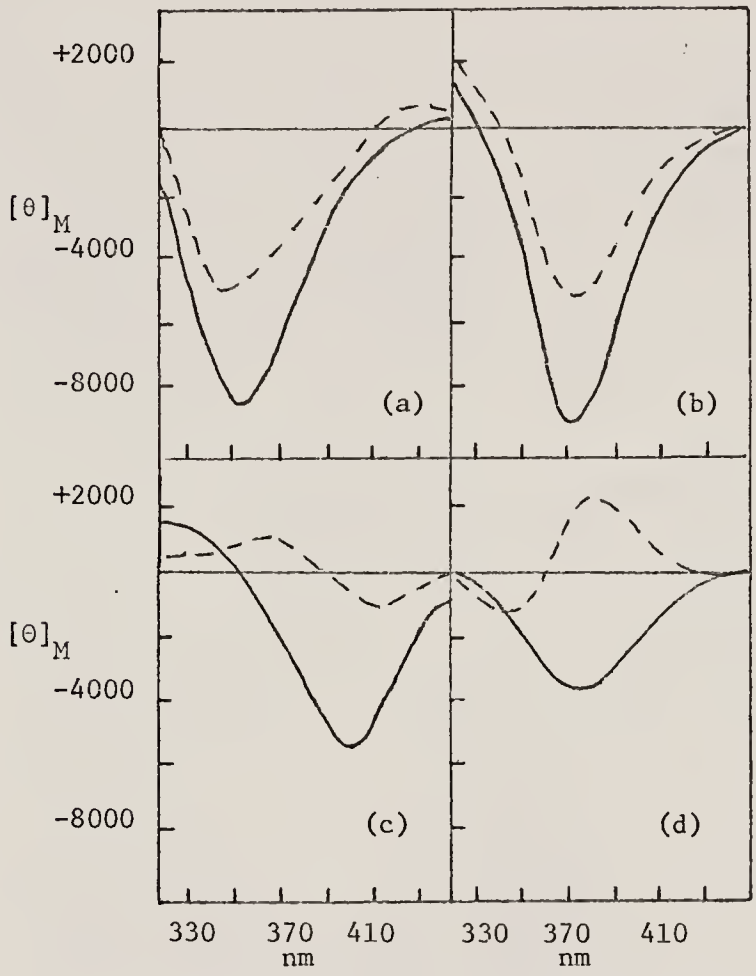

Figure 44. The Induced Circular Dichroism Spectra of the DNA-Bound Reporters 8, 14, 15, and 17 at High (———) and Low (- - - -) P/R Ratios, i.e., at 70/1 and 5.7/1: (a) DNA-Reporter 8; (b) DNA-Reporter 14; (c) DNA-Reporter 15; (d) DNA-Reporter 17.

are ten distinctly different intercalating sites in DNA as a consequence of the right-handed Watson-Crick-Wilkins double helix with the A-T and G-C base pairs (Figure 45). It is theoretically possible that the

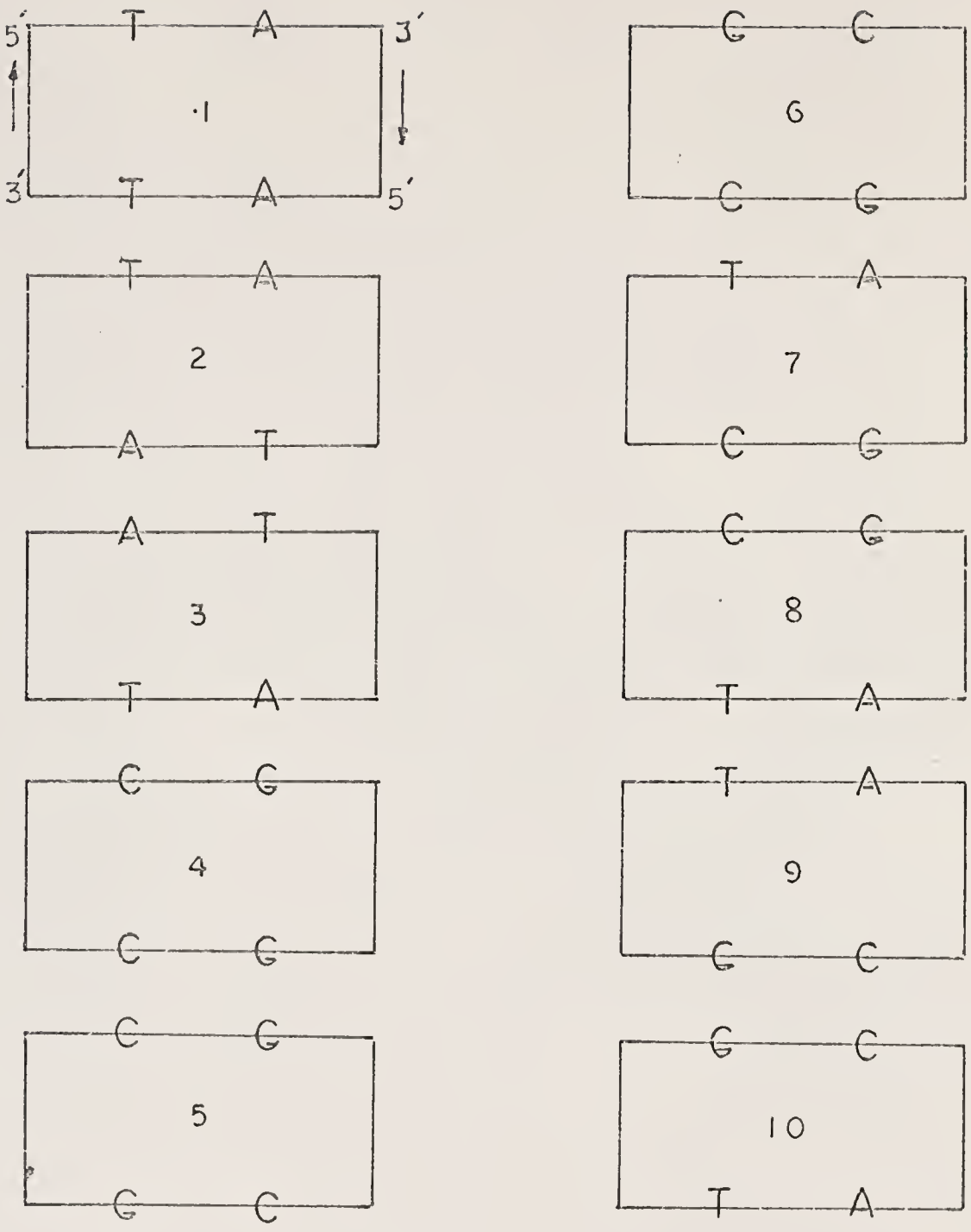

Figure 45. The Ten Different Intercalating Sites of DNA.

reporters could have different affinities for each of the 10 sites, and this line of reasoning is in agreement with the data. For example, it is instructive to examine first the results shown in Figure 44a. At high P/R ratio (2×10^{-3} M P/1 and 3×10^{-5} M 8), a limiting value for the molar ellipticity, $[\theta]_M$, is obtained, i. e., further excess of DNA gives the same value for $[\theta]_M$. Under these conditions, the reporter molecule 8 is fully intercalated and could presumably discriminate among the 10 possible sites since the base pair to reporter concentration ratio is 35/1. At low P/R ratio (3.2×10^{-4} M P/1 and 5.55×10^{-5} M 8), a lower value of $[\theta]$ is obtained. If it is assumed that all intercalating sites ellicit a negative CD band of the same magnitude in the 4-nitroaniline transition of 8, it is possible to calculate the concentration of the intercalated reporter molecule at the low P/R ratio (equation 11).

$$\frac{[\theta]_{\text{low P/R}}}{[\theta]_{\text{high P/R}}} \times (3 \times 10^{-5}\ \text{M}) = 1.75 \times 10^{-5}\ \text{M} \qquad (11)$$

If this were the true concentration of intercalated reporter 8, there would be one reporter per 9 base pairs of DNA. However, under the conditions of the low P/R experiment, all possible intercalating sites should be filled. The binding studies already discussed showed that there must be at least one reporter per 3.57 base pairs (Table 19). Hence, the assumption that all intercalating sites ellicit a negative CD band of the same magnitude is an erroneous one. In line with this is the finding by Gabbay and Gaffney that poly dAT-poly dAT and poly dG-poly dC induce molar ellipticities of -9.2×10^3 and -0.72×10^3 respectively.[59] Similar arguments can also be applied to the induced CD spectra of the DNA-reporter 14 complex shown in Figure 44b.

Figures 44c and 44d dramatically demonstrate the different induced CD of the 4-nitroaniline transition of the DNA-reporter 15 and DNA-reporter 17 complexes at high and low P/R ratios. The results seem to strongly suggest that each of the possible intercalating sites may have different affinity for the reporter molecules and could ellicit significantly different CD signals.

Significance of the Results

The ramifications of these findings are quite important, especially in the field of protein-nucleic acid interactions. It appears that one possible recognition mechanism could involve the selective interactions of aromatic amino acids with the nucleic acid double helix. This theory actually has some experimental support based on the work of Gabbay and Sanford.[75] Their studies showed that specificity exists and is dependent upon the primary sequence of the di- and tripeptide model systems used. They also showed that the peptides competed for the same binding sites used by the p-nitroaniline reporter molecules. It is then quite reasonable to assume that the forces demonstrated to be important in the interactions of the reporter molecules with nucleic acids may also be important in the protein-nucleic acid interactions. This argument assumes, of course, that the peptide models used are fair approximations to the much larger and more complex polypeptide chains of the proteins.

EXPERIMENTAL

Analyses were performed by Atlantic Microlab, Inc., Atlanta, Georgia. Proton magnetic resonance spectra were recorded on either a Varian A60A or a Varian XL-100 spectrometer by Dr. C.S. Baxter. Chemical shifts of deuterium oxide solutions were determined relative to the standard sodium 2,2-dimethyl-2-silapentane sulfonate, and chemical shifts of solutions in organic solvents were determined relative to the standard tetramethylsilane. Circular dichroism spectra were recorded using a Jasco J-20 spectropolarimeter, and the molar ellipticities were determined relative to the standard D-camphor sulfonic acid (Durrum Instrument Company). Viscosity studies were performed utilizing a low-shear Zimm viscometer from Beckman Instrument Company. Ultraviolet and visible absorption measurements were recorded using either a Cary 15 or a Gilford 240 spectrophotometer. The melting point determinations were carried out on a Thomas-Hoover Unimelt apparatus and are uncorrected.

All organic chemicals were reagent grade and were not further purified unless noted in the text. The calf thymus and salmon sperm DNA preparations were obtained from Worthington Biochemical Corporation, and the remaining polynucleotides used in these studies were obtained from Miles Laboratories. Nitroaniline reporter molecules not synthesized during the course of this work were obtained from Dr. E.J. Gabbay.

All of the various solutions used in these studies were prepared in buffers made from deionized water, and any solutions containing polynucleotides or proteins were routinely protected from bacterial

growth by refrigeration and the addition of 2-3 drops of chloroform. The biological macromolecules were stored as concentrated solutions and diluted just prior to use. In the case of the DNA preparations, the concentration of the stock solution was about 4-6 x 10^{-3} M P/1, and the ribopolymers were usually 2.5 x 10^{-3} M P/1. Polylysine hydrobromide was stored as a 0.2 mg/ml solution.

Preparation of N,N,N-Trimethyl-N',N'-dimethyl-N'(β-N-methyl 1-2,4-dinitroanilinoethyl)-1,3-diammoniumpropane dibromide, 9.

This compound was made via the synthetic route outlined in Figure 46. 1-Fluoro-2,4-dinitrobenzene (2.00 g, 0.011 moles) and N-methyl-N', N'-dimethylethylenediamine (1.11 g, 0.011 moles) were dissolved in 2-3 ml of absolute ethanol and heated to 120°C for 24 hr in a sealed tube. The solvent was then evaporated, and the resulting oil was dissolved in water (10 ml) and extracted with ethyl ether (2 x 20 ml). The water layer was then made basic to litmus by the addition of sodium hydroxide pellets and extracted with ethyl acetate (2 x 30 ml). The ethyl acetate layers were pooled, dried over anhydrous magnesium sulfate, and flash-evaporated. The resulting oil was dissolved in a minimum amount of acetone, and aqueous hydrobromic acid (47%) was added dropwise until turbidity was noted. Refrigeration, vacuum filtration, and recrystallization from ethanol-acetone yielded 2.40 g (62%) of Va, mp 197-200°C. The pmr spectrum ($CDCl_3$) showed a one-proton doublet at 8.32δ (J_{AB} = 3.0 Hz), a one-proton doublet of doublets at 8.00δ (J_{AB} = 3.0 Hz, J_{BC} = 9.5 Hz), a one-proton doublet at 7.12δ (J_{BC} = 9.5 Hz), a four-proton multiplet at 3.42δ, a six-proton singlet at 2.73δ, and a three-proton singlet at 1.97δ. Anal. Calculated for $C_{11}H_{17}N_4O_4Br$: C, 37.80; H, 4.89. Found: C, 37.84; H, 4.88.

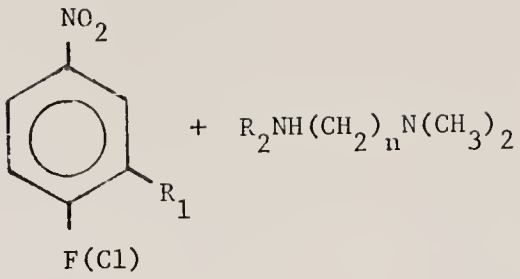

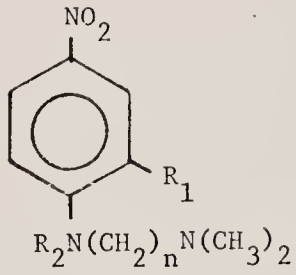

IV a $R_1=NO_2$, $R_2=CH_3$, n=2

b $R_1=NO_2$, $R_2=C_2H_5$, n=2

c $R_1=H$, $R_2=CH_3$, n=2

d $R_1=CF_3$, $R_2=H$, n=3

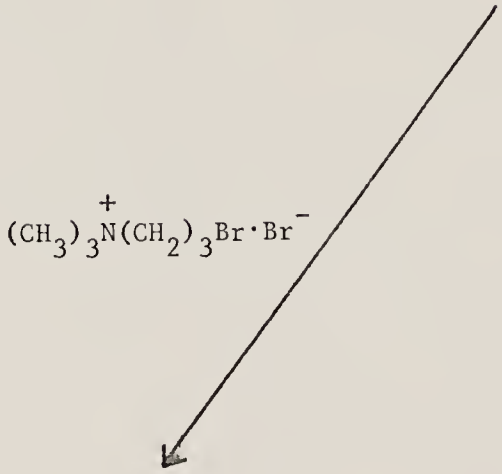

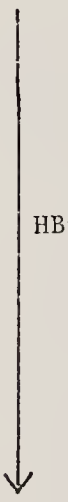

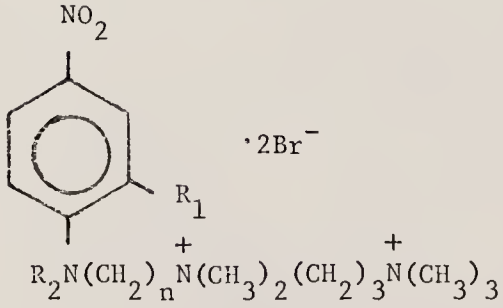

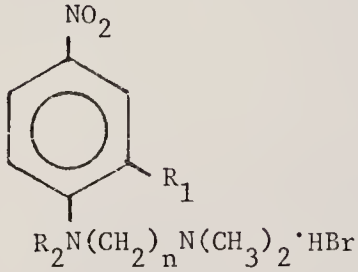

V a $R_1=NO_2$, $R_2=CH_3$, n=2

b $R_1=NO_2$, $R_2=C_2H_5$, n=2

c $R_1=H$, $R_2=CH_3$, n=2

d $R_1=CF_3$, $R_2=H$, n=3

Figure 46. Synthesis of Nitroaniline Reporter Molecules.

Va (0.52 g, 1.5 mmoles) was dissolved in water, and the solution was made basic with sodium hydroxide pellets and extracted with ethyl acetate. The ethyl acetate layer was dried over anhydrous magnesium sulfate and evaporated to an oil. The oil was dissolved in about 2-3 ml of absolute ethanol, and N,N,N-trimethyl-N-3-bromopropylammonium bromide (0.50 g, 1.65 mmoles) was added. The mixture was heated to 120°C for 24 hr in a sealed tube, then cooled to room temperature. Addition of excess acetone resulted in the precipitation of a yellow solid. Recrystallization from ethanol-acetone produced 0.58 g (73%) of the desired product, mp 215-17°C. The pmr spectrum (D_2O) showed a one-proton doublet at 8.73δ (J_{AB} = 2.5 Hz), a one-proton doublet of doublets at 8.38δ (J_{AB} = 2.5 Hz, J_{BC} = 9.4 Hz), a one-proton doublet at 7.48δ (J_{BC} = 9.4 Hz), a ten-proton multiplet at 3.80δ, a six-proton singlet at 3.38δ, a nine-proton singlet at 3.32δ, and a three-proton singlet at 3.10δ. Anal. Calculated for $C_{17}H_{31}N_5O_4Br_2$: C, 38.57; H, 5.90. Found: C, 38.68; H, 5.95.

Preparation of N,N,N-Trimethyl-N',N'-dimethyl-N'-(β-N-ethyl-2,4-dinitroanilinoethyl)-1,3-diammoniumpropane Dibromide, 10.

1-Fluoro-2,4-dinitrobenzene (2.00 g, 0.011 moles) and N-ethyl-N', N'-dimethylethylenediamine (124 g, 0.011 moles) were coupled according to the procedure used to make Va above and yielded 2.84 g (71%) of Vb. After a single recrystallization from ethanol-acetone, the mp was 201-2°C, and the pmr spectrum (D_2O) showed a one-proton doublet at 9.00δ (J_{AB} = 2.6 Hz), a one-proton doublet of doublets at 8.67δ (J_{AB} = 2.6 Hz, J_{BC} = 9.4 Hz), a one-proton doublet at 7.28δ (J_{BC} = 9.4 Hz), a six-proton multiplet at 3.38δ, a six-proton singlet at 2.08δ, and a three-proton singlet at 0.98δ. Anal. Calculated for $C_{12}H_{19}N_4O_4Br$: C, 39.68; H, 5.26. Found: C, 39.49; H, 5.37.

Vb (0.54 g, 1.5 mmoles) and N,N,N-trimethyl-N-3-bromopropyl-ammonium bromide (0.50 g, 1.65 mmoles) were allowed to react according to the procedure used to make 9 above and yielded 0.54 g (66%) of the desired product. After a single recrystallization from ethanol-acetone, the mp was 140-43°C, and the pmr spectrum (D_2O) showed a one-proton doublet at 8.83δ (J_{AB} = 2.6 Hz), a one-proton doublet of doublets at 8.47δ (J_{AB} = 2.6 Hz, J_{BC} = 9.4 Hz), a one-proton doublet at 7.52δ (J_{BC} = 9.4 Hz), a twelve-proton multiplet at 3.70δ, a pair of overlapping singlets accounting for fifteen protons at 3.27-3.32δ, and a three-proton triplet at 1.22δ (J = 7.0 Hz). Anal. Calculated for $C_{18}H_{33}N_5O_4Br_2 \cdot H_2O$: C, 38.51; H, 6.29. Found: C, 38.35; H, 6.35.

Preparation of N,N,N-Trimethyl-N'N'-dimethyl-N'-(β-N-methyl-4-nitroanilinoethyl)-1,3-diammoniumpropane Dibromide, 13.

1-Fluoro-4-nitrobenzene (2.00 g, 0.014 moles) and N-methyl-N', N'-dimethylethylenediamine (1,23 g, 0.014 moles) were coupled according to the procedure used to make Va above and yielded 1.67 g (55%) of Vc. After a single recrystallization from ethanol-acetone, the mp was 248-50°C (dec.), and the pmr spectrum (D_2O) showed a two-proton doublet at 8.18δ (J = 9.4 Hz), a two-proton doublet at 6.88δ (J = 9.4 Hz), a four-proton multiplet at 3.77δ, a three-proton singlet at 3.20δ, and a six-proton singlet at 3.05δ. Anal. Calculated for $C_{11}H_{18}N_3O_2Br$: C, 43.17; H, 5.92. Found: C, 43.39; H, 6.14.

Vc (0.30 g, 0.74 mmoles) and N,N,N-trimethyl-N-3-bromopropyl-ammonium bromide (0.29 g, 0.96 mmoles) were allowed to react according to the procedure used to make 9 above and yielded 0.36 g (63%) of the desired product. After a single recrystallization from ethanol-acetone, the mp was 156-9°C, and the pmr spectrum (D_2O) showed a two-proton

doublet at 8.07δ (J = 9.6 Hz), a two-proton doublet at 6.77δ (J = 9.6 Hz), a ten-proton multiplet at 3.75δ, a six-proton singlet at 3.30δ, a nine-proton singlet at 3.18δ, and a three-proton singlet at 3.13δ. Anal. Calculated for $C_{17}H_{32}N_4O_2Br_2$: C, 42.19; H, 6.66. Found: C, 41.98; H, 6.73.

Preparation of N,N,N-Trimethyl-N',N'-dimethyl-N'-(γ-2-trifluoromethyl-4-nitroanilinopropyl)-1,3-diammoniumpropane Dibromide, 18.

2-Chloro-5-nitro-benzotrifluoride (5.60 g, 25 mmoles) and N,N-dimethylpropylenediamine (5.10 g, 50 mmoles) were coupled according to the procedure used to make Vc above, and the workup was carried out up to the point where the water layer is extracted with ethyl acetate. Flash-evaporation of the ethyl acetate layer yielded 7.19 g (96%) of IVd. After a single recrystallization from ethanol-water, the mp was 82-3°C, and the pmr spectrum ($CDCl_3$) showed a two-proton multiplet at 8.20δ, a one-proton doublet at 6.95δ (J = 10 Hz), a four-proton multiplet at 3.51δ, a six-proton singlet at 3.21δ, and a two-proton multiplet at 2.34δ.

IVd (0.80 g, 2.75 mmoles) and N,N,N-trimethyl-N-3-bromopropyl-ammonium bromide (0.65 g, 2.49 mmoles) were dissolved in 2-3 ml of absolute ethanol and heated to 120°C for 24 hr in a sealed tube. Cooling and the addition of excess acetone yielded 0.83 g (62%) of the desired product. After a single recrystallization from ethanol-acetone, the mp was 129-31°C, and the pmr spectrum (D_2O) showed a two-proton multiplet at 8.12δ, a one-proton doublet at 6.01δ (J = 9.5 Hz), a pair of overlapping triplets integrating for four protons at 3.37δ (J = 5-6 Hz), a four-proton triplet at 2.55δ (J = 5.6 Hz), a fifteen-proton singlet at 2.25δ, and a four-proton multiplet at 1.06δ. Anal. Calculated for

$C_{18}H_{31}N_4O_2Br_2F_3$: C, 39.14; H, 5.66. Found: C, 39.33; H, 5.75.

Preparation of 4,8-Di (β-aminoethyl)-2,6-di-t-butyl-naphthalene Dihydrobromide, 1.

This molecule was made via the synthetic route shown in Figure 47. 2,6-Di-t-butylnaphthalene (8.0 g, 0.03 moles) (prepared according to the procedure of Crawford and Glessman[89]) and chloromethyl methyl ether (4.0 g, 0.05 moles) were dissolved in 40 ml of carbon disulfide contained in a 100 ml three-necked roundbottom flask equipped with a dropping funnel and a calcium chloride drying tube. The solution was stirred magnetically and cooled to 0°C with an ice-water bath. Stannic chloride (2.4 g, 0.01 moles) was added dropwise to the stirred solution, and the stirring was continued for one hour after the addition was completed. The mixture was then poured onto 50 g of cracked ice. The resulting water and carbon disulfide layers were then transferred to a 250 ml separatory funnel and extracted twice with 150 ml portions of ethyl ether. The ether layers were pooled, dried over anhydrous magnesium sulfate, and evaporated to dryness. The resulting light yellow viscous liquid was dissolved in chloroform, and the solution was concentrated to about 10 ml and refrigerated. The resulting solid was recrystallized once from ethyl ether to yield 1.23 g (12%) of VI, mp 192.5-94.5°C. The pmr spectrum (CS_2) showed an eighteen-proton singlet at 1.37δ, a four-proton singlet at 4.87δ, a two-proton doublet at 7.41δ (J = 2.0 Hz), and a two-proton doublet at 7.89δ (J = 2.0 Hz). Anal. Calculated for $C_{20}H_{26}Cl_2$: C, 71.35; H, 7.72. Found: C, 71.22; H, 7.80.

VI (1.25 g, 3.75 mmoles) and potassium cyanide (0.65 g, 10 mmoles) were dissolved in 50 ml of absolute ethanol and heated to reflux for 24 hours in a 100 ml roundbottom flask equipped with a reflux condenser and

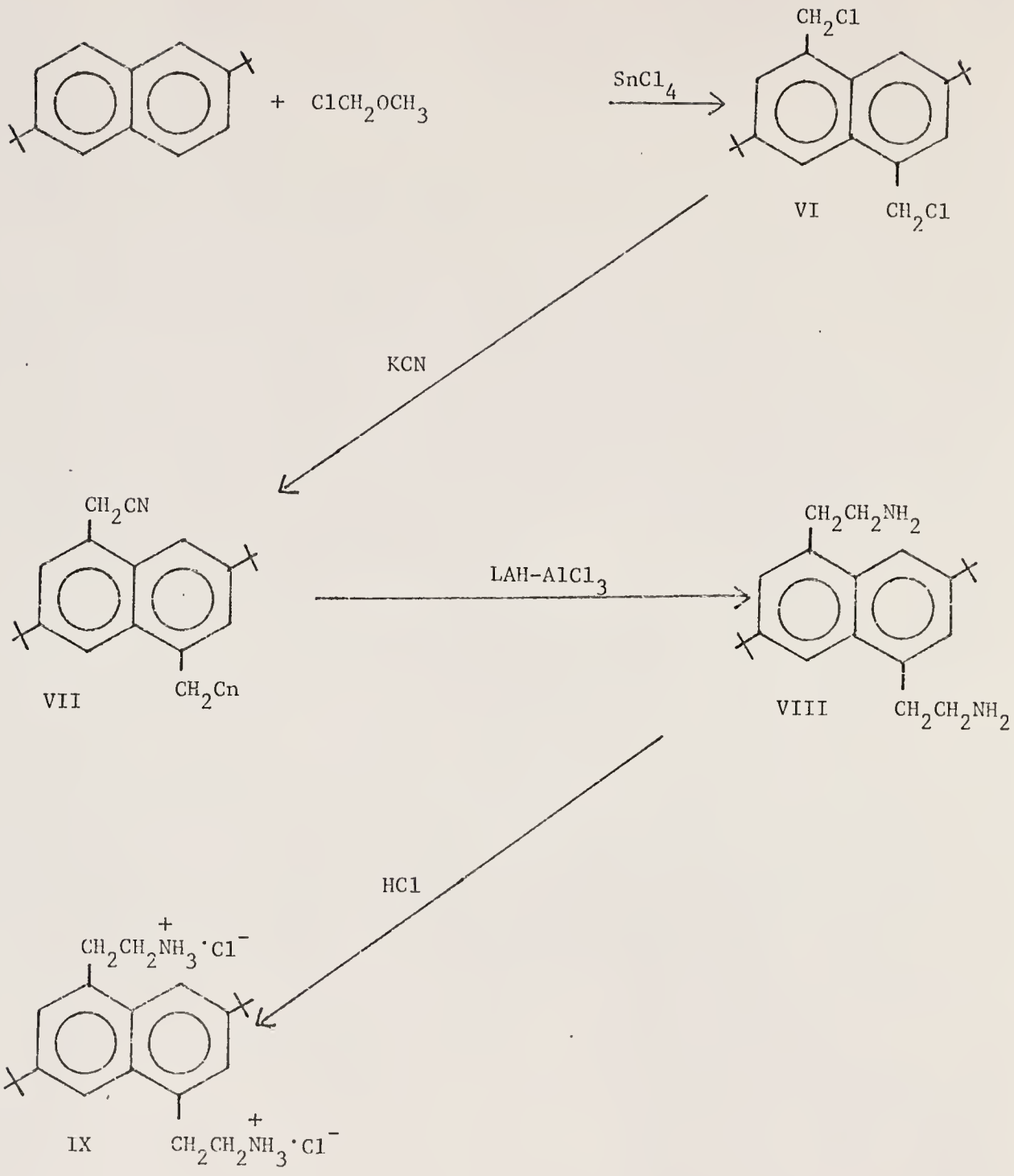

Figure 47. Synthesis of Naphthalene Reporter 1.

a calcium chloride drying tube. The flask was then cooled, and the precipitate of potassium chloride was filtered off and discarded. The filtrate was evaporated to dryness, and the resulting residue was partitioned between 50 ml of chloroform and 50 ml of water. The water layer was then separated and extracted with another 50 ml portion of chloroform. The chloroform layers were pooled, dried over anhydrous magnesium sulfate, and then evaporated to dryness. The resulting red-brown solid was recrystallized twice from acetone-pentane to yield 350 mg (30%) of VII, mp 172.4°C. The pmr spectrum ($CDCl_3$) showed an eighteen-proton singlet at 1.41δ, a four-proton singlet at 4.14δ, and a four-proton doublet at 7.70δ ($J = 3.0H_3$).

Lithium aluminum hydride (80 mg, 2.0 mmoles) was suspended in 30 ml of anhydrous ethyl ether contained in a 200 ml roundbottom flask equipped with a reflux condenser, a 20 ml addition funnel, a calcium chloride drying tube, and magnetic stirring. Anhydrous aluminum chloride (270 mg, 2.0 mmoles) in 20 ml of absolute ethyl ether and VII (320 mg, 1.0 mmoles) in 10 ml of freshly distilled tetrahydrofuran were then added to the suspension in quick succession. The mixture was brought to reflux for 5 hours, cooled to room temperature, poured into a 500 ml Erlenmeyer flask, and acidified with 6N sulfuric acid. The solution was then extracted with 250 ml of ethyl ether. The water layer was separated, made basic with sodium hydroxide pellets, and extracted with another 250 ml portion of ethyl ether. The second ether layer was separated, dried over anhydrous magnesium sulfate, filtered, and finally flash-evaporated. The resulting colorless crystalline solid was dissolved in tetrahydrofuran and acidified with concentrated hydrochloric acid. The resulting precipitate was collected by vacuum filtration and dried under vacuum to

give 190 mg (45%) of IX. The pmr spectrum (D_2O) showed an eighteen-proton singlet at 1.52δ, a ten-proton complex multiplet at 3.50δ, a two-proton doublet at 7.57δ (J = 2.0 Hz), and a two-proton doublet at 7.80δ (J = 2.0 Hz). Anal. Calculated for $C_{22}H_{36}N_2Cl_2 \cdot H_2O$: C, 63.30; H, 9.18. Found: C, 63.57; H, 9.25.

Preparation of Salmon Sperm DNA-Polylysine Complexes

Direct mixing of DNA and polylysine in buffers of moderate ionic strength results in precipitation of the complex. To avoid this complication, the DNA-polylysine complexes were prepared in buffers of high ionic strength and then dialyzed exhaustively against the desired buffer system. 12.5 ml of a 6×10^{-4} M P/1 salmon sperm DNA solution in 0.01 M MES (pH 6.2, 0.005 M in Na^+), 5.0 ml of 0.10 M MES (pH 6.2, 0.05 M in Na^+), and 25 ml of 5 M NaCl solution were mixed in a 50 ml volumetric flask. The calculated amount of polylysine stock solution (0.2 mg/ml in 0.001 M MES, 0.0005 M in Na^+, pH 6.2) was then added dropwise to the vigorously stirred DNA solution in the volumetric. The solution was then brought up to the mark with deionized water and transferred to Visking dialysis sacs. The DNA-polylysine complexes were exhaustively dialyzed against four one-liter portions of 0.01 M MES (pH 6.2, 0.10 M in Na^+). The complexes were stored in tightly stoppered glass vials and were bacteriostatted with 2-3 drops of chloroform.

Proton Magnetic Resonance Spectra

Pmr studies of reporter molecules with DNA require special preparation of the DNA in order to reduce the viscosity of the solutions. The necessary reduction in viscosity is achieved by ultrasonic cleavage of the DNA molecule to give shorter double-helical fragments.[90]

To a 250 ml beaker containing 100 ml of 0.001 M sodium phosphate buffer (pH 7.0, 0.001 M in Na^+), 3.0 g of salmon sperm DNA (Worthington Biochemicals) was added. The solution was stirred for several hours to dissolve the DNA, and 75 ml of deionized water was added to reduce the viscosity slightly. Nitrogen gas was bubbled through the stirred solution for 15 minutes prior to the start of the procedure and throughout the course of the experiment to prevent the dissolution of oxygen in the solution. The beaker containing the DNA solution was placed in an ice-water bath and sonicated in a Bio-Sonic II-A apparatus (Bronwill Scientific Company) at three-minute intervals for two hours. The solution was then filtered through an 0.8 micron Millipore filter membrane using suction and lyophilized to dryness. The sonicated DNA was collected and stored in a brown bottle at 0°C. The yield was 2.8 g of DNA with a molecular weight below 500,000.

The pmr stock solutions were made by dissolving 75 mg of the sonicated DNA in 1 ml of a deuterium oxide solution containing 1 mg of DSS. This yields a DNA concentration of 0.32 M P/1. The actual pmr samples were prepared by diluting 0.2 ml of this solution with 0.2 ml of a 4.0×10^{-2} M reporter solution made in D_2O DSS. The ionic strength was 0.01 M in Na^+, and the pD was 7.3.

Viscosity Measurements

A DNA solution ($5\text{-}6 \times 10^{-4}$ M P) was pipetted into a low-shear Zimm viscometer (Beckman Instrument Co.) which was thermostatted at 37°C with a Haake constant-temperature circulator. A glass rotor containing a steel pellet was washed with the solution to be titrated and then inserted into the viscometer. The height of the rotor with respect to an etched line on the outside of the viscometer was then

adjusted to assure free rotation of the rotor when the magnetic arms of the viscometer were spinning. The total volume of solution used for each determination was 2.7 ml. An arbitrary number of rotations of the rotor was timed on a Lab-Chron timer (Lab-Line Instrument Co.) in order to obtain the number of revolutions per second of the rotor. This number was then compared to the number of revolutions per second of the rotor in the buffer solution alone to get the relative viscosity (η_{rel}) of the DNA. The calculation of the specific viscosity (η_{sp}) is straightforward, i.e., $\eta_{sp} = \eta_{rel} - 1$. To the DNA solution, 2-3 µl additions of 1×10^{-2} M reporter solutions were added. The solution was gently mixed by rapidly drawing some of it into a pipette and forcing it back into the solution remaining in the viscometer. This was repeated several times and a viscosity measurement was then made.

Melting Temperature Measurements

These studies were done in 1.0 ml quartz cuvettes thermostatted with a Haake constant temperature water circulator equipped with a Neslab temperature programmer. A Gilford Model 240 spectrophotometer equipped with automatic recording accessories was used and the temperature of the cell compartment was measured with an iron-constantan thermocouple connected to a Leeds-Northrup Model 8680 potentiometer.

A typical experiment consisted of mixing 0.15 ml of a 6×10^{-4} M P/l solution of salmon sperm DNA in 0.01 M MES buffer (pH 6.2, 0.005 M in Na^+), 0.85 ml of the same buffer, and 1-2 µl of a 1×10^{-2} M solution of a reporter molecule. The solutions were placed in the thermostatted compartment of the spectrophotometer with a buffer blank. The Neslab temperature programmer was set at a rate of increment of 0.45°/minute. Initial optical densities were recorded for each sample at the beginning

of the run. Temperature readings were taken periodically until the DNA started to melt and were taken at every third cycle of the automatic cuvette positioner after this time.

Circular Dichroism Measurements

Circular dichroism spectra for reporter-DNA complexes were typically taken in 50 mm cells at DNA and reporter concentrations of 4-6 x 10^{-4} M P/1 and 3-10 x 10-5 M, respectively. All experiments were done in 0.01 M MES (pH 6.2. 0.005 M in Na^{+}) at ambient temperature. The spectra were all determined on a Jasco J-20 spectropolarimeter. A scan rate of 50 nm/min and a sensitivity of 0.001°/cm were usually used.

Measurement of Visible Spectra

Absorption spectra for reporters and reporter-nucleic acid complexes were usually determined using either 10 mm or 50 mm quartz cells with a Cary-15 spectrophotometer at ambient temperature. Concentrations were adjusted to give an absorbance as close to full scale as possible and were typically 3-10 x 10^{-5} M and 1-10 x 10^{-4} M P/1 for the reporters and the nucleic acids, respectively. Spectra were recorded between 420 nm and 320 nm in most cases.

Determination of Binding Constants

The determination of binding constants by equilibrium dialysis was done in the following manner. Visking dialysis tubing (26/100 ft. Nojax casings) was cut into 20 cm strips and carefully cleaned by boiling for three one-hour periods in fresh portions of a 50% aqueous ethanol solution containing 5 x 10^{-3} M EDTA and 5 x 10^{-2} M sodium bicarbonate. The membranes were then boiled for six five-hour periods in fresh portions of deionized water. The clean membranes were then stored in deionized water containing 0.2% chloroform as a bacteriostat.

The dialysis experiments were conducted in a pair of plexiglass blocks which had ten semicircular depressions (3 cm x 0.25 cm) located on one edge. Each half of the pair was lightly coated with silicone grease, and a clean dialysis membrane was then placed between the two blocks to form two chambers in each of the depressions. The blocks were then securely fastened together by means of twelve screws and four C-type clamps. Into one side of each cell was introduced 0.200 ml of a nucleic acid solution containing 1.5-3.0 x 10^{-4} M P/l in either 0.01 M MES (pH 6.2, 0.005 M in Na^+) or BPES buffer (0.08 M Na_2HPO_4, 0.02 M NaH_2PO_4, 0.18 M NaCl, and 0.01 M Na_2EDTA, pH 6.9). Into the other side of each cell was introduced 0.200 ml of a 5-10 x 10^{-5} M solution of the reporter in the same buffer system. Bacterial growth was suppressed by the addition of 0.001 ml of chloroform to each compartment. The top of the cells was covered with a strip of lightly greased Parafilm to prevent evaporation. Equilibration was achieved by gentle shaking at either room temperature or 10°C for 16-20 hours. The contents of the chambers containing only the reporter molecule was then pipetted into a 10 mm quartz cuvette, and the optical density at the absorption maximum of the reporter was determined. Blank determinations showed that less than 1% of the DNA passed through the membrane and that the reporter was fully equilibrated.

Kinetic Measurements

All measurements were done using a Durrum-Gibson stopped-flow spectrophotometer (Durrum Instrument Corp.) thermostatted with a Lauda K-2/R circulator. The block diagram for this equipment is shown in Figure 48. The two solutions to be combined were loaded into separate reservoir syringes to a volume of 5-15 ml. The nucleic acid solutions

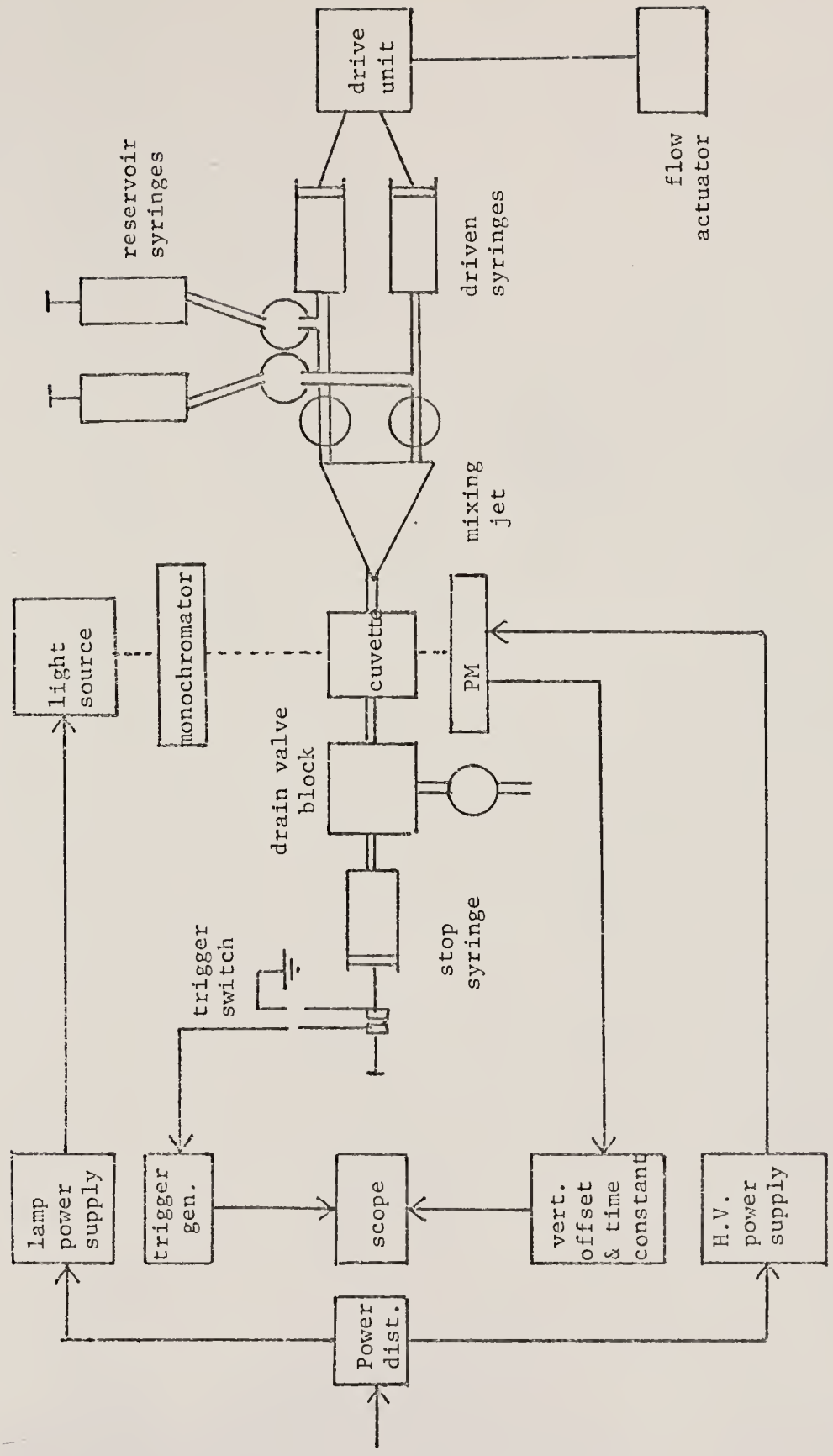

Figure 48. Block Diagram of Stopped-Flow Spectrophotometer System.

were typically 1.0-3.0 x 10^{-4} M P/1, and the reporter solutions were 5-40 x 10^{-6} M. The buffer systems used were either BPES or 0.01 M MES (pH 6.2, 0.10 M in Na^{+}). The driven syringes were cleaned by filling from the reservoir syringes and manually emptying three times. The loaded drive syringes were then allowed 5-10 minutes to equilibrate with the thermostatted bath. At this point, the instrument was triggered several times to rid the system of air bubbles. This was continued until the equilibrium transmittance line pictured on the oscilliscope was reproducible three successive times. The dynode voltage was then adjusted to give a displacement which was as close as possible to full scale. Kinetic measurements were then made using several time spans. The time constant was always selected such that it was no larger than 10% of the value for one division on the oscilliscope grid. After all suitable time spans had been recorded on the oscilliscope screen, a photograph of the screen was taken using the Tektronix C-27 oscilliscope camera and the C-27 camera bezel attached to the oscilliscope screen.

BIBLIOGRAPHY

1. Watson, J. D., and Crick, F. H. C. (1953) Nature, 171, 737.

2. Watson, J. D., and Crick, F. H. C. (1953) Nature, 171, 964.

3. Watson, J. D. (1970) Molecular Biology of the Gene, N. Y., N. Y., W. A. Benjamin, Inc.

4. Bram, S. (1972) Biochem. Biophys. Res. Comm., 48, 1088.

5. Bram, S. (1971) J. Mol. Biol., 58, 277.

6. Bram, S. (1971) Nature New Biology, 233, 161.

7. Donahue, J. (1970) Science, 167, 1700.

8. Donahue, J. (1969) Science, 165, 1091.

9. Donahue, J. (1971) J. Mol. Biol., 59, 381

10. Feugelman, M., Langridge, R., Sieds, W., Stokes, A., Wilson, H., Hooper, C., Wilkins, M., Barclay, R., and Hamilton, L. (1955) Nature, 175, 834.

11. Chargaff, E., and Lipschitz, R. (1953) J. Am. Chem. Soc., 75, 3658.

12. Josse, J., Kaiser, A. D., and Kornberg, A. (1961) J. Biol. Chem., 236. 964.

13. Langridge, R., Wilson, H. R., Hooper, C. W., Wilkins, M. H. F., and Hamilton, L. P. (1960) J. Mol. Biol., 2, 19.

14. Donahue, J. (1956) Proc. Natl. Acad. U. S., 42, 60.

15. Donahue, J. (1960) J. Mol. Biol., 2, 263.

16. Nash, H. A., and Bradley, D. F. (1966) J. Chem. Phys., 45, 1380.

17. Hoogstein, K. (1963) Acta Cryst., 16, 907.

18. Haschemeyer, A. E. V., and Sobell, H. M. (1963) Proc. Natl. Acad. Sci. U. S., 50, 782.

19. Haschemeyer, A. E. V., and Sobell, H. M. (1965) Acta Cryst., 18, 525.

20. O'Brien, E. J. (1963) J. Mol. Biol., 7, 107.

21. O'Brien, E. J. (1966) J. Mol. Biol., 22, 377.

22. Tuppy, H. T., and Kuechler, E. K. (1964) Biochim. Biophys. Acta, 80, 669.

23. Katz, L., and Penman, S. (1965) J. Mol. Biol., 15, 220.

24. Katz, L., Tomaita, K., and Rich, A. (1965) J. Mol. Biol., 13, 340.

25. Ts'o, P. O. P., Melvin, I. S., and Olson, A. C. (1963) J. Am. Chem. Soc., 85, 1289.

26. Ts'o, P. O. P., and Chan, S. I. (1964) J. Am. Chem. Soc., 86, 4176.

27. Ts'o, P. O. P. (1968) Molecular Associations, N. Y., N. Y., Academic Press, 40.

28. Hanlon, S. (1966) Biochem. Biophys. Res. Comm., 23, 861.

29. Chan, S. I., Schweizer, M. P., Ts'o, P. O. P., and Helmkamp, G. R. (1964) J. Am. Chem. Soc., 86, 4182.

30. Broom, A. D., Schweizer, M. P., and Ts'o, P. O. P. (1967) J. Am. Chem. Soc., 89, 3612.

31. Chan, S. I., and Nelson, J. A. (1969) J. Am. Chem. Soc., 91, 168.

32. Tinoco, I., Jr., Davis, R. C., and Jaskunas, S. R. (1968) Molecular Associations, N. Y., N. Y., Academic Press, 81.

33. Warner, R. (1957) J. Biol. Chem., 229, 711.

34. Steiner, R. F., and Beers, R. F., Jr. (1961) Polynucleotides, N. Y., N. Y., Elsevier.

35. Griffin, B. E., Haslan, W. J., and Reese, C. B. (1964) J. Mol. Biol., 10, 353.

36. Van Holde, K. E., Brahms, J., and Michaelson, A. M. (1965) J. Mol. Biol., 12, 726.

37. Thomason, J. F., Cartter, M. S., and Tourtellotc, W. W. (1954) Radiation Res., 1, 165.

38. Leng, M., and Felsenfeld, G. (1964) J. Mol. Biol., 15, 455.

39. Stevens, C. L., and Felsenfeld, G. (1964) Biopolymers, 2, 293.

40. Cohen, G., and Eisenberg, H. (1969) Biopolymers, 35, 251.

41. Tinoco, I., Jr. (1960) J. Am. Chem. Soc., 82, 4745.

42. Tinoco, I., Jr. (1961) J. Chem. Phys., 34, 1067.

43. Devoe, H., and Tinoco, I., Jr. (1962) J. Mol. Biol., 4, 518.

44. Tinoco, I., Jr. (1964) J. Am. Chem. Soc., 86, 297.

45. Printz, M. P., and von Hippel, P. H. (1965) Proc. Natl. Acad. Sci. U. S., 53, 363.

46. McConnell, B., and von Hippel, P. H. (1970) J. Mol. Biol., 50, 297.

47. McConnell, B., and von Hippel, P. H. (1970) J. Mol. Biol., 50, 317.

48. Robinson, D. R., and Grant, M. E. (1966) J. Biol. Chem., 241, 4030.

49. Dove, W. F., and Davidson, N. (1962) J. Mol. Biol., 5, 467.

50. Bunville, L. G., Geiduschek, E. P., Raurtscher, M. R., and Sturtevant, J. M. (1965) Biopolymers, 3, 213.

51. Haselkorn, R., and Doty, P. (1961) J. Biol. Chem., 236, 2738.

52. Von Hippel, P. H., and Wong, K. Y. (1971) J. Mol. Biol., 61, 587.

53. Mueller, W., and Crothers, D. (1968) J. Mol. Biol., 35, 251.

54. Burr, M., and Koshland, D. E., Jr. (1967) J. Am. Chem. Soc., 89, 5945.

55. Burr, M., and Koshland, D. E., Jr. (1964) Proc. Natl. Acad. Sci. U. S., 52, 1017.

56. Gabbay, E. J. (1969) J. Am. Chem. Soc., 91, 5136.

57. Gabbay, E. J., and Mitschele, J. (1969) Biochem. Biophys. Res. Comm., 34, 53.

58. Gabbay, E. J. (1968) J. Am. Chem. Soc., 90, 6574.

59. Gabbay, E. J., and Gaffney, B. (1970) J. Macromol. Sci. Chem., A4, 1315.

60. Mahler, H. R., and Mehrotra, B. D. (1963) Biochim. Biophys. Acta., 68, 211.

61. Gabbay, E. J. (1966) Biochemistry, 5, 3036.

62. Gabbay, E. J. and Shimshak, R. R. (1968) Biopolymers, 6, 255.

63. Lerman, L. S. (1961) J. Mol. Biol., 3, 18.

64. Drummond, D. S., Pritchard, N. J., Simpson-Gildmeister, V. F. W., and Peacocke, A. R. (1966) Biopolymers, 4, 971.

65. Luzzati, V., Masson, F., and Lerman, L. S. (1961) J. Mol. Biol., 3, 634.

66. Passero, F., Gabbay, E. J., Gaffney, B. L., and Kurucsev, T. (1970) Macromol., 3, 158.

67. Gabbay, E. J., Glaser, R., and Gaffney, B. L. (1970) Ann. N. Y. Acad. Sci., 171, 810.

68. Fischer, J. J., and Jardetsky, O. (1965) J. Am. Chem. Soc., 87, 3237.

69. McDonald, C. C., Phillips, W. D., and Penman, J. (1964) Science, 144, 1234.

70. Gabbay, E. J., and DeStefano, R., unpublished results.

71. Gabbay, E. J., and DePaolis, A. (1971) J. Am. Chem. Soc., 93, 562.

72. Raska, M., and Mandel, M. (1971) Proc. Natl. Acad. Sci. U. S., 68, 1190.

73. Helene, C., Montenay-Garestier, T., and Dimicoli, J. L. (1971) Biochim. Biophys. Acta, 254, 349.

74. Helene, C., Dimicoli, J. L., and Brun, F. (1971) Biochemistry, 10, 3802.

75. Gabbay, E. J., Sanford, K. J., and Baxter, C. S. (19712) Biochemistry, 11, 3249.

76. Gabbay, E. J., and Baxter, C. S. unpublished results.

77. Pople, J. A., Schneider, W. G., and Bernstein, H. H. (1959) High Resolution Nuclear Magnetic Resonance, New York, McGraw-Hill Book Co.

78. Cram, D. J., and Hammond, G. S. (1964) Organic Chemistry, 2nd ed., New York, John Wiley and Sons, Inc., 13.

79. Frost, A. A., and Pearson, R. G. (1961) Kinetics and Mechanism, 2nd ed., New York, John Wiley and Sons, Inc., 13.

80. Gabbay, E. J., DeStefano, R., and Baxter, C. S. (1973) Biochem. Biophys. Res. Comm., 51, 1083.

81. Frost, A. A., and Pearson, R. G. (1961) Kinetics and Mechanism, 2nd ed., New York, John Wiley and Sons, Inc., 44.

82. Printz, M. P., and von Hippel, P. H. (1965) Proc. Natl. Acad. Sci. U. S., 53, 363.

83. Frost, A. A., and Pearson, R. G. (1961) Kinetics and Mechanism, 2nd ed., New York, John Wiley and Sons, Inc., 23.

84. Scatchard, G. (1949) Ann. N. Y. Acad. Sci., 51, 660.

85. Salem, L. (1966) Molecular Orbital Theory of Conjugated Systems. New York, W. A. Benjamin, Inc., 458.

86. Gabbay, E. J. (1967) Biopolymers. 5, 727.

87. Sharpe, V. V. (1973) Undergraduate Research Participant, National Science Foundation.

88. Sanford, K. J. (1972) The Interaction Specificities of Oligopeptide Amides and Reporter Molecules with DNA. Ph.D. Dissertation, University of Florida, Gainesville, Florida.

89. Crawford, H. M., and Glessman, M. C. (1954) J. Am. Chem. Soc., 76, 1108.

90. Strauss, V. P., Heffgott, C., and Pink, H. (1967) J. Phys. Chem., 71, 2550.

APPENDIX

Model 1: Rate-Determining Nucleic Acid Preequilibrium

$$CH \underset{-1}{\overset{1\,(slow)}{\rightleftharpoons}} 2(OH)$$

$$(OH) + (R) \underset{-2}{\overset{2}{\rightleftharpoons}} (OH\cdot R) \xrightarrow{3} (CH\cdot R)$$

$$\frac{d(CH\cdot R)}{dt} = k_3(OH\cdot R)$$

$$\frac{d(OH\cdot R)}{dt} = 0 = -k_3(OH\cdot R) + k_2(OH)(R) - k_{-2}(OH\cdot R)$$

$$(OH\cdot R) = \left[k_2/(k_{-2} + k_3)\right](OH)(R)$$

$$\frac{d(OH)}{dt} = 0 = k_1(CH) - k_{-1}(OH)^2 - k_2(OH)(R) + k_{-2}(OH\cdot R)$$

$$(OH) = \frac{-k_2k_3(R)}{(k_{-2}+k_3)2k_{-1}} \pm \left[\left(\frac{k_2k_3(R)}{k_{-2}+k_3}\right)^2 + \frac{4k_1(CH)}{1/2\ k_{-1}}\right]^{1/2}$$

$$4k_1(CH) >> \left(\frac{k_2k_3R}{k_{-2}+k_3}\right)^2$$

$$(OH) = \frac{k_1^{1/2}(CH)^{1/2}}{k_{-1}} - \frac{k_2k_3(R)}{2k_{-1}(k_{-2}+k_3)}$$

$$\frac{d(CH\cdot R)}{dt} = k_3(OH\cdot R) = \frac{k_2k_3(R)}{(k_{-2}+k_3)}\left[\frac{k_1^{1/2}(CH)^{1/2}}{k_{-1}} - \frac{k_2k_3(R)}{2k_{-1}(k_{-2}+k_3)}\right]$$

Model 2: Product Inhibition

$$(CH) \underset{-1}{\overset{1}{\rightleftharpoons}} 2(OH)$$

$$(OH) + (R) \underset{-2}{\overset{2}{\rightleftharpoons}} (OH\cdot R) \xrightarrow{3} (CH\cdot R)$$

$$(CH\cdot R) + 2(OH) \xrightarrow{4} (CH\cdot R) + (CH)$$

$$\frac{d(CH\cdot R)}{dt} = k_3(OH\cdot R)$$

$$(OH\cdot R) = \frac{k_2(OH)(R)}{k_{-2}+k_3}$$

$$\frac{d(OH)}{dt} = 0 = k_1(CH) - k_{-1}(OH)^2 - k_4(CH\cdot R)(OH)^2 - k_2(OH)(R) + k_{-2}(OH\cdot R)$$

$$= [k_1 + k_4(CH\cdot R)](OH)^2 + \frac{k_2k_3(R)(OH)}{(k_{-2}+k_3)} - k_1(CH)$$

$$(OH) = \frac{k_1^{1/2}(CH)^{1/2}}{k_{-1}+k_4(CH\cdot R)} - \frac{k_2k_3(R)}{2[k_{-1}+k_4(CH\cdot R)](k_{-2}+k_3)}$$

$$\frac{d(CH\cdot R)}{dt} = k_3(OH\cdot R) = \frac{k_2k_3(R)}{(k_{-2}+k_3)}\left[\frac{k_1^{1/2}(CH)^{1/2}}{k_{-1}+k_4(CH\cdot R)} - \frac{k_2k_3(R)}{2[k_{-1}+k_4(CH\cdot R)]}\quad(k_{-2}+k_3)\right]$$

Model 3: Catalysis by an Intermediate Complex

$$(CH) \underset{-1}{\overset{1}{\rightleftharpoons}} 2(OH)$$

$$(OH) + (R) \underset{}{\overset{2}{\rightleftharpoons}} (OH\cdot R) \xrightarrow{3(slow)} (CH\cdot R)$$

$$(OH\cdot R) + (CH) \xrightarrow[-2]{4} (OH\cdot R) + 2(OH)$$

$$\frac{d(CH\cdot R)}{dt} = k_3(OH\cdot R) = \frac{k_3k_2(OH)(R)}{(k_{-2}+k_3)}$$

$$\frac{d(OH)}{dt} = 0 = k_1(CH) - k_{-1}(OH)^2 - k_2(OH)(R)\quad 1 - \frac{k_{-2}+k_4(CH)}{(k_{-2}+k_3)}$$

$$= k_1(CH) - k_{-1}(OH)^2 - k_2(OH)(R)\ \frac{k_3-k_4(CH)}{(k_{-2}+k_3)}$$

$$(OH) = 1/2\ k_{-1}\left[\left(\frac{k_2[k_3-k_4(CH)](R)}{(k_{-2}+k_3)}\right) + 4k_1(CH)\right] - \frac{k_2[k_3-k_4(CH)](R)}{2k_{-1}(k_{-2}+k_3)}$$

$$4k_1(CH) >> \left[\frac{k_2[k_3-k_4(CH)](R)}{(k_{-2}+k_3)}\right]^2$$

$$(OH) = \frac{k_1^{1/2}(CH)^{1/2}}{k_{-1}} - \frac{k_2(R)[k_3-k_4(CH)]}{2k_{-1}(k_{-2}+k_3)}$$

$$\frac{d(CH\cdot R)}{dt} = \frac{k_2}{k_{-2}+k_3}(R)\left[\frac{k_1^{1/2}(CH)^{1/2}}{k_{-1}} - \frac{k_2(R)[k_3-k_4(CH)]}{2k_{-1}(k_{-2}+k_3)}\right]$$

Model 4: Rate-Determining Formation of Intermediate Complex

$$(CH) \underset{-1}{\overset{1}{\rightleftharpoons}} 2(OH)$$

$$(OH) + (R) \xrightarrow{2} (OH \cdot R) \underset{-3}{\overset{3}{\rightleftharpoons}} (CH \cdot R)$$

$$\frac{d(CH \cdot R)}{dt} = k_2(R)(OH)$$

$$\frac{d(OH)}{dt} = 0 = k_1(CH) - k_{-1}(OH)^2 - k_2(OH)(R)$$

$$(OH) = 1/2\ k_{-1}\left[\left([k_2(R)]^2 + 4k_1(CH)\right)^{1/2} - k_2R\right]$$

$$4k_1(CH) >> [k_2(R)]^2$$

$$(OH) = \frac{k_1^{1/2}(CH)^{1/2}}{k_{-1}} - \frac{k_2(R)}{2k_{-1}}$$

$$\frac{d(CH \cdot R)}{dt} = k_2(R)\left[\frac{k_1^{1/2}(CH)^{1/2}}{k_{-1}} - \frac{k_2(R)}{2k_{-1}}\right]$$

Ronald Phillip DeStefano

1947	Born April 6 in New Castle, Pennsylvania.
1965	Graduated fron New Castle High School, New Castle, Pennsylvania.
1965-69	Attended Case Institute of Technology, Cleveland, Ohio; majored in chemistry.
1969	B. S. degree in chemistry, Case Institute of Technology.
1969	Married Karen Audia.
1969-73	Graduate work in chemistry, University of Florida, Gainesville, Florida.
1971	Daughter Kimberly Ann born.
1969-70	Teaching Assistant, School of Chemistry.
1970-73	Research Assistant, School of Chemistry.
1972	Article with E. J. Gabbay and K. Sanford: "Topography of Nucleic Acid Helices in Solution XXIV. Intercalation Specificities of DNA and their Possible Role in the Recognition Process." Biochemical and Biophysical Research Communications, vol. 46, 155-161.
1973	Article with E. J. Gabbay and C. S. Baxter: "Topography of Nucleic Acid Helices in Solution XXVIII. Evidence for a Dynamic Structure of DNA in Solution." Biochemical and Biophysical Research Communications, vol. 51, 1083-1089.
1973	Ph.D. in chemistry, University of Florida.

I certify that I have read this study and that in my opinion it conforms to acceptable standards of scholarly presentation and is fully adequate, in scope and quality, as a dissertation for the degree of Doctor of Philosophy.

Edmund Gabbay, Chairman
Associate Professor of Chemistry

I certify that I have read this study and that in my opinion it conforms to acceptable standards of scholarly presentation and is fully adequate, in scope and quality, as a dissertation for the degree of Doctor of Philosophy.

George Butler
Professor of Chemistry

I certify that I have read this study and that in my opinion it conforms to acceptable standards of scholarly presentation and is fully adequate, in scope and quality, as a dissertation for the degree of Doctor of Philosophy.

Willis Person
Professor of Chemistry

I certify that I have read this study and that in my opinion it conforms to acceptable standards of scholarly presentation and is fully adequate, in scope and quality, as a dissertation for the degree of Doctor of Philosophy.

Paul Tarrant
Professor of Chemistry

I certify that I have read this study and that in my opinion it conforms to acceptable standards of scholarly presentation and is fully adequate, in scope and quality, as a dissertation for the degree of Doctor of Philosophy.

Phillip Ackey
Assistant Professor of Radiology

This dissertation was submitted to the Department of Chemistry in the College of Arts and Sciences and to the Graduate Council, and was accepted as partial fulfillment of the requirements for the degree of Doctor of Philosophy.

December, 1973

_____

Dean, Graduate School